CHALMERS
UNIVERSITY OF TECHNOLOGY

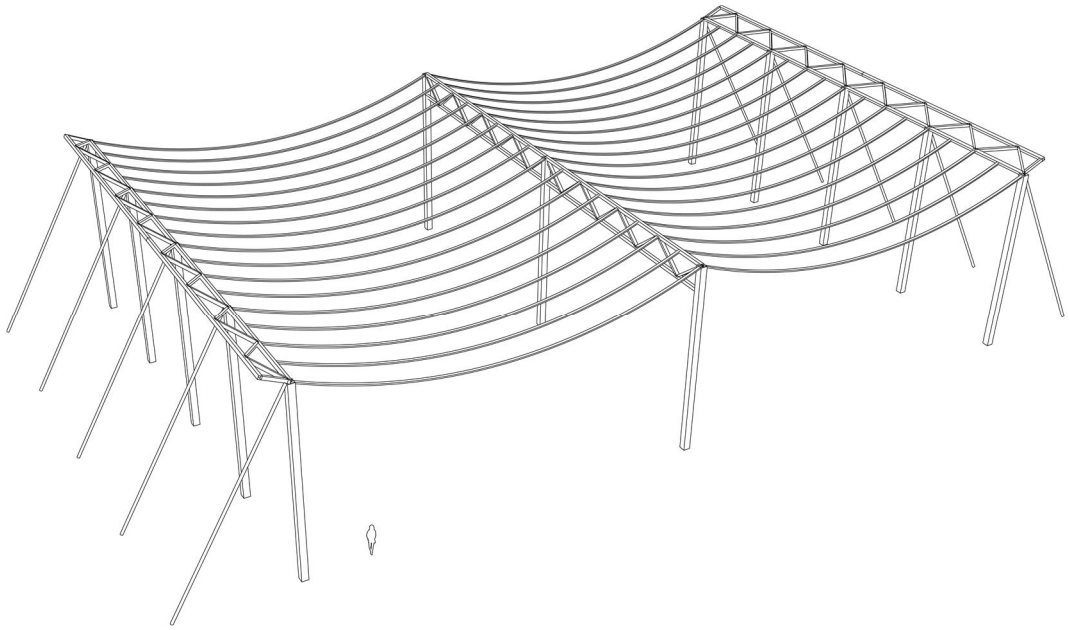

Long-span tensile timber roof structures

Development of design proposals adopting the Stress Ribbon concept

Master's Thesis in the Master's Programme Structural Engineering and Building Technology

SAMUEL HOFVERBERG

Department of Civil and Environmental Engineering
Division of Structural Engineering
CHALMERS UNIVERSITY OF TECHNOLOGY
Gothenburg, Sweden 2016
Master's Thesis BOMX02-16-30

MASTER'S THESIS BOMX02-16-30

Long-span tensile timber roof structures

Development of design proposals adopting the Stress Ribbon concept

Master's Thesis in the Master's Programme Structural Engineering and Building Technology

SAMUEL HOFVERBERG

Department of Civil and Environmental Engineering
Division of Structural Engineering
CHALMERS UNIVERSITY OF TECHNOLOGY
Göteborg, Sweden 2016

Long-span tensile timber roof structures
Development of design proposals adopting the Stress Ribbon concept
Master's Thesis in the Master's Programme Structural Engineering and Building Technology

SAMUEL HOFVERBERG

Examensarbete BOMX02-16-30/ Institutionen för bygg- och miljöteknik,
Chalmers tekniska högskola 2016

Department of Civil and Environmental Engineering
Division of Structural Engineering
Chalmers University of Technology
SE-412 96 Göteborg
Sweden
Telephone: + 46 (0)31-772 1000

Cover:
One of the developed proposals, with closely spaced Stress Ribbons. More information is found in Chapter 5.

Chalmers Reproservice
Göteborg, Sweden, 2016

Long-span tensile timber roof structures

Development of design proposals adopting the Stress Ribbon concept

Master's thesis in the Master's Programme Structural Engineering and Building Technology

SAMUEL HOFVERBERG
Department of Civil and Environmental Engineering
Division of Structural Engineering
Chalmers University of Technology

ABSTRACT

In construction, one factor that affects the impact made on the environment by a building is the choice of construction material; timber is often considered a sustainable choice compared to other conventional building materials, such as steel and concrete. From an ecological point of view, replacing these less environmental friendly materials with timber can therefore be seen as beneficial. Another way of reducing the environmental impact of buildings is to reduce the overall material consumption. A study has been initiated by the furniture company IKEA, where the possibility to replace the steel roof systems commonly used in their warehouses with material efficient timber structures is investigated.

This thesis was a part of that study, with the aim to investigate the possibility of utilising timber in structurally efficient long-span roof structures. The material efficiency was strived for by primarily adopting cable-like behaviour with the Stress Ribbon concept.

The theory of the Stress Ribbon concept, its properties and reference buildings were studied, and three possible design solutions were established. The different concepts were analysed by use of analytical expressions derived for the hanging cable and main members were designed in the Ultimate Limit State according to Eurocode. Three different span lengths, 24, 36 and 48 m, were studied. The design proposals were then compared, both to each other and to more conventional structural systems in order to evaluate their material efficiency. Finally some connection details were studied and possible solutions were developed.

The results of the study showed that all of the proposals and considered span lengths are feasible with regard to member design. Furthermore, it was concluded that implementation of the Stress Ribbon concept in long-span roof structures is not only possible, but has the potential of reducing the material usage significantly compared to conventional systems.

Key words: Stress Ribbon, cable shape, timber, long-span, roof structure, tension, material efficiency, preliminary design

Dragna trätakkonstruktioner för långa spännvidder

Utveckling av designförslag enligt Stress Ribbon-konceptet

Examensarbete inom masterprogrammet Structural Engineering and Building Technology

SAMUEL HOFVERBERG
Institutionen för bygg- och miljöteknik
Avdelningen för Konstruktionsteknik
Chalmers tekniska högskola

SAMMANFATTNING

En av faktorerna som avgör en byggnads klimatpåverkan är valet av material i den bärande stommen. Trä ses ofta som ett ekologiskt hållbart alternativ i jämförelse med andra vanliga konstruktionsmaterial, såsom stål och betong. I ett hållbarhetsperspektiv är det därför fördelaktigt att välja trä som konstruktionsmaterial. Ytterligare ett sätt att minska klimatpåverkan är att dra ner på den totala materialåtgången. Möbelföretaget IKEA har inlett en undersökning om möjligheten att ersätta de stålfackverkssystem som idag används i deras varuhus med materialeffektiva träsystem.

Det här examensarbetet var en del i denna studie. Målet var att undersöka och utveckla ett system som nyttjar trä i materialeffektiva takkonstruktioner. Metoden som undersöktes för att nå materialeffektivit var det så kallade Stress Ribbon-konceptet, som innebär att de lastbärande elementen primärt arbetar i drag genom kabelverkan.

I examensarbetet undersöktes Stress Ribbon-konceptet, dess egenskaper och referensbyggnader. Sedan skapades tre förslag på hur ett sådant system skulle kunna se ut. De tre koncepten analyserades med hjälp av analytiska uttryck härledda för den hängande kabeln och systemens huvudelement dimensionerades i brottgränstillstånd enligt Eurocode. Tre olika spännvidder, 24, 36 och 48 m undersöktes. Designförslagen jämfördes sedan både sinsemellan och med mer konventionella system, främst med avseende på materialeffektivitet. Slutligen studerades några infästningsdetaljer och möjliga lösningar togs fram.

Resultaten av studien visar att samtliga designförslag och spännvidder som undersöktes är rimliga med avseende på tvärsnittsdesign. Utöver detta drogs slutsatsen att implementering av Stress Ribbon-konceptet i trätak med långa spännvidder inte bara är rimligt, utan dessutom har potential att reducera materialanvändningen i jämförelse med konventionella system.

Nyckelord: Stress Ribbon, kabelform, trä, långa spännvidder, takkonstruktioner, drag, materialeffektivitet, preliminär design

Contents

Preface

In this project the Stress Ribbon concept has been studied, and three design proposals for long-span roof structures have been generated. The project has been carried out at the Division of Structural Engineering, Department of Civil and Environmental Engineering, Chalmers University of Technology, Sweden, in collaboration with IKEA Fastigheter and WSP Sweden, business area WSP Construction Design.

Examiner was Senior Lecturer Joosef Leppänen and supervisors were Alexander Sehlström at WSP Byggprojektering and Professor Roberto Crocetti at the Division of Structural Engineering, Lund University, Sweden.

As initiators to the collaboration and the project itself, Marcus Hedman at IKEA Fastigheter and Linda Leijonberg at WSP Byggprojektering have been very valuable and their involvement is much appreciated. Furthermore, the original idea of Stress Ribbon roofs in this context was generated by Roberto Crocetti, and I therefore have him to thank for the subject of this thesis.

I would also like to thank Alexander Sehlström for the continuous support and good advice, and Joosef Leppänen for the valuable input.

Finally, I would like to thank everybody at WSP Construction Design in Gothenburg for keeping me company during this spring and for continuously showing interest in the progress of my work.

Göteborg June 2016

Samuel Hofverberg

Notations

Roman upper case letters

A	Cross-section area
A_{ef}	Effective cross-section area with regard to fire
E	Modulus of elasticity
E_{05}	5 %-fractile of modulus of elasticity at normal temperature
E_{20}	20 %-fractile of modulus of elasticity at normal temperature
$E_{0,\mathrm{g,mean}}$	Mean modulus of elasticity of glulam
$E_{0,\mathrm{Q,mean}}$	Mean modulus of elasticity of Kerto-Q
E_{d}	Design modulus of elasticity
$E_{\mathrm{d,fi}}$	Design modulus of elasticity with regard to fire
$E_{\mathrm{mean,fin}}$	Mean modulus of elasticity with regard to creep
G_{k}	Characteristic value of permanent load
$G_{\mathrm{kj,sup}}$	Upper characteristic value for permanent load *j*
H	Horizontal force
H_{col}	Total horizontal force at column
I	Moment of inertia
L	Span length
L_0	Cable/Stress Ribbon length
M_{Ed}	Design bending moment
$M_{\mathrm{Ed,bt}}$	Design bending moment in boundary truss
$M_{\mathrm{Ed,it}}$	Design bending moment in intermediate truss
N	Normal force
N_{Ed}	Design normal force
$N_{\mathrm{Ed,bt}}$	Design normal force in boundary truss
$N_{\mathrm{Ed,it}}$	Design normal force in intermediate truss
$N_{\mathrm{t,Rd}}$	Design tensile capacity
$Q_{\mathrm{k,1}}$	Characteristic value of main variable load
$Q_{\mathrm{k,i}}$	Characteristic value of variable load i
R_{d}	Design strength value
R_{k}	Characteristic strength value
V	Vertical force
V_{col}	Vertical force in column
$V_{\mathrm{Ed,bt}}$	Design shear force in boundary truss

$V_{\mathrm{Ed,it}}$ Design shear force in intermediate truss

Roman lower case letters

b Cross-section width

b_{ef} Effective cross-section width with regard to fire

b_{col} Concrete column cross-section width

b_{strut} Strut cross-section width

c Ribbon spacing

$c_{\mathrm{col,b}}$ Boundary column spacing

$c_{\mathrm{col,i}}$ Internal column spacing

$d_{\mathrm{char,n}}$ Equivalent design charring depth

d_{ef} Cross-section reduction depth with regard to fire

f Sag

f_{20} 20 %-fractile of strength at normal temperature

$f_{\mathrm{d,fi}}$ Design strength during fire

f_{k} Characteristic strength

$f_{\mathrm{m,0,Q,flat,k}}$ Characteristic bending strength of Kerto-Q, flatwise, parallel to grain

$f_{\mathrm{m,g,k}}$ Characteristic bending strength of glulam

$f_{\mathrm{m,y,d}}$ Design bending strength

$f_{\mathrm{t,0,d}}$ Design tensile strength parallel to fibres

$f_{\mathrm{t,0,g,k}}$ Characteristic tensile strength of glulam, parallel to fibres

$f_{\mathrm{t,0,Q,k}}$ Characteristic tensile strength of Kerto-Q, parallel to grain

f_{u} Ultimate steel strength

f_{y} Steel yield strength

g Permanent load

g_{k} Characteristic self-weight

$g_{\mathrm{k,sheet}}$ Characteristic self-weight of metal sheeting

h Cross-section height

h_{ef} Effective cross-section height with regard to fire

h_{col} Concrete column cross-section height

h_{strut} Strut cross-section height

$k_0 d_0$ Thickness of non-charred material layer without strength and stiffness

k_{def} Creep factor

k_{fi}	Factor for calculation of 20 %-fractile of strength property
k_{h}	Size factor
k_{mod}	Modification factor for duration of load and moisture content
$k_{\mathrm{mod,fi}}$	Modification factor during fire
m_{col}	Column concrete mass
m_{cs}	Compression strut steel mass
m_{bs}	Total back-stay steel mass
m_{bt}	Self-weight of one boundary truss
$m_{\mathrm{bt,tot}}$	Total mass of boundary trusses
m_{it}	Mass of one intermediate truss
$m_{\mathrm{it,tot}}$	Total mass of intermediate trusses
m_{pri}	Mass of one primary beam
$m_{\mathrm{pri,tot}}$	Total mass of primary beams
m_{rb}	Total mass of reinforcement bars
m_{sec}	Mass of one secondary beam
$m_{\mathrm{sec,tot}}$	Total mass of secondary beams
$m_{\mathrm{sheet,tot}}$	Total mass of metal sheeting
m_{SR}	Mass of one stress ribbon
$m_{\mathrm{SR,tot}}$	Total mass of stress ribbons
n_{bs}	Number of back-stay members
n_{bt}	Number of boundary trusses
n_{it}	Number of intermediate trusses
n_{pri}	Number of primary beams
n_{rb}	Number of reinforcement bars
n_{sec}	Number of secondary beams
n_{span}	Number of spans
n_{SR}	Number of stress ribbons
s_{k}	Characteristic snow load on ground
t	Steel thickness
w	Deflection
w_{max}	Maximum deflection
q	Distributed load
$q_{\mathrm{d,bt}}$	Design line load in ULS on boundary truss
$q_{\mathrm{d,it}}$	Design line load in ULS on intermediate truss

$q_{\mathrm{d,max}}$	Maximum surface load in ULS
z	Cable shape function

Greek lower case letters

β_{n}	Equivalent design charring speed
γ_{d}	Safety factor
γ_{G}	Partial coefficient for permanent load
γ_{M}	Partial factor for material property
γ_{M2}	Partial factor for steel in tension
$\gamma_{\mathrm{M,fi}}$	Partial factor for material property during fire
$\gamma_{\mathrm{Q,1}}$	Partial coefficient for main variable load
ε	Strain
η_{fi}	Reduction factor
μ	Shape factor for snow
ξ	Reduction factor for unfavourable permanent load
$\rho_{\mathrm{g,mean}}$	Mean glulam density
$\rho_{\mathrm{Q,mean}}$	Mean Kerto-Q density
σ_{m}	Bending stress
$\sigma_{\mathrm{m,y,d}}$	Design bending stress
σ_{t}	Tensile stress
$\sigma_{\mathrm{t,0,d}}$	Design normal stress parallel to fibres
ϕ_{rb}	Reinforcement bar diameter
ψ_0	Factor for combination value of variable action
ψ_1	Factor for frequent value of variable action
ψ_2	Factor for quasi-permanent value of variable action
ψ_{fi}	Factor for frequent value of variable action during fire

Abbreviations

CEN	European Committee for Standardization
CLT	Cross-Laminated Timber
CS	Cross-Section
EWP	Engineered Wood Product
Glulam	Glued laminated timber
LCA	Life Cycle Assessment
LVL	Laminated Veneer Lumber
SLS	Service Limit State
SR	Stress Ribbon
ULS	Ultimate Limit State

1 Introduction

1.1 Background

Ecological sustainability is a very timely subject, which is discussed and sought for in a wide variety of contexts. In construction, one factor that affects the environmental impact is the choice of construction material; timber is often considered a sustainable material compared to other conventional building materials, such as steel and concrete. From an ecological point of view, replacing these less environmental friendly materials with timber can therefore be seen as beneficial.

With this in mind the furniture company IKEA has initiated an inquiry of the possibility to use structural timber as parts of their future department stores, and thus replace the steel structures most commonly used in their present buildings. Today the IKEA department stores contain a lot of steel in their roof structures, both truss beams and metal sheeting. To instead introduce a timber roof structure could therefore imply a significant environmental benefit.

Apart from the environmental aspect timber has a significant advantage compared to steel when it comes to fire safety. As steel is exposed to high temperatures it loses its strength and thus its load-bearing capacity, which makes the material very vulnerable during fire. This problem is usually solved by covering the steel, often by fire proof painting or other type of coating, which can be very expensive. Timber on the other hand does not lose its strength significantly when exposed to high temperatures, but is only affected by the flames themselves. The core of a timber cross-section which is not directly exposed to the flames will therefore maintain its load-bearing capacity during fire, and cover is thus not essential. However, it should be noted that when designing a timber member with regard to fire one has to account for the reduction of cross-sectional size as material at the surface is charred. Due to recently tightened fire regulations in Sweden, there is an increased demand on the load-carrying capacity of a structure in case of fire. For a steel structure, this implies an increased cost and amount of work, since cover is required. The beneficial property of timber during fire is therefore another argument for using the material in load-bearing constructions.

An important function of a department store is to enable the tenant to dispose of an open and flexible floor plan, with possibility for alterations. One of the main constraints for the roof structure is therefore a long span length with few supports.

Together with producers and representatives of the timber industry IKEA Fastigheter (IKEA's property department) has conducted some workshops on the subject, with help from Professor Roberto Crocetti at Lund University[1]. During these workshops a few interesting ideas on innovative timber roof structures have been generated. There is one solution of particular interest, where the timber is used primarily in tension in a so-called Stress Ribbon System.

At this stage the proposals are literally only sketches on a piece of paper. There is therefore a need for further investigation of the ideas, their possibilities and consequences and to refine them into something more concrete.

[1] Marcus Hedman, IKEA Fastigheter AB, and Roberto Crocetti, Lund University, meeting in Helsingborg, Sweden (2016-02-02).

1.2 Aim

The main aim of this thesis is to investigate the concept of Stress Ribbon Systems, and to assess its applicability as load-bearing roof structures of large department store buildings. The characteristics of the system are identified, and possible design proposals are generated and evaluated by comparison to more conventional structural systems.

The aim of the thesis can be summarized into the following questions:

- What is a Stress Ribbon System?
- What is an appropriate structural design of a Stress Ribbon System intended for long-span timber roofs?
- What benefits can be gained by implementing the concept in large roof structures, compared to more conventional systems? What are the consequences?
- What critical issues does the concept involve with regard to structural performance, delivery and assembly? How can these issues be solved?

In addition to the aim of the thesis, the main aim of the studied systems is to decrease the amount of steel in the roof structure and to achieve structural efficiency in comparison to conventional systems.

1.3 Limitations

The study will focus on investigating load-carrying systems with regard to structural performance. Environmental benefits are only discussed briefly and in general terms. Economical aspects are kept in mind throughout the process in order to keep the work realistic, but will not be studied explicitly.

The main load-carrying members of the roof structure are of primary interest in this thesis. Other parts of the structural system, such as foundations and intermediate floor structures, are therefore not covered.

As the main goal for the project is to develop, present and assess an innovative system in more general terms, in-depth studies of detailing and connections are considered secondary and are thus only treated briefly.

The building is assumed to be placed in Stockholm, Sweden, and characteristic climate data is determined accordingly. All calculations with regard to structural design are based on the Eurocodes with consideration to the Swedish annex presented by Boverket (2015). The design is primarily performed in the Ultimate Limit State, and design in the Service Limit State is therefore not treated. Furthermore, no studies with regard to the dynamic properties of the roof structure are performed.

1.4 Method

The work of this thesis is divided into four major phases – Theory Phase, Design Phase, Evaluation Phase and Detailing Phase.

The thesis work is initiated by the Theory Phase, which comprises a literature study. First the general properties and use of timber is addressed briefly, in order to get an overview of the material and to understand the mechanical properties and environmental benefits of using timber. This is followed by a study of references related to the subject of the thesis; projects where Stress Ribbon Systems have been used will be studied, in order to define the characteristics of the concept and to identify different possible applications. Furthermore, the Theory Phase will cover some theoretical background of analytical structural analysis of the system. This is performed in order to establish analytical expression for use in the design.

After acquiring the required knowledge on the subject, the Design Phase is initiated. The aim of this phase is to establish a number of possible design proposals, and to acquire estimations of reasonable geometrical properties, such as span length and cross-section dimensions of main members. This is achieved by analysing a number of geometrically different cases by use of theoretical expressions previously derived. For the different cases external and internal forces are estimated and preliminary sizing is performed.

In the Evaluation Phase the established Stress Ribbon Systems are evaluated and compared to more conventional structural systems. The evaluation is focused on structural efficiency, which is addressed in terms of overall material consumption.

The final stage of the project is the Detailing Phase. Here a few principal connection details are developed in order to exemplify how such issues can be solved.

Finally the results of the thesis are evaluated and reviewed. General conclusions are drawn and a discussion of topics for further studies on the subject is presented.

2 Timber as Construction Material

In this chapter the general mechanical properties of timber are presented, complemented by a brief discussion on the environmental benefits of using timber.

2.1 Mechanical properties

Wood is an organic material mainly built up by cellulose fibres and lignin. The fibres are to a large extent oriented in one main direction, giving the material one of its major characteristics; anisotropy. The word anisotropy simply means that a physical property is different in different directions ("Anisotropi", n.d.). In timber the anisotropic structure results in a significant variation of strength and stiffness properties in different directions.

Loaded perpendicular to the grains wood is very weak, especially in tension (Crocetti et al., 2011), and such loading conditions should if possible be avoided. Parallel to the fibres, on the other hand, the material is very strong; according to Johansson, Samuelsson & Engström (2000) the tensile strength of wood fibres in relation to its weight is even comparable to steel. Of course, this statement disregards the negative influence of defects in timber, but does still imply that the material can be highly capable as construction material when utilised properly. Before steel was introduced in a constructional context, timber was actually unique as the only easily available material being able to resist tensile forces (c.f. stone and masonry) (Johansson et al., 2000).

As timber is a natural material it contains aberrations, such as knots, which affect its properties. Also moisture content, member size and load duration are factors that influence the strength and stiffness of timber. When designing timber structures all of these factors therefore have to be accounted for. Temperature is another factor affecting the structural properties of timber; with increased temperature the strength and stiffness decreases. However, in ordinary design situations the effect is relatively small, and temperature differences are therefore seldom taken into account in design codes (Crocetti et al., 2011).

2.2 Engineered wood products

As sawn timber is limited in dimensions and shape, various wood products fabricated from smaller timber members have been invented. These are referred to as Engineered Wood Products (EWPs). EWPs come in many different shapes, with different properties and suitable for different purposes. Two EWPs commonly used as beams are glulam and Laminated Veneer Lumber (LVL), as illustrated in Figure 2.1. With regard to the subject of this thesis the focus will here be on such EWPs, and these products are therefore explained more in detail in the following sections.

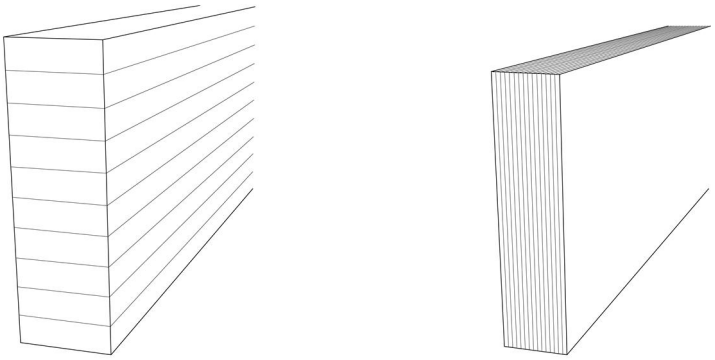

a) b)

Figure 2.1 Examples of EWPs, a) Glulam, b) LVL.

2.2.1 Glulam

Glulam is the oldest and perhaps the most common type of EWP used as beams. It is built up by sawn timber boards bonded together by adhesives, as implied in Figure 2.1a. All of the timber boards in a beam can be made of same strength timber; the cross-section is then referred to as homogeneous. The beam can also consist of timber boards of different strength; the cross-section is then referred to as combined. The homogeneous cross-section is suitable when the member is primarily subjected to a homogeneous stress distribution, i.e. tension or compression. The combined cross-section, on the other hand, is suitable when the member is used primarily in bending, as high strength material is used in the higher stresses regions, while lower strength timber can be used in lower stressed parts of the cross-section.

Since the number of boards glued together is unlimited glulam can be produced with a larger cross-section height than sawn timber. The width on the other hand, is usually restricted due to the natural restriction of the width of timber boards. In certain cases however, multiple members can be glued together side-by-side to form wider cross-sections. Swedish standard cross-section sizes according to Carling (2001) are presented in Appendix A. The length of glulam members is often extended by finger jointing several boards. Apart from the beneficial dimensional properties, glulam has other advantages compared to plain timber, as explained below.

Even though the mean strength is not significantly larger than for sawn timber, the variability in strength between different specimens is lower for glulam. This can be explained by the fact that during production larger defects in the lumber are distributed into smaller, not as critical, defects when the material is sawn and glued together (Crocetti et al., 2011).

Another advantage of glulam is its flexibility. Before the boards are fixed together they have rather low bending stiffness and can therefore be bent, shaping the beam into a curved member. This can be very beneficial, for example as pre-cambering can lower the final deflection of a structure (Crocetti et al., 2011).

2.2.2 LVL

Another typical EWP used in beam elements is laminated veneer lumber (LVL). LVL consists of thin veneers fixed together by adhesives, as implied in Figure 2.1b. In general it has high strength and stiffness properties, and similar to glulam it has lower strength variability than ordinary sawn timber. LVL can be used as beams when placed edge up as seen in Figure 2.1b, but can also be produced in dimensions up to 3 m × 24 m (Crocetti et al., 2011) and thereby be used as high strength sheeting.

Examples of commonly used LVL products are Kerto-S and Kerto-Q produced by Metsä Wood (VTT, 2009). Kerto-S is arranged with the grains of every veneer oriented in the same direction, while Kerto-Q has a few veneers with their grains perpendicular to the main grain direction. The latter configuration gives the product a certain transversal stiffness. Standard sizes of Kerto are presented in Appendix A. In contrast to glulam, LVL is not easily produced with a curvature.

2.3 Environmental benefits

The arguments for the environmental benefits of using timber are numerous. Wood is a renewable material. It requires low amount of energy during production and processing. It can be used in multiple cycles; firstly as timber product, secondly as recycled wood-based panel, and finally for energy production. Timber can be considered a CO_2-neutral material, as the emission of CO_2 at combustion corresponds to the amount bound by the tree when grown (Frühwald, Welling & Scharai-Rad, 2003).

A commonly used approach to evaluate the environmental impact of a structure is Life Cycle Assessment (LCA). LCA is a science in itself and there are a lot of factors to take into consideration, especially when it comes to timber. For example Peñaloza (2015) discusses common assumptions, as well as not so common aspects of timber in LCA and their impact. As this thesis does not focus on environmental aspects, no thorough investigation will be carried out. General conclusions are instead drawn from other investigations.

On behalf of IKEA, the engineering consultant Tyréns has performed an LCA in order to assess the benefits of replacing the steel roof systems used in IKEA department stores today with corresponding timber systems[2]. The systems considered in the study are the existing steel truss system with corrugated steel sheeting, and a system of glulam beams with either steel sheeting or cross-laminated timber (CLT) panels. The investigation is performed both with generic data based on European average values, as presented in Table 2.1, and with specific data provided by the timber suppliers Martinsons and Moelven and steel supplier Skonto Prefab, as presented in and Table 2.2. It should be noticed that the study is limited to only consider material production and does not include the construction, use or maintenance of the building.

[2] Internal report by Tyréns (2015), received by email from Marcus Hedman, IKEA Fastigheter AB (2016-02-02)

Table 2.1 Generic emission data used in internal LCA study[2].

Material	Emission
Glulam	236.0 kg CO_2eq/m^3
Steel beams and sheeting	7.1 kg CO_2eq/kg

Table 2.2 Specific emission data used in internal LCA study[2].

Material	Emission
Glulam, Martinsons	39.0 kg CO_2eq/m^3
Glulam, Moelven	121.0 kg CO_2eq/m^3
Steel beams, Skonto	1.36 kg CO_2eq/kg
Steel sheeting, Skonto	2.75 kg CO_2eq/kg

Without going further into details of the investigation the results are presented in Table 2.3.

Table 2.3 Comparison of CO_2 equivalent[2].

System	Generic data	Specific data	
		Martinsons	Moelven
Steel trusses with steel sheeting	100%	100%	100%
Glulam beams with corrugated steel sheeting	89%	163%	169%
Glulam truss with cross-laminated panels	19%	14%	18%

The results of the study with regard to generic data give an implication of the benefits of using timber; more timber means less emissions. When looking at specific data this is also the case for the consistent timber system. However, specific data on the composite structure show an increase of emissions compared to the consistent steel system.

The problem with this study is that the steel system is based on shorter beam spacing than the timber system. This results in longer spans for the sheeting in the timber system which therefore required thicker sheeting, i.e. more material. By comparing generic and specific data it can be observed that the CO_2 equivalent is significantly lower both for the steel used for truss beams and for timber with specific data. This is due to shorter transports and more use of wind and water power at the specific suppliers mentioned above. The steel sheeting, however, experiences less reduction from the generic to the specific data of the study. As a result of this the steel sheeting becomes the decisive factor in the specific case, and in the study a larger volume of steel sheeting is used in the timber system, as previously explained.

The conclusion to be drawn from this study is that timber per se is more beneficial than steel with regard to CO_2 equivalent. However, careful choices must be made and consequences analysed in order to ensure that environmental benefits are actually gained.

In order to somewhat verify the results of the internal report presented above, other sources are also reviewed. There are a lot of studies performed on LCA of different

materials and building components. One study, performed by Frühwald et al. (2003), is rather similar to the one performed by Tyréns; Frühwald et al. (2003) use LCA to investigate a simple three-storey building constructed either entirely in steel or in a combination of steel and timber, and then compare the results. The results show that by partly replacing steel with timber leads to a decrease of CO_2 equivalent of about 68 % with regard to total energy consumption. As it is not evident from the study what the system looks like or how large amount of steel is actually replaced it is hard to compare the numbers to the study performed by Tyréns. It can however be considered an implication of the correctness of the conclusion that timber in general is more beneficial than steel with regard to CO_2 equivalent.

3 Stress Ribbon Systems

This chapter treats the concept of Stress Ribbon (SR) systems. Its general properties are discussed and some applications are presented.

3.1 Structural efficiency

In order to understand the SR concept and its benefits, it is necessary to first understand the basics of efficient load paths.

The task of transferring vertical loads to adjacent supports in order to bridge a gap is an evident problem in structural engineering. There are however an endless number of solutions, all of them with their different strengths and weaknesses.

The structurally most efficient load paths between two supports can be illustrated by the principal stresses of a simply supported beam (Strasky, 2011). In Figure 3.1 below, the compressive and tensile principal stresses of such a beam, subjected to a uniformly distributed load, can be seen.

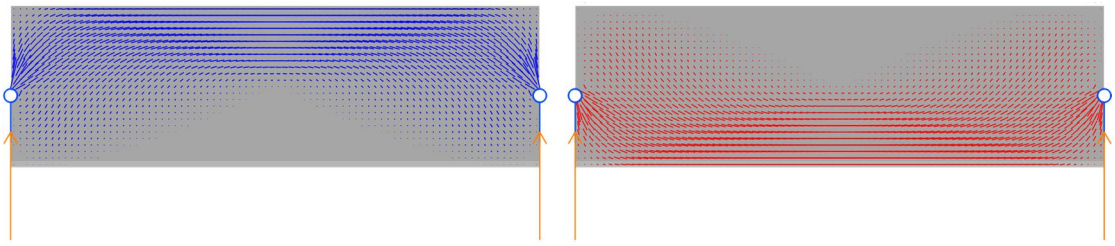

a) b)

Figure 3.1 Principal stresses of a simply supported beam subjected to a uniformly distributed load, a) Compressive stresses, and b) Tensile stresses.

In Figure 3.1 it can be observed that the pattern implies two main load paths; one in compression and one in tension. By so-called topology optimisation the beam can be optimised with regard to material efficiency, i.e. by removal of low-utilised material. By applying this method to the beam in Figure 3.1 the shapes of the two load paths appear even more pronounced, as seen in Figure 3.2.

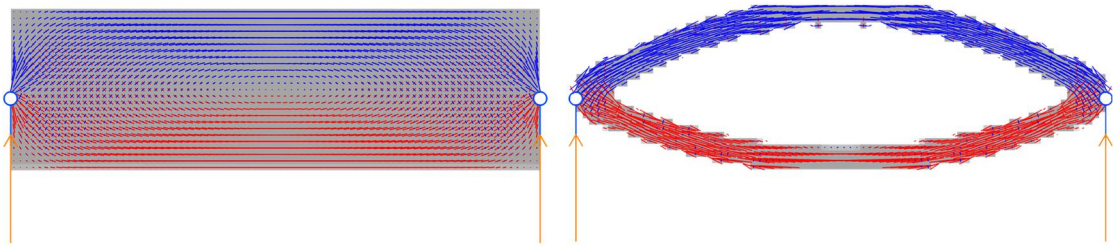

a) b)

Figure 3.2 The same beam as in Figure 3.1, a) unoptimised, b) optimised with regard to structural efficiency. Blue = compression, red = tension.

From this figure the two most efficient shapes can thus be derived; the arch working purely in compression and the suspension cable working purely in tension; the two

structural members are illustrated in Figure 3.3. Structures like these are called funicular structures (Bechthold & Schodek, 2008).

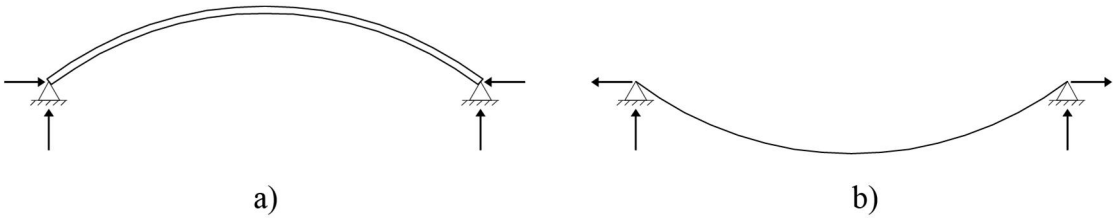

Figure 3.3 Structurally efficient shapes under a uniformly distributed load, a) Compression arch, b) Suspension cable. Notice the horizontal reaction forces.

That members exposed to pure axial force are better utilised than members in bending is no surprising fact. It can easily be illustrated by the distribution of stresses in a cross-section exposed to the two types of load. As seen in Figure 3.4 the normal stress is evenly distributed, allowing full utilisation of the cross-section capacity. The bending stress however, has a linear distribution and the full capacity of the material can thus only be reached at the outermost fibres of the cross-section, whereas the middle of the cross-section is left under-utilised. Note that this only applies for the case of elastic material response.

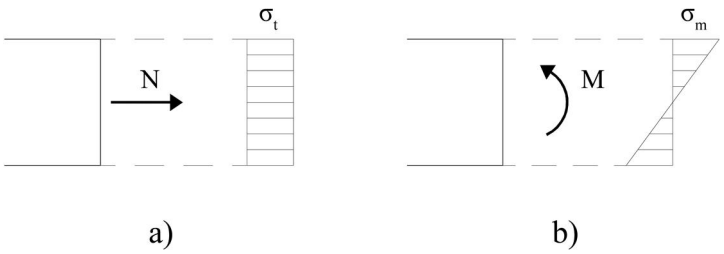

Figure 3.4 Distribution of stresses in a cross-section subjected to a) normal force, b) bending moment.

It should be noticed that the structural efficiency of both the arch and the cable has its price; as seen in Figure 3.3 horizontal reaction forces are introduced at the supports, which must be resisted in order to keep equilibrium in the system. To handle these horizontal forces more sophisticated supports are required, in comparison to a simple beam with only vertical reaction forces.

The arch and the cable can be seen as each other's mirror images, and as a result of this their properties with regard to stability can also be seen as opposites. The arch is geometrically stiff in the sense that for a change of load distribution the arch will only experience minor deformations. As it is in compression it is however susceptible to structural instability, i.e. with an increase of load there is a risk for buckling and thus collapse of the structure. The cable, which works purely in tension, is at no risk of buckling as this is a phenomenon only associated with compressive stresses. On the other hand, the cable has no geometrical stiffness; with a change of load distribution the shape is altered to agree with the new configuration of loads.

With regard to material-to-capacity ratio, it can thus be concluded that the cable is superior to the arch; the arch must be designed with consideration to buckling while

the cable only has to withstand the pure tensile force it is subjected to. The lack of geometrical stiffness in the cable is though an issue, and this problem is further discussed in Section 3.3.

3.2 The Stress Ribbon concept

The SR concept is based on the suspension cable. According to Frei, cited in Ludescher, Braun & Bachmann (2007), it is considered one of the most material efficient systems for long-span structures, which can be explained by the arguments presented in the previous section. What actually defines an SR system is however a bit vague; different sources state slightly different definitions.

Baus & Schlaich (2008) imply that simple ropes tied to either side of a ravine can be considered an SR system, which makes it a simple hanging cable.

Marti (2013) addresses the topics of SR structures and suspended roofs in the same section, but gives no clear definition or distinction between them. By studying calculation examples given in the book one can deduce that SR structures and suspended roofs are similar, but SR structures seem to have less sag and higher bending stiffness than suspended roofs.

Strasky (2011) covers SR bridges built up by tension cables and prestressed concrete decks. He stresses the property of stiffness in an SR system, as he in his definition describes how the concrete deck provides tension stiffness as well as transverse stiffness to the system. Furthermore, the incorporation of prestressing in an SR system is seemingly essential according to Strasky's (2011) definition. Looking at reference projects, the most common structures described as SR systems are also prestressed concrete bridges.

However, in this thesis the interpretation of the SR concept is a suspended structure with the shape of a hanging cable, somehow provided with in-plane stiffness.

Further definition of the concept and its fundamental properties is presented in the following Sections.

3.3 Cable stiffening

With regard to stiffness two different types of structural elements can be defined, rigid and non-rigid ones. A rigid element does not change its shape significantly under a change of load, it has a certain stiffness. A non-rigid element, on the other hand, does change its shape at different loading conditions (Bechthold & Schodek, 2008). This is of course a simplified view on the matter; for example a 'rigid' member will at critical loading lose its stiffness due to plasticity and/or instability and thus turn into a non-rigid member.

A cable is a typical non-rigid structural element. It is very efficient in carrying loads, but has the disadvantage of adapting its shape to the load applied, as illustrated with an example in Figure 3.5. If the magnitude of the point load is increased the influence of the cable self-weight decreases and the shape of the cable will approach two straight segments.

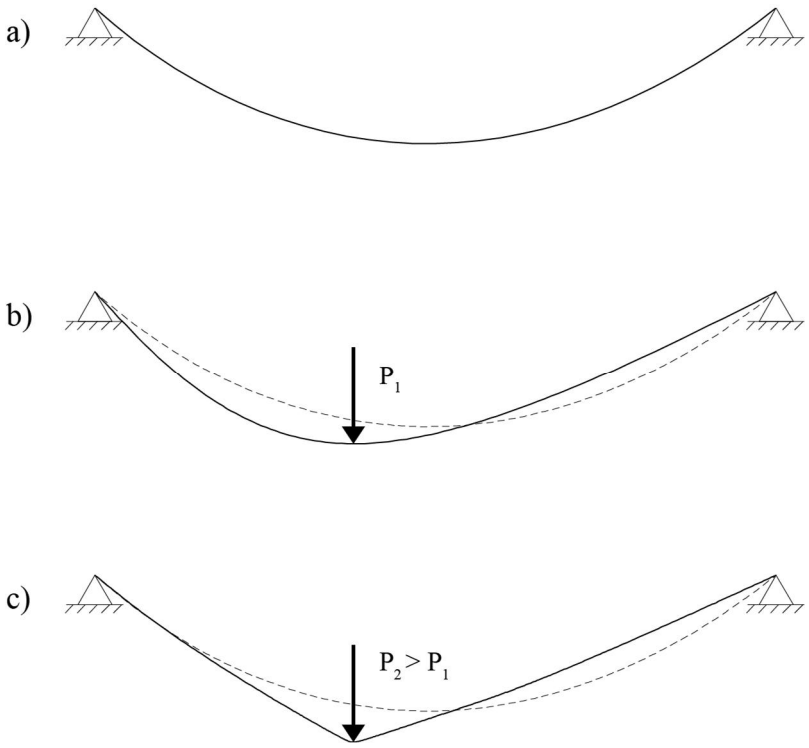

Figure 3.5 Suspension cable subjected to a) self-weight only, b) self-weight and additional point load P_1, c) self-weight and additional point load $P_2 > P_1$.

The lack of stiffness can in many cases be problematic. In bridges uneven loading is a frequently recurring phenomenon, as the imposed load by pedestrians and/or traffic moves across the structure in an irregular pattern. The continuously changing shape can be uncomfortable or even pose a threat to the structural integrity of the structure (e.g. fatigue). For roof structures the non-symmetric loading can for example occur due to uneven snow load or installations on the roof. As roofs are generally not walked on by people the uncomfortableness might not be an issue. Here however, compatibility can be problematic as the roof should somehow be connected to the façades, and connections allowing for large deformations are hard to design. Another problem is that the tightness of wind and moisture barriers in the building envelope is endangered when the structure is exposed to large deformations.

In order to be able to use the cable in structural systems it is therefore necessary to provide it with sufficient stiffness. According to Strasky (2011) there are four general methods to achieve stiffness of a cable; adding extra dead weight, stiffening it by an external system of cables, adding bending stiffness to the cable itself, or by a beam distributing the load on the cable. The four principles are shown in Figure 3.6.

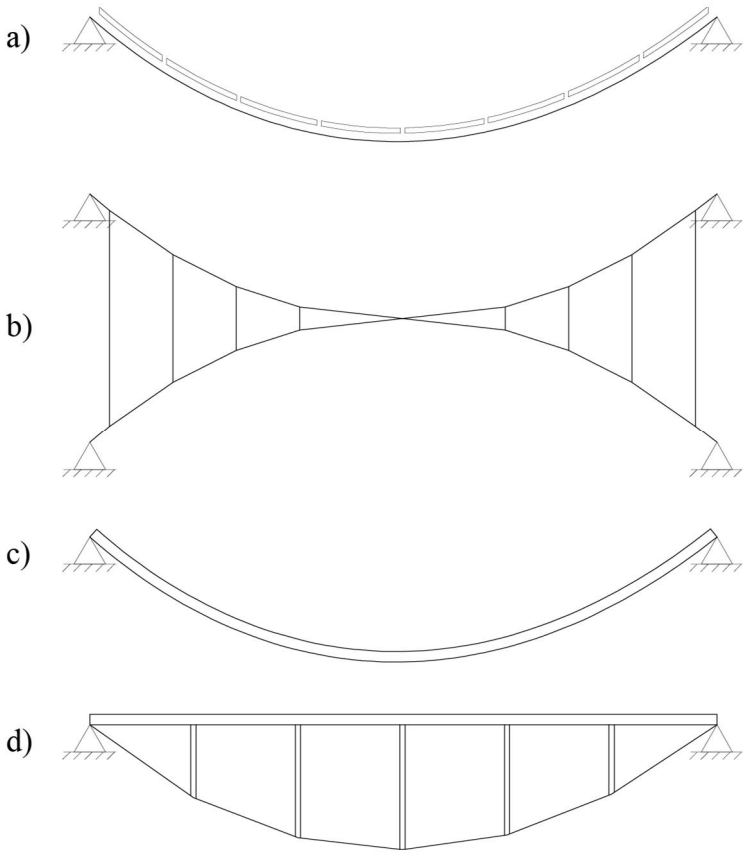

Figure 3.6 Principles for stiffening a cable, a) Extra dead weight, b) External cables, c) Bending stiffness, d) Distributing beam.

In Section 3.5 some reference projects where the different stiffening methods have been used are presented.

3.4 Horizontal forces

As mentioned in Section 3.1 the structurally efficient shape of the hanging cable will produce horizontal forces that must somehow be resisted at the supports (c.f. Figure 3.3). In bridges where the suspended structure is used directly as bridge deck, these horizontal forces are generally resisted by the supports themselves; as the cables meet the ground the horizontal forces can be directly anchored into the bridge foundations. In buildings however, the suspended structure is often elevated from the ground in order to enclose a volume below. For this reason the horizontal forces cannot be directly anchored to the ground, but must be resisted by other means.

Bechthold & Schodek (2008) presents four different principles for resisting horizontal forces in a suspended roof structure. The principles, with internal stresses and reaction forces indicated, are illustrated in Figure 3.7.

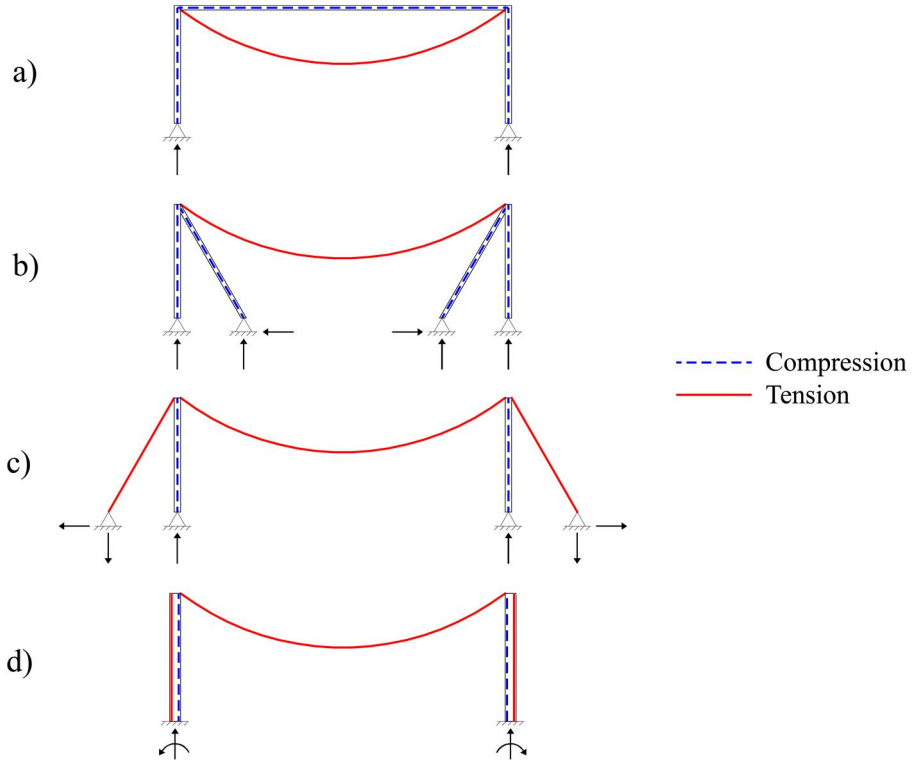

Figure 3.7 *Principles for resisting horizontal forces, a) Compression strut between columns, b) Compression strut from column to ground, c) Tie from column to ground, d) Bending stiff column.*

The first method, see Figure 3.7a, relies on a compression strut between the two columns. Note that this is only a method for resisting the horizontal forces produced by the cable; in addition, overall horizontal stability with regard to e.g. wind loads must be provided. The primary benefits of this solution are that horizontal and rotational reaction forces are prevented in the foundations, and that it requires no extra ground space in- or outside of the structure. The main disadvantage is the long compression member, which is highly susceptible to buckling. In order to prevent buckling the compression strut has to be of large dimensions, and the material efficiency is thereby lost. For this reason it is seldom used, and will not be treated further in this thesis.

In the second method, see Figure 3.7b, the horizontal forces are transferred to the ground through inclined compression struts. The struts are shorter than in the first method and thus not as prone to buckle, i.e. more efficient. This principle though requires foundations which are able to resist not only vertical, but also horizontal forces. Furthermore, the compression struts will claim space inside the structure and possibly be in conflict with activities in the building.

The third method, see Figure 3.7c, can be considered an opposite to the second one. Here the horizontal forces are resisted by a tie connected to the ground, and as it works in tension it is a structurally efficient solution. Similar to the second method the foundations have to resist both vertical and horizontal forces. This alternative also requires additional space, but outside of the structure rather than inside.

For both the second and the third method the force in the inclined supporting member can be adjusted by changing the inclination; as the angle between the strut/tie and the vertical column increases the force in the member decreases.

The last method, see Figure 3.7d, includes no additional members to handle the horizontal forces, but instead relies on bending stiffness of the columns themselves. A benefit of this principle is that, as in the first method, it claims no extra space. However, to carry loads in bending is structurally inefficient, and there is a risk for very bulky columns. Moreover, the foundation design becomes rather complicated as rotational stiffness must be achieved.

3.5 Reference projects

Below follows a number of reference projects illustrating some applications of the Stress Ribbon concept. The main focus is on timber structures, but also steel and concrete projects are presented in order to address the different methods for achieving stiffness and resisting horizontal forces.

3.5.1 Essing Timber Bridge, Germany

The Essing Timber Bridge, as seen in Figure 3.8, crosses the Rhein-Main-Donau Canal in Essing, Germany. It was designed by architect Richard J. Dietrich and structural engineer Heinz Brüninghoff, and was taken into service in 1992 (Brüninghoff, 1993).

Figure 3.8 Overview of Essing Timber Bridge [1].

The bridge is designed as a continuous SR structure in four spans, of which the longest is 73 m long. The main load-carrying members are nine glulam beams of dimensions 220 mm × 650 mm, arranged as seen in Figure 3.9.

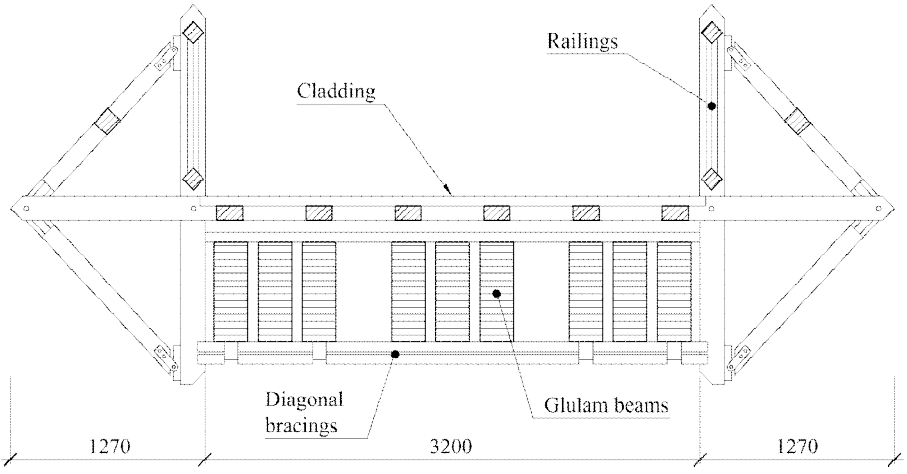

Figure 3.9 Bridge cross-section.

The glulam beams are curved to give the bridge the characteristic sag of an SR structure. The shape is derived from the criterion that the maximum normal force should be approximately the same in each span under a uniformly distributed load. The height-width ratio of the beam cross-section is rather low which is favourable when bending moments are to be minimised in favour of tensile forces. Consequently, approximately 90 % of the vertical load on the bridge is resisted by tensile forces, while 10 % is resisted in bending (Brüninghoff, 1993). The glulam beams were produced in lengths of 40-45 m and connected on site by finger joints.

Geometrical in-plane stiffness of the structure is provided by the bending stiffness of the glulam beams, in accordance with the principle presented in Figure 3.6c. In order to achieve sufficient lateral stiffness the bridge is provided with a system of diagonal bracing members underneath the bridge deck, as seen in Figure 3.10.

Figure 3.10 The bridge from below. The diagonal members provide the structure with lateral stiffness [2].

The intermediate supports are designed as glulam trusses with a force pattern according to Figure 3.11. At the bridge landings on either side the nine glulam beams are anchored into concrete abutments which transfer both the horizontal and the vertical forces into the ground.

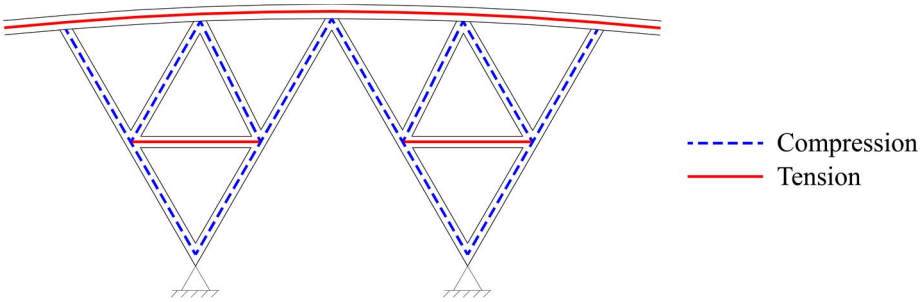

Figure 3.11 Force pattern of intermediate truss supports.

The Essing Timber Bridge was in some sense a pioneer among tensile timber structures of such large size. It is therefore a good example of what can be achieved with timber, and shows that critical issues such as connections and splices can be solved in a satisfying manner. It also evinces that prestressing is not essential for the structural stability of an SR structure, as the bridge is only stabilized by the integrated bending stiffness of the timber ribbons.

3.5.2 Nagano Olympic Memorial Arena

The Nagano Olympic Memorial Arena, situated in Nagano, Japan, was constructed in 1996 and was host for the speed skating competitions in the Olympic Games in 1998.

It was designed by a joint venture of the companies Kajima, Kume, Okumura, Nissan, Iijima and Takagi.

The building, which can be seen in Figure 3.12, consists of 15 suspended roof sections, each with a width of 18 m, span length of 80 m and 5 m sag (Ban, Yoshida & Motohashi, 1998).

Figure 3.12 Nagano Olympic Memorial Arena [3].

The main load-carrying structure of the roof consists of a combination of steel plates and glulam beams, distributed along the roof with a spacing of 600 mm. As seen in Figure 3.13 each composite member consists of two glulam beams of dimensions 300 mm × 125 mm, with a steel plate of dimensions 200 mm × 12 mm in between. The composite beams are connected to each other and stabilised by intermediate steel tie plates and plywood sheeting (Ban et al., 1998).

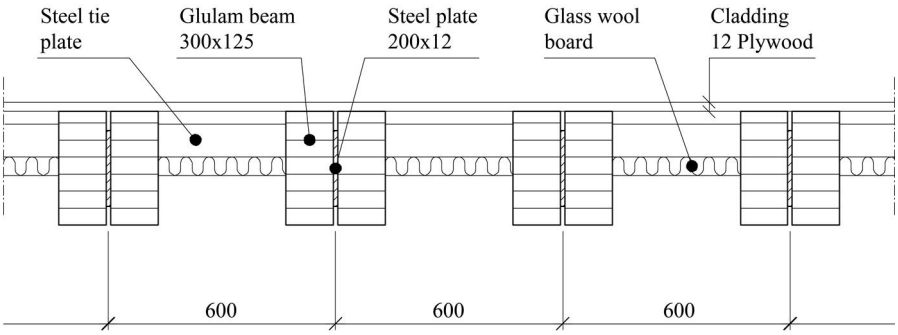

Figure 3.13 Cross-section of the roof structure.

The forces in the roof are transmitted to the ground via inclined walls with a force pattern corresponding to the principle presented in Figure 3.7c. The walls consist of an upper part, made of steel posts, and a lower part made of prestressed concrete. The prestressing rods in the lower part of the walls are anchored into large concrete foundations which work as counter-weights to the horizontal forces produced by the roof shape (Ban et al., 1998).

The assembly is one of the major challenges of a building with such large flexible members. The stability of the ribbons is dependent on the introduction of axial tension, and handling the members before stressed is therefore a difficult matter. During construction lift-up units of six composite members were assembled, and temporarily connected to vertical lift-up towers at the ends. The lift-up units were then one by one slowly lifted into position, and as the members left ground the necessary tension was introduced. When in place, the lift-up units were pin-connected to the supporting steel columns. The lift-up towers were placed on rails, which enabled them to be moved along the structure as the construction progressed (Ban et al., 1998).

The Nagano Olympic Memorial Arena is another good example of how timber can be used in long-span tensile structures. Furthermore, the project shows an interesting construction method, which could be adopted also for the structures addressed in this thesis.

3.5.3 Stuttgart Trade Fair Exhibition Halls, Germany

The New Stuttgart Trade Fair was designed by architect Wulf & Associates and structural engineer Mayr + Ludescher Ingenieure, and was finalised in 2007. It comprises seven Standard Exhibition Halls á 10,000 m^2 and one Grand Exhibition Hall of 25,000 m^2 (Ludescher, Braun & Bachmann, 2007). One of the standard exhibition halls is illustrated in Figure 3.14.

The roof structure of each of the smaller exhibition hall consists of a steel SR system in one span, with a span length of 56.5 m. The larger hall has a free span of 126.8 m, which is built up by an SR system in two spans, in the middle supported by a large steel truss.

Figure 3.14 One of the Standard Exhibition Halls [4].

The main load bearing members, i.e. the ribbons, are pinned to their supports and distributed along the roof with a spacing of 6.75 m. The cross-section is a double-T shape, as seen in Figure 3.15, made of high performance steel. The cross-section shape provides the system with bending stiffness, and thus stabilises the structure according to the principle shown in Figure 3.6c. This is however not the only measure taken in order to stabilise the structure; as seen in Figure 3.15 the ribbons are prestressed by a system of cables forming a cable truss, similar to the principle

presented in Figure 3.6b. Furthermore, the structure is loaded with additional self-weight from roof landscaping, which contributes to the geometrical stiffness in accordance with the principle presented in Figure 3.6a. Thus three of the four principles for stiffening a cable presented in Section 3.3 are combined in order to achieve sufficient stiffness of the roof structure.

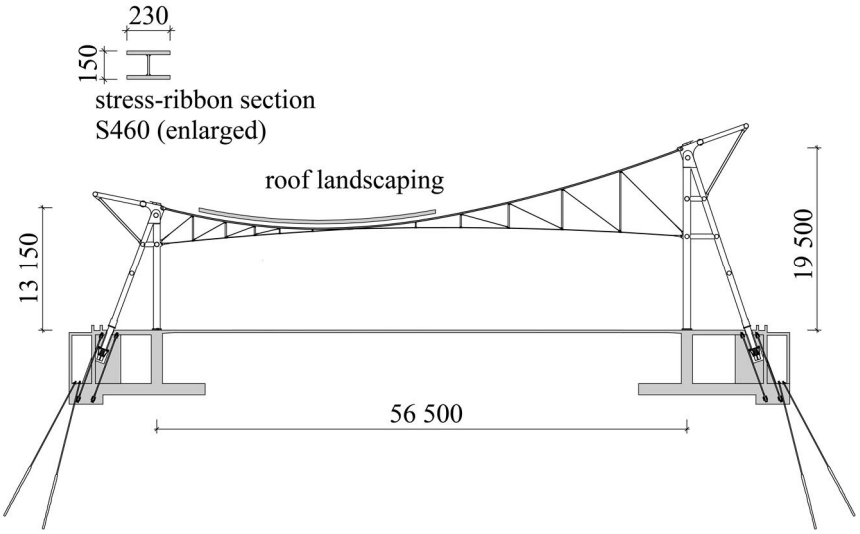

Figure 3.15 Cross-section of the Standard Hall [5].

The roof structure is on each side supported by a number of A-shaped trestles, as indicated in Figure 3.15. The force pattern in the supporting structures follows the principle shown in Figure 3.7c. As the supporting trestles are not as closely spaced as the tensile ribbons, longitudinal boundary trusses with an inclination tangential to the ribbon shape distributes the forces from the ribbons to the supports. The boundary trusses are situated outside of the building envelope, as seen in Figure 3.14.

The forces in the trestles are transferred to the ground via longitudinal concrete foundations connected to the ground by prestressed soil anchors in order to resist the tensile forces in the inclined ties. The foundation structure also forms channels used for building service installations (Ludescher et al., 2007).

The ribbons were fabricated with an initial curvature according to the catenary shape, based on the support spacing and maximum cable sag. The ribbons were delivered on sight in three parts each and assembled by welding. During erection the ribbons were temporarily loaded, as seen in Figure 3.16. This was done in order to compensate for the additional self-weight not yet applied and thus achieve the shape of the final structure (Ludescher et al., 2007).

Figure 3.16 Preloading of the ribbons in the Grand Exhibition Hall [6].

Though not a timber structure, the thin roof of the Stuttgart Trade Fair Exhibition Halls is a good example of the structural efficiency of the SR concept. The project also highlights some of the main difficulties of the concept, as well as possible solutions; it shows how the stability problem can be handled by a combination of different stiffening methods, and also demonstrates an effective way of resisting the horizontal load produced by the ribbons.

3.5.4 Washington Dulles International Airport

The previous reference buildings both adopt the method for resisting horizontal forces illustrated in Figure 3.7c, i.e. the back-stay cable alternative. In order to demonstrate that also other methods have been used, the Washington Dulles International Airport is here briefly presented. The building was designed by architect Eero Saarinen and engineers Ammann and Whitney, and was constructed in 1962. As seen in Figure 3.17, the building comprises a thin prestressed concrete roof spanning 49 m, supported on concrete columns. The columns are inclined in order to counteract the horizontal forces produced by the roof, and are thus working both in bending and compression. The method for resisting the horizontal forces can thus be seen as a combination of the principles presented in Figure 3.7b and d.

Figure 3.17 Washington Dulles International Airport [7].

4 Analytical Expressions

The analysis and design of the SR systems in this thesis is performed using analytical expressions based on the hanging cable. This chapter is dedicated to present and derive these expressions.

4.1 Cable equations

As explained before, the SR concept is based on the shape of a hanging cable. In order to analyse such structures it is therefore essential to first establish the fundamental equations of the hanging cable. Below follows the derivation of these equations, as explained by Marti (2013) and Samuelsson & Wiberg (1980).

Figure 4.1a shows a cable suspended between two supports, subjected to an arbitrary distributed load. In Figure 4.1b a small segment of the same cable is illustrated with corresponding internal forces. The cable is assumed to have a constant axial stiffness and no bending stiffness.

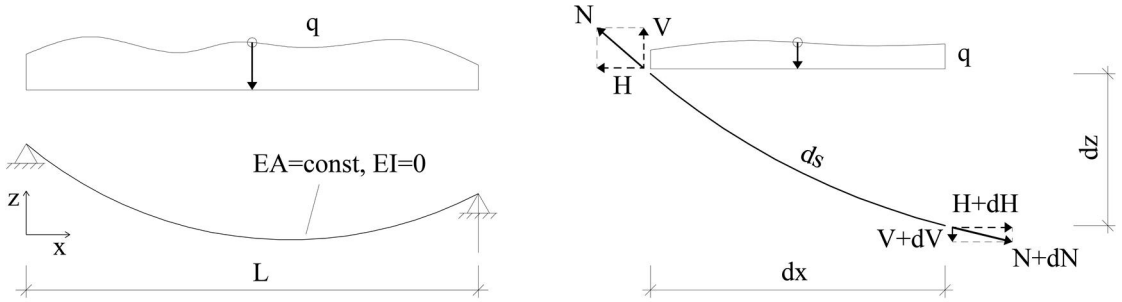

a) b)

Figure 4.1 a) Cable suspended between two supports, subjected to a distributed vertical load. b) Small cable segment.

For the small cable segment the shape can be approximated to be a straight line. The arc length ds can then be expressed by the Pythagorean Theorem as

$$ds = \sqrt{dx^2 + dz^2} = dx\sqrt{1 + z'^2} \tag{4.1}$$

where

$$z' = \frac{dz}{dx}$$

From Figure 4.1b the horizontal equilibrium condition can be established as

$$H + dH - H = 0 \;\rightarrow\; dH = 0;\; H = \text{constant} \tag{4.2}$$

Moment equilibrium around the right end of the cable segment gives

$$H \cdot dz - V \cdot dx = 0 \;\rightarrow\; z' = \frac{V}{H} \tag{4.3}$$

Note that the term related to the external load q is excluded in Equation (4.3). The reason for this is that the term contains the factor dx^2. As $dx \to 0, dx^2 \ll dx$, which makes it negligible.

The vertical equilibrium is then established and rewritten by use of Equation (4.3) according to

$$q \cdot dx + dV = 0 \;\; \rightarrow \;\; z'' = -\frac{q}{H} \tag{4.4}$$

where

$$z'' = \frac{d^2 z}{dx^2}$$

By use of the Pythagorean Theorem and Equation (4.3) the normal force in the cable can be expressed according to

$$N = \sqrt{H^2 + V^2} = H\sqrt{1 + z'^2} \tag{4.5}$$

The length of the cable L_0, assuming infinite axial stiffness, can be expressed by

$$L_0 = \lim_{ds \to 0} \sum ds = \lim_{dx \to 0} \sum \sqrt{dx^2 + dz^2} = \lim_{dx \to 0} \sum dx \sqrt{1 + \left(\frac{dz}{dx}\right)^2} \tag{4.6}$$

Rewriting Equation (4.6) on integral form gives

$$L_0 = \int_0^L \sqrt{1 + z'^2}\, dx \tag{4.7}$$

L Span length [m]

However, for an elastic material the material strain will affect the cable length. If an accurate length is demanded, the assumption of infinite axial stiffness is thus inapplicable. The axial strain can be considered by transforming Equation (4.6) according to

$$L_0 = \lim_{ds \to 0} \sum \frac{ds}{1 + \varepsilon} \approx \lim_{ds \to 0} \sum ds(1 - \varepsilon) = \lim_{ds \to 0} \sum ds \left(1 - \frac{N}{EA}\right) \tag{4.8}$$

ε Elastic strain [-]

N Normal force in cable [N]

E Modulus of elasticity [Pa]

A Cross-section area [m^2]

With ds and N according to Equation (4.1) and (4.5) respectively, Equation (4.8) can be written as

$$L_0 = \int_0^L \sqrt{1+z'^2}\left(1 - \frac{H}{EA}\sqrt{1+z'^2}\right)dx \tag{4.9}$$

The equations above enable analysis of the fundamental properties of a hanging cable.

4.1.1 Special case

As a special case a cable suspended between two horizontal supports, subjected to a uniformly distributed load q, is considered. Integrating Equation (4.4) twice yields

$$z' = -\frac{q}{H}\,x + C_1 \tag{4.10}$$

$$z = -\frac{q}{2H}\,x^2 + C_1 x + C_2 \tag{4.11}$$

Boundary conditions give the constants C_1 and C_2 as

$$z(0) = 0 \;\rightarrow\; C_2 = 0$$

$$z(L) = 0 \;\rightarrow\; C_1 = \frac{qL}{2H}$$

Due to the uniform load q, the maximum sag f will occur in the middle of the span. Thus, an expression for the horizontal force H can be derived according to

$$f = z\left(\frac{L}{2}\right) = -\frac{q}{2H}\left(\frac{L}{2}\right)^2 + \frac{qL}{2H}\frac{L}{2} \;\rightarrow\; H = \frac{qL^2}{8f} \tag{4.12}$$

It can be observed that the horizontal force increases for an increased span length, but decreases for an increased sag, according to the graphs shown in Figure 4.2.

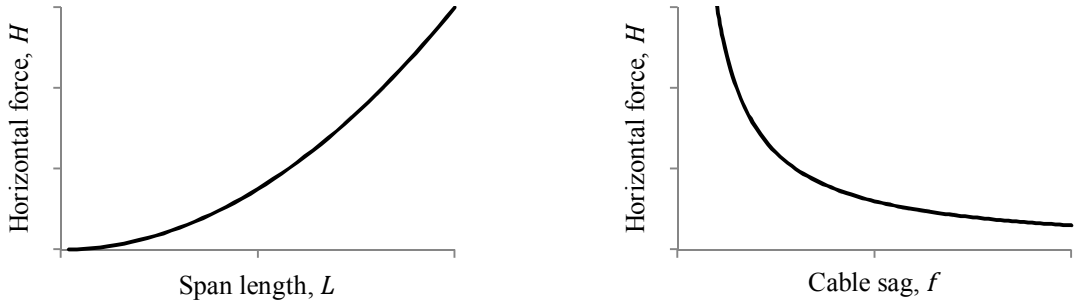

Figure 4.2 The horizontal force H as a function of a) span length L, and b) cable sag f.

Small cable sag f thus results in large horizontal forces, and an entirely straight cable, i.e. $f = 0$, would require an infinite horizontal force.

By inserting Equation (4.12) and boundary conditions into Equation (4.11), the cable shape function can be written as

$$z = -\frac{4f}{L^2}x^2 + \frac{4f}{L}x \tag{4.13}$$

And its first two derivatives are

$$z' = -\frac{8f}{L^2}x + \frac{4f}{L} \tag{4.14}$$

$$z'' = -\frac{8f}{L^2} \tag{4.15}$$

Assuming that e.g. the maximum allowed sag is known the fundamental properties of the cable can be calculated; the shape is given by Equation (4.13), horizontal reaction force by Equation (4.12) and the normal force in the cable can be calculated from Equation (4.5). Furthermore, assuming inextensible cable and inserting Equation (4.10) into (4.7), gives the cable length as

$$L_0 = \int_0^L \sqrt{1 + \left(-\frac{8f}{L^2}x + \frac{4f}{L}\right)^2} = \frac{1}{2}\sqrt{16f^2 + L^2} + \frac{L^2 \sinh^{-1}\left(\frac{4f}{L}\right)}{8f} \tag{4.16}$$

It can be noticed that a cable subjected to a uniformly distributed load has the shape of a quadratic parabola, c.f. Equation (4.13). If instead studying a cable subjected to its self-weight the shape will change from parabolic to catenary. This is due to the fact that the self-weight is not evenly distributed along the horizontal length of the span L, but rather evenly distributed along the length of the cable L_0. However, the deviation from the parabolic shape is negligible if the sag is small, and assuming a parabolic shape under self-weight is therefore considered reasonable. Marti (2013) shows this by studying the horizontal reaction forces of a parabolic curve and a catenary. The horizontal force in the parabola for a sag-to-span ratio of 1/8 is calculated and used as input to calculate the corresponding cable sag of a catenary. The result shows that the sag for the catenary is only about 2 % higher. Furthermore, Goldack, Schlaich & Meiselbach (2016) states that if assuming a parabolic shape for the self-weight a satisfactory accuracy is kept for a sag-to-span ratio of $f/L \leq 0.1$.

4.2 Combined cable and beam action

In many cases a load-carrying system works not only in pure tension but also has a certain amount of bending stiffness. An SR stiffened according to the principle shown in Figure 3.6c is a typical example of this. In order to assess such systems analytically it is therefore necessary to find expressions for the combination of the two different modes. According to Marti (2013) this can be performed as explained below.

From beam theory the following expression for a beam in pure bending can be recalled:

$$q = EIw'''' \tag{4.17}$$

q Distributed load [N/m]

E Modulus of elasticity [Pa]

I Moment of inertia [m^4]

w Deflection [m]

Combining Equation (4.17) with Equation (4.4) gives

$$EIw'''' - (H + \Delta H)(z + w)'' = g + q \tag{4.18}$$

g Permanent load [N/m]

q Variable load [N/m]

H Horizontal tension due to permanent load g [N]

ΔH Horizontal tension due to variable load q [N]

It is reasonable to assume that the system is designed in such way that the permanent load is resisted by pure cable-like behaviour. This implies that Equation (4.4) alone applies for the self-weight, and Equation (4.18) can thus be rewritten as

$$EIw'''' - (H + \Delta H)w'' = q - g\frac{\Delta H}{H} \tag{4.19}$$

The general solution to this differential equation is

$$w = C_1 + C_2 x + C_3 \cosh(\lambda x) + C_4 \sinh(\lambda x) + w_p \tag{4.20}$$

where

$$\lambda^2 = \frac{H + \Delta H}{EI}$$

Since cable-like behaviour is assumed for the permanent load, the horizontal force H related to the self-weight can be expressed according to Equation (4.12). The additional horizontal force ΔH can according to Marti (2013) be derived from the expression

$$\int_0^L w'z'dx = \frac{\Delta HL}{EA} \tag{4.21}$$

Integration by parts of the left hand side of Equation (4.21) gives

$$\int_0^L w'z'dx = wz'\Big|_0^L - \int_0^L wz''dx \tag{4.22}$$

Insertion of Equation (4.22) and boundary conditions $w(0) = w(L) = 0$ into Equation (4.21), and assuming z'' according to Equation (4.15) gives the following expression for ΔH:

$$\Delta H = \frac{8f}{L^2}\int_0^L w\,dx \tag{4.23}$$

It can be noticed that the assumption of z'' is derived from a case assuming a uniformly distributed load, i.e. a parabolic cable shape. As mentioned in Section 4.1.1, this is a reasonable simplification of the shape, even for a cable loaded only by its self-weight.

Equations (4.20) and (4.23) can be used to calculate the deflection and the horizontal component of the variable load. From the horizontal force the normal force in the SR can be calculated according to Equation (4.5). The bending moment M in the member can according to beam theory be calculated as

$$M = -EIw'' \tag{4.24}$$

4.2.1 Special case

The expressions presented above are derived for the general case, but it will now be studied what these expressions look like for a specific case. As in Section 4.1.1, the example of a cable suspended between two horizontal supports, subjected to a uniformly distributed load is considered, only this time the cable is provided with an additional bending stiffness EI.

Defining the horizontal coordinate x from the middle of the span, gives the boundary and continuity conditions $w'(0) = w'''(0) = w(L/2) = w''(l/2) = 0$. According to Marti (2013) Equation (4.20) then becomes

$$w = \frac{q - g\frac{\Delta H}{H}}{2(H + \Delta H)}\left(\frac{L^2}{4} - \frac{2}{\lambda^2} + \frac{2\cosh(\lambda x)}{\lambda^2 \cosh\left(\frac{\lambda L}{2}\right)} - x^2\right) \tag{4.25}$$

Differentiation twice of Equation (4.25) yields

$$w' = \frac{q - g\frac{\Delta H}{H}}{(H + \Delta H)}\left(\operatorname{sech}\left(\frac{\lambda L}{2}\right)\sinh(\lambda x)\frac{1}{\lambda} - x\right) \tag{4.26}$$

$$w'' = \frac{q - g\frac{\Delta H}{H}}{(H + \Delta H)}\left(\operatorname{sech}\left(\frac{\lambda L}{2}\right)\cosh(\lambda x) - 1\right) \tag{4.27}$$

Insertion of (4.27) into Equation (4.24) gives the bending moment M as

$$M = -EI\,\frac{q - g\frac{\Delta H}{H}}{2(H + \Delta H)}\left(2\operatorname{sech}\left(\frac{\lambda L}{2}\right)\cosh(\lambda x) - 2\right) \tag{4.28}$$

The expression for ΔH is given by inserting Equation (4.25) into Equation (4.23) and integrating, which yields

$$\Delta H = \frac{q - g\frac{\Delta H}{H}}{2(H + \Delta H)} 16 f E A \left(\frac{1}{12} - \frac{1}{(\lambda L)^2} + \frac{2\tanh(\lambda L/2)}{(\lambda L)^3} \right) \tag{4.29}$$

Finally the normal force in the ribbon can similar to Equation (4.5) be calculated according to

$$N = (H + \Delta H)\sqrt{1 + (z' + w')^2} \tag{4.30}$$

where H, ΔH, z' and w' are defined according to Equations (4.12), (4.29), (4.14) and (4.26) respectively.

With these equations at hand it is possible to perform a preliminary assessment of a SR structure with integrated bending stiffness with regard to forces and dimensions.

5 Possible design solutions

After studying the SR concept, its properties and references, three promising design proposals for long-span roof structures have been generated. All the proposals aim at utilising timber as much as possible in the main load-carrying structure, and therefore no composite sections are considered. Furthermore, the geometrical stiffness gained from using timber SRs is assumed to be sufficient, and thus no additional stiffening methods are considered.

All the proposals are compatible with all the methods for resisting the horizontal forces (c.f. Figure 3.7). This is therefore not included in the proposals themselves but investigated separately. Furthermore, overall horizontal stability of the building is not considered in this thesis, and members possibly required for this purpose are therefore also excluded from the proposals.

The design proposals are based on a number of geometrical constraints. Below follows a description of these constraints and their background, followed by a presentation of the three proposals.

5.1 Geometrical constraints

In order to limit the number of design variables, and to secure that the design fulfils reasonable user requirements, some geometrical constraints are introduced. These constraints are based on construction drawings of an existing IKEA store, recently erected in Umeå, Sweden.

5.1.1 Reference building: IKEA, Umeå

The IKEA store in Umeå is a building approximately 170 m long and 120 m wide. The structural system consists of primary and secondary steel trusses supported on concrete columns, with cross-section dimensions 400 mm x 400 mm. The columns are arranged in a general grid of 16 m × 24 m, as seen in Figure 5.1. At the building boundaries the column spacing is reduced to 8 m in order to support the façade against wind loads.

The primary trusses span 16 m between the columns, at a spacing of 24 m. The secondary trusses span the distance of 24 m between the primary trusses with a spacing of 5.4 m. The layout of the roof system is also illustrated in Figure 5.1. As seen in the principal cross-section, the total height of the building is 11.6 m. The vertical clearance inside the building is 8.8 m, disregarding intermediate floors.

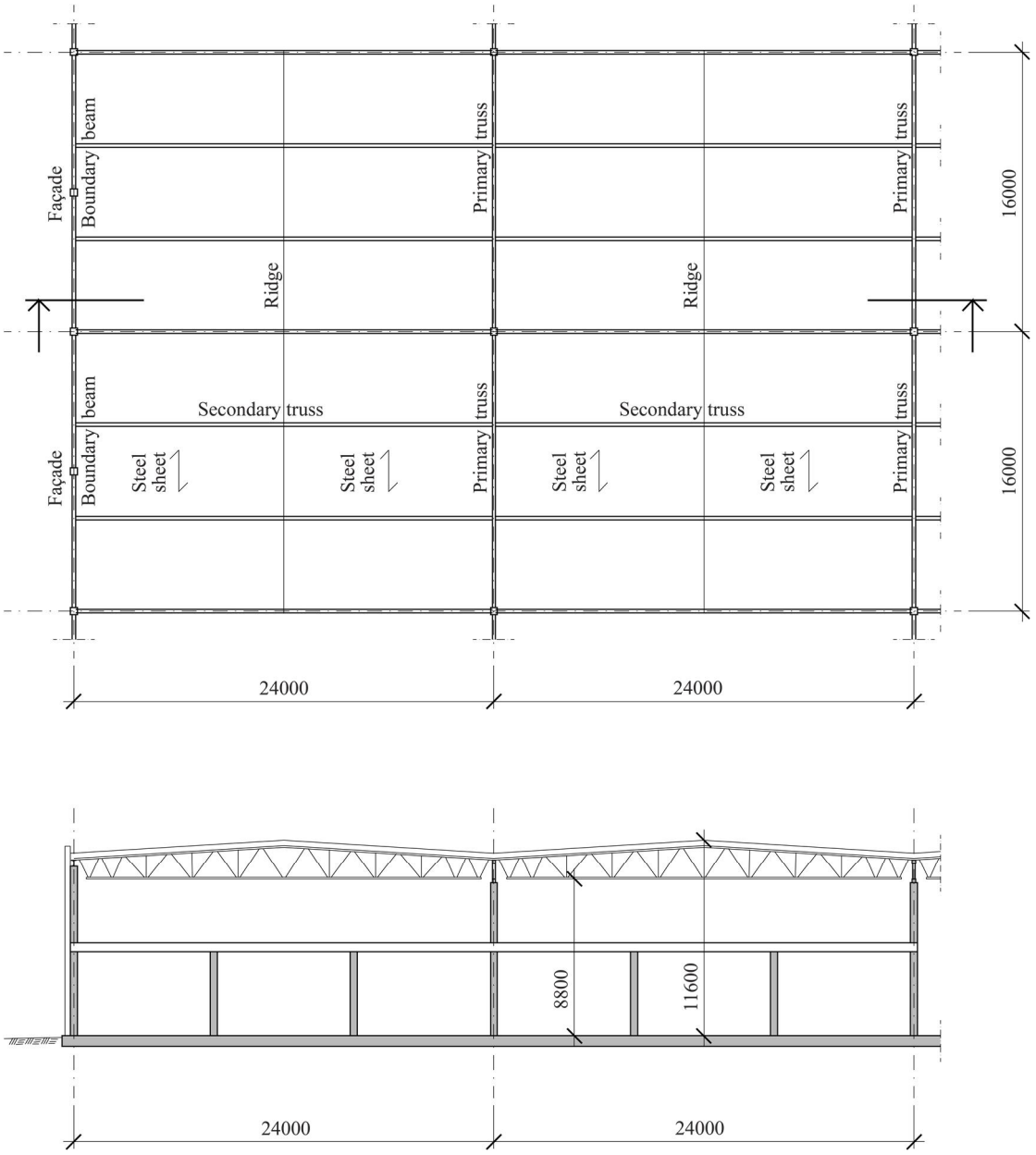

Figure 5.1 Principal roof plan and section of a part of the building.

5.1.2 Establishment of constraints

As flexibility and an open layout are of high importance for department stores, the column spacing of the reference building is assumed a minimum requirement. An internal column spacing of 16 m in the direction perpendicular to the ribbons, and a spacing of 8 m in the façade is considered reasonable and are therefore directly adopted as constraints. Regarding the span length of the ribbons, the measurement of 24 m is kept as a minimum length, but because of the structural efficiency of the SR concept, the possibility of longer spans is also investigated.

The vertical clearance of 8.8 m is assumed important in order to supply adequate room for intermediate floors. In order not to alter the total height of the building significantly, a maximum height of 12 m is assumed. The difference between internal and external height is then 3.2 m, and taking the depth of the roof and eventual

complementary parts into consideration a sag of 2.5 m is considered a reasonable restriction. With these constraints the sag-to-span ratio becomes

$$\frac{f}{L} = \frac{2.5\text{ m}}{24\text{ m}} = 0.104$$

Recalling the discussion of shape presented in Section 4.1.1, it can be noticed that the chosen sag-to-span ratio fulfils the limit of 1/8 in Marti's (2013) example and is very close to the limit of 1/10 given by Goldack et al. (2016). To assume a parabolic shape in the analysis is therefore considered reasonable.

The constraints are summarised in Table 5.1.

Table 5.1 Design constraints.

Intermediate column spacing (perpendicular to ribbons), $c_{\text{col,i}}$	16.0 m
Column spacing along building boundary, $c_{\text{col,b}}$	8.0 m
Ribbon span length, L	min. 24.0 m
Vertical clearance inside building	8.8 m
Total building height	12.0 m
Allowed sag, f	2.5 m

5.2 Proposal 1 – Sparse ribbons

The first proposal is based on a sparse system of ribbons, as seen in Figure 5.2 and Figure 5.3. The ribbons are assumed to be made of rectangular glulam beams, with a spacing of 8 m, curved to fit the predetermined initial sag. The choice of spacing implies that the ribbons coincide with the columns in the façade. As the column spacing is 16 m inside the building every other ribbon has to be supported by a transversal primary beam. The rather large spacing implies that the ribbons could be subjected to considerable loads, and large cross-section dimensions can therefore be expected.

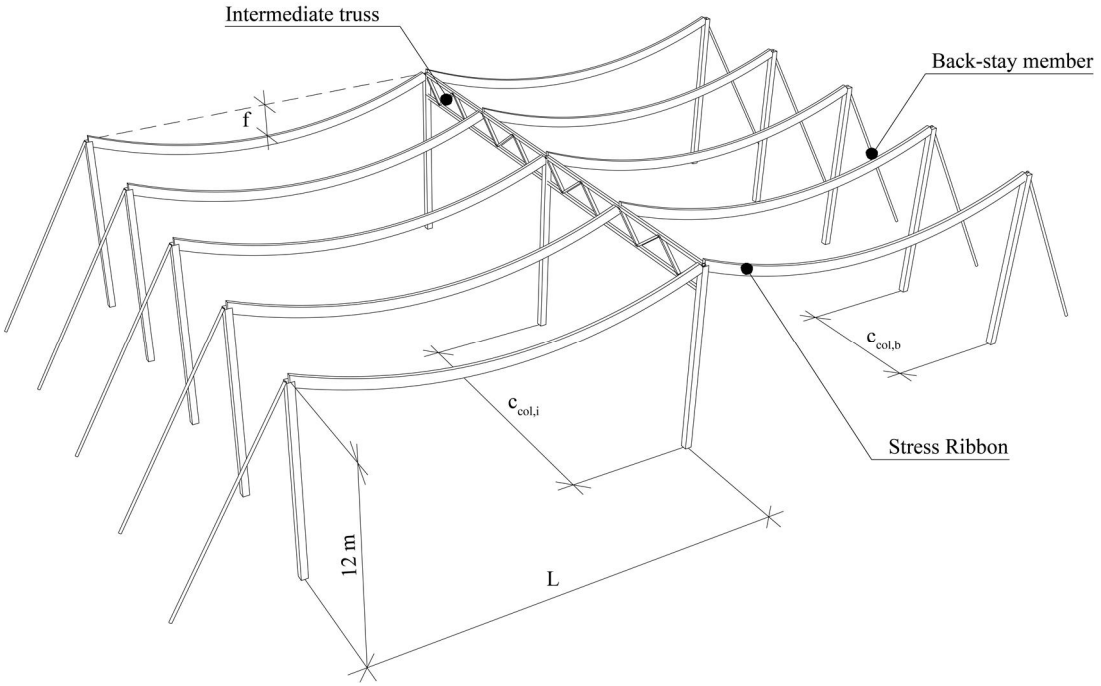

Figure 5.2 Overview of Proposal 1, here illustrated with the back-stay member alternative. Note though that the other alternatives for resisting horizontal forces, see Section 3.4, are also applicable.

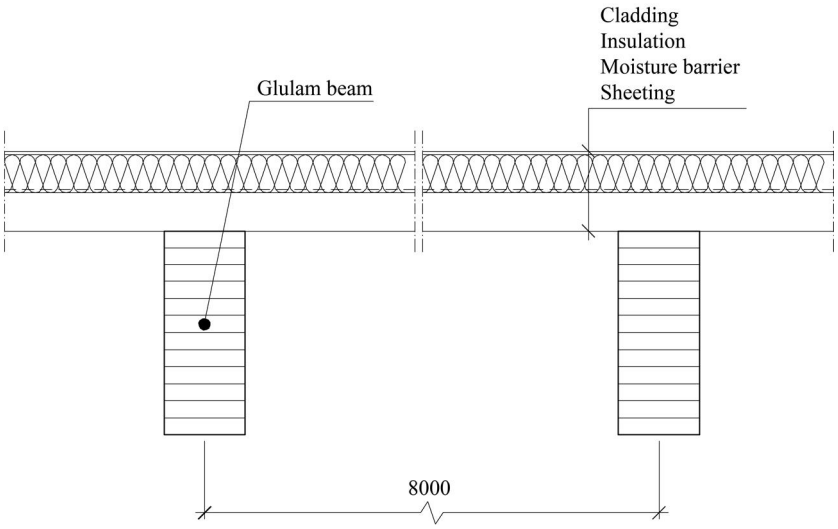

Figure 5.3 Cross-section of Proposal 1.

In order to cover the gap between the ribbons, a tertiary system spanning transversally across the ribbons is required. This could be achieved by e.g. corrugated metal sheeting or prefabricated timber elements. The tertiary system must also be able to work as a continuous diaphragm in order to provide the building with overall stability.

The main benefit of this system is that the ribbon spacing coincides with the column spacing in the façade, and the horizontal forces from the ribbons can thus be directly anchored in the columns. Inside the building the horizontal forces from two adjacent spans are assumed to be in equilibrium, and the internal columns and primary beams are thus assumed to be without significant horizontal forces.

One disadvantage of the system is that the span length might be limited in order to keep the cross-section size reasonable. Furthermore, a critical issue is how to anchor the large axial forces which the system gives rise to. A conventional way of producing such connections is to slit the member and insert steel plates which are fastened by bolts through the member. The removal of material for the slits will however weaken the member, which further increases the requirement for large cross-section dimensions.

5.3 Proposal 2 – Closely spaced ribbons

The second proposal consists of closely spaced ribbons connected to a beam along the boundary transferring the forces into the more sparsely placed columns, as seen in Figure 5.4 and Figure 5.5.

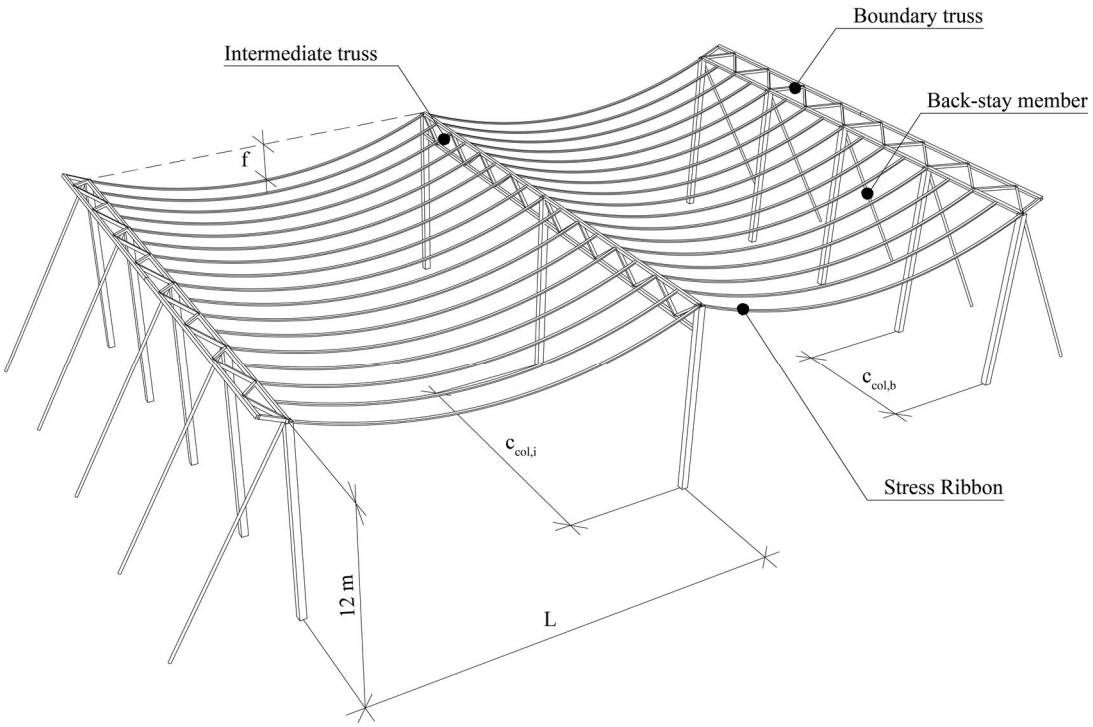

Figure 5.4 Overview of Proposal 2, here illustrated with the back-stay member alternative. Note though that the other alternatives for resisting horizontal forces, see Section 3.4, are also applicable.

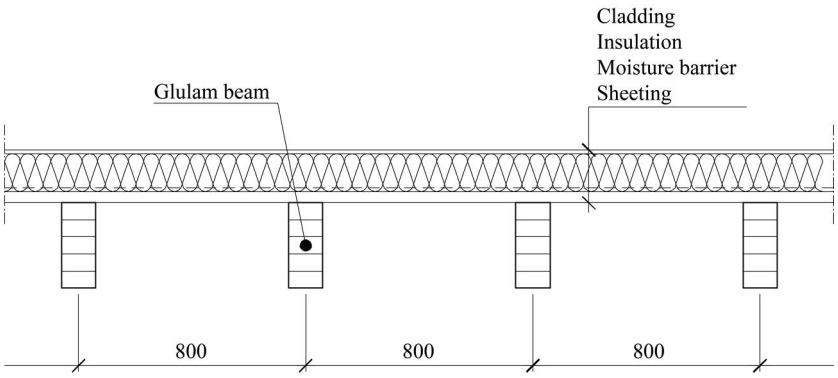

Figure 5.5 Cross-section of Proposal 2.

Similar to the first proposal, the ribbons are assumed to be made of rectangular glulam beams with an initial curvature. With regard to the connection of the ribbons to the boundary beam, it will be shown convenient with a spacing of 0.8 m, which is therefore assumed.

With small ribbon spacing the demand on the load-carrying capacity of the tertiary system is reduced, and thus a thinner and more material efficient roof construction can be achieved.

As the vertical loads are distributed on a large number of ribbons the system can be designed to maintain its load-carrying capacity even if one ribbon would break. The system can therefore be considered beneficial with regard to structural redundancy.

The main disadvantage of the proposal is that an extra structural element, the boundary beam, has to be added in order to transfer the forces from the ribbons into the supporting columns. The boundary beam must be able to resist both horizontal and vertical forces, will add to the material usage, and might complicate production and assembly. Furthermore, the system will contain many elements and thus many connections, which might complicate the assembly.

5.4 Proposal 3 – Continuous ribbon

As explained in Section 2.2, glulam is the only EWP which can be pre-cambered in an uncomplicated way. However, an SR system could be designed with initially straight members, relying on the deflection of the member under its self-weight. Provided a low bending stiffness of the ribbon, the deflection under its self-weight can be sufficient for the member to act in axial tension rather than bending. If the self-weight is insufficient, additional dead weight can be added to achieve the desired shape.

The third proposal consists of such a system, where LVL panels are arranged side by side, forming a continuous sheet, as seen in Figure 5.6 and Figure 5.7. Since the panels cannot be produced with initial sag, the system relies on the deflection of the panel. Similar to Proposal 2, the ribbon forces must somehow be transferred to the supports. The solution with a distributing beam along the building boundary adopted in Proposal 2 is a possible solution also here, as implied in Figure 5.6.

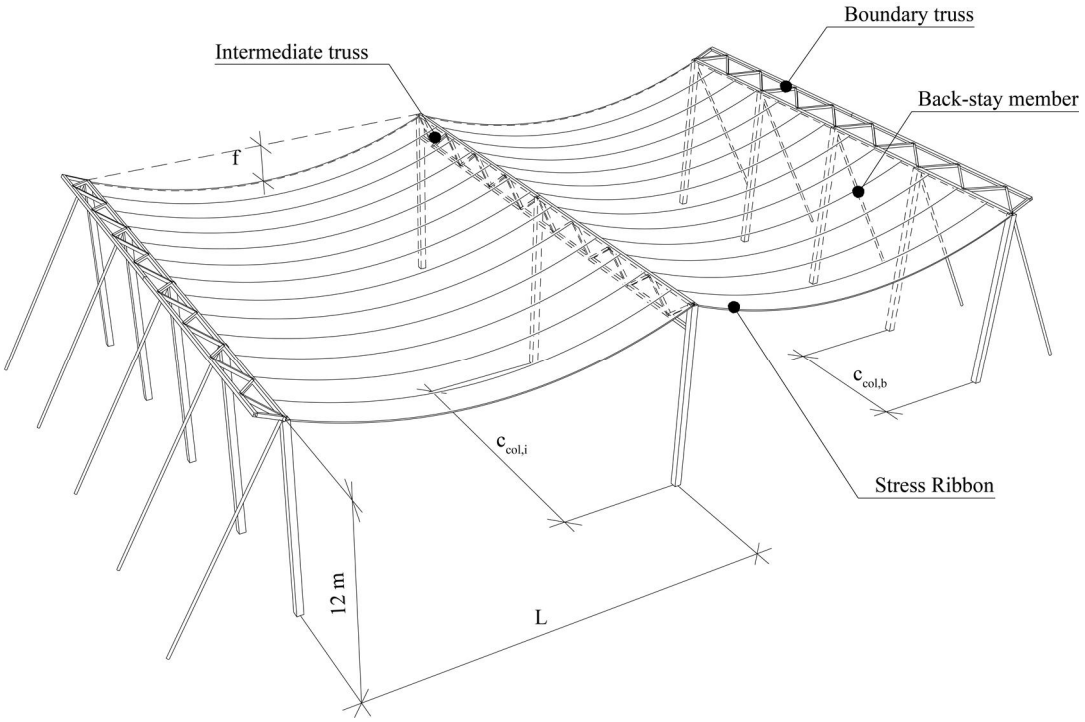

Figure 5.6 Overview of Proposal 3, here illustrated with the back-stay member alternative. Note though that the other alternatives for resisting horizontal forces, see Section 3.4, are also applicable.

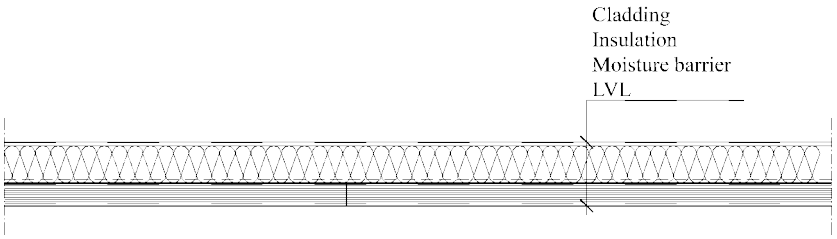

Figure 5.7 Cross-section of Proposal 3.

The ribbons form a continuous surface, and thus no tertiary system is required to span transversally across the ribbons. Furthermore, the ribbons can be utilised in resisting horizontal forces by diaphragm action. The total number of elements in the system is thus limited, which can be assumed to simplify the assembly.

As for the other proposals, one of the main issues of the concept is how to design connections. Another matter that has to be addressed is the geometrical stability of the ribbons during both erection and use of the building; because of the limited thickness of the ribbons, minimum bending stiffness is provided, and thus the behaviour during installation and under concentrated loads might be critical. Also, the aerodynamic properties of the roof must be investigated.

6 Preliminary Design

In this chapter a preliminary design of the main members of the three concepts presented in Sections 5.2-5.4 is performed. This is done in order to get an estimation of forces involved and reasonable geometrical properties.

6.1 Design constraints

In order not to complicate the calculations at this stage, the preliminary design is limited to only consider a single span with uniformly distributed loads and non-deformable supports. The only loads considered are self-weight and snow load; effects due to e.g. wind load and imposed load are thus not considered.

The ribbon design is primarily performed in the Ultimate Limit State (ULS). However, small cross-sections are highly vulnerable to fire exposure, and as rather thin cross-section dimensions are expected for the third proposal, design with regard to fire is also performed.

In the ULS design the target value for the utilisation ratio is set to 50 %. This is done in order to give room for the negative influence of connections, which is not explicitly accounted for at this stage.

The general geometrical properties considered are the ones presented in Section 5.1.2. Regarding the span lengths, the minimum value of 24 m is investigated, but also spans of 36 and 48 m are considered. Regarding the given sag of 2.5 m, this is used as input value; additional deflection is assumed to be small, and not interfere with the requirement for vertical clearance.

The different proposals and span lengths are evaluated and compared to each other, mainly with regard to material efficiency.

Apart from design of the ribbons, also an estimation of required dimensions for trusses and members resisting the horizontal forces is performed.

6.2 Ribbon design – ULS

Below follows a general presentation of the method of calculation with references to considered design codes, followed by the design results. The explicit calculation procedure for the glulam proposals is presented in Appendix B1 and for the LVL proposal in Appendix B2.

6.2.1 Material properties

6.2.1.1 Characteristic material properties – Glulam

The glulam considered for the ribbons in Proposals 1 and 2 is GL30h. Since the ribbons are intended to be used primarily in tension the full cross-section can be utilised (c.f. Figure 3.4), and a homogeneous cross-section is therefore considered suitable.

The characteristic material properties according to SS-EN 14080:2013 (CEN, 2013) are given in Table 6.1.

Table 6.1 Characteristic material properties of glulam GL30h.

Bending strength, $f_{\mathrm{m,g,k}}$	30.0 MPa
Tensile strength, $f_{\mathrm{t,0,g,k}}$	24.0 MPa
Modulus of elasticity, $E_{\mathrm{0,g,mean}}$	13.6 GPa
Density, $\rho_{\mathrm{g,mean}}$	4.8 kN/m^3

6.2.1.2 Design strength – Glulam

Design strength values are according to Equation 2.17 in Eurocode SS-EN 1995-1-1 (CEN, 2009, p. 27), calculated as

$$R_{\mathrm{d}} = k_{\mathrm{mod}} \frac{R_{\mathrm{k}}}{\gamma_{\mathrm{M}}} \tag{6.1}$$

R_{d} Design strength value

R_{k} Characteristic strength value

k_{mod} Modification factor for duration of load and moisture content

γ_{M} Partial factor for material property

The modification factor k_{mod} is determined from Table 3.1 in Eurocode SS-EN 1995-1-1 (CEN, 2009, p. 29) based on Load Duration Class and Service Class. According to Table 2.2 in Eurocode SS-EN 1995-1-1 (CEN, 2009, p. 24) the Load Duration Class for snow load is medium term action. The Service Class is determined according to Section 2.3.1.3 in Eurocode SS-EN 1995-1-1 (CEN, 2009, p. 24), and here Service Class 1 is assumed. This gives the value of k_{mod} as

$$k_{\mathrm{mod}} = 0.8$$

The partial factor for glulam is obtained from Table 2.3 in Eurocode SS-EN 1995-1-1 (CEN, 2009, p. 26) as

$$\gamma_{\mathrm{M}} = 1.25$$

For members in tension or bending an additional factor with consideration to member size can be considered for the design strength, according to Equation 3.2 in Eurocode SS-EN 1995-1-1 (CEN, 2009, p. 30). For members in tension with a width smaller than 600 mm and members in bending with a height smaller than 600 mm the following value for the size factor k_{h} applies

$$k_{\mathrm{h}} = \min \begin{cases} \left(\frac{600}{h}\right)^{0.1} \\ 1.1 \end{cases} \tag{6.2}$$

h Height for member in bending, width for member in tension [mm]

6.2.1.3 Design modulus of elasticity – Glulam

The design modulus of elasticity is according to Equation 2.15 in Eurocode SS-EN 1995-1-1 (CEN, 2009, p. 26) calculated as

$$E_{\mathrm{d}} = \frac{E_{\mathrm{mean}}}{\gamma_{\mathrm{M}}} \tag{6.3}$$

In addition, Section 2.3.2.2 in Eurocode SS-EN 1995-1-1 (CEN, 2009, p. 25) states that the influence of creep should be considered in ULS design, if the distribution of member forces is affected by the stiffness distribution in the structure.

According to Equation 2.10 in Eurocode SS-EN 1995-1-1 (CEN, 2009, p. 25) creep is considered by replacing E_{mean} in Equation (6.3) by $E_{\mathrm{mean,fin}}$, determined according to the expression

$$E_{\mathrm{mean,fin}} = \frac{E_{\mathrm{mean}}}{1 + \psi_2 k_{\mathrm{def}}} \tag{6.4}$$

ψ_2 Factor for quasi-permanent load for main variable action

k_{def} Creep factor

The factor ψ_2 can be determined from Table B-1 in Boverket (2015, p. 21), and k_{def} from Table 3.2 in Eurocode SS-EN 1995-1-1 (CEN, 2009, p. 31).

The distribution of member forces in the SR systems studied in this thesis is dependent on the stiffness distribution in the structure, and hence $E_{\mathrm{mean,fin}}$ should be used.

However, it is here of importance to understand how the stiffness affects the member forces. In Figure 6.1 three graphs can be seen, illustrating how the deflection, normal force and bending moment depend on the modulus of elasticity in an SR system. The graphs are obtained by studying a general case of an SR with bending stiffness, using the equations presented in Section 4.2.1.

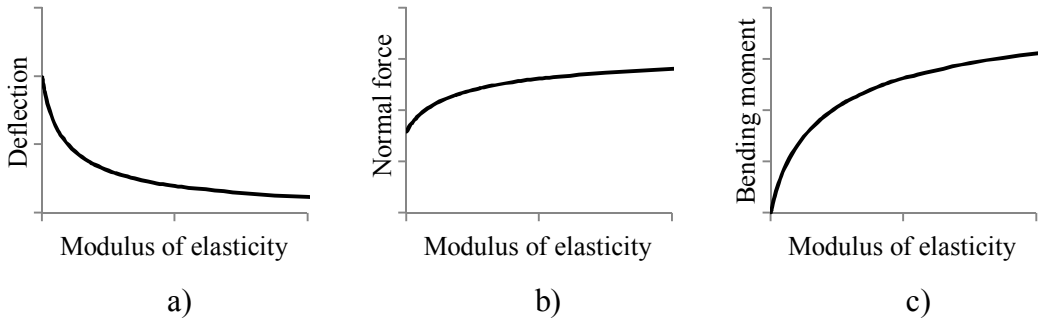

Figure 6.1 Principal relation between modulus of elasticity and a) deflection, b) normal force, and c) bending moment.

As seen in graph a in Figure 6.1, a decreased modulus of elasticity, i.e. decreased stiffness, imply larger deflection. Since the design is here performed in ULS the deflection is not of significant importance, if not shown to be unreasonably large. What is more interesting is the relation between the modulus of elasticity and the internal member forces. As seen in graphs b and c in Figure 6.1, both the normal force and the bending moment are reduced with a reduced modulus of elasticity.

The effect of creep decreases the member stiffness, and is often accounted for by reducing the modulus of elasticity, as in Equation (6.4). Creep can thus be deemed favourable with regard to internal member forces.

As this is a preliminary design a safe-side-approach is chosen, and creep is thus not considered.

6.2.1.4 Characteristic material properties – LVL

The material considered for the ribbons in Proposal 3 is Kerto-Q, a commonly used LVL product, as explained in Section 0.

The characteristic material properties according to VTT (2009) are given in Table 6.1.

Table 6.2 Characteristic material properties of Kerto-Q.

Bending strength, flatwise, parallel to grain, $f_{\mathrm{m,0,Q,flat,k}}$	36.0 MPa
Tensile strength, parallel to grain, $f_{\mathrm{t,0,Q,k}}$	26.0 MPa
Modulus of elasticity, parallel to grain, along, $E_{\mathrm{0,Q,mean}}$	10.5 GPa
Density, $\rho_{\mathrm{Q,mean}}$	5.1 kN/m^3

6.2.1.5 Design strength – LVL

Design strength values are calculated according to Equation (6.1). The value of k_{mod} should for Kerto-Q, according to Section 6.3 in VTT (2009, p. 8), be based on plywood data. The modification factor k_{mod} is determined from Table 3.1 in Eurocode SS-EN 1995-1-1 (CEN, 2009, p. 29) as

$$k_{\mathrm{mod}} = 0.8$$

The partial factor for LVL is obtained from Table 2.3 in Eurocode SS-EN 1995-1-1 (CEN, 2009, p. 26) as

$$\gamma_{\mathrm{M}} = 1.2$$

6.2.1.6 Design modulus of elasticity – LVL

The design modulus of elasticity is calculated according to Equation (6.3). As explained in Section 6.2.1.3, the effect of creep is favourable and therefore disregarded. If creep was to be included it should be noticed that the factor k_{def}, similar to k_{mod}, for Kerto-Q should be based on plywood data, according to Section 6.3 in VTT (2009, p. 8).

6.2.2 Loads

The loads considered in the preliminary design are self-weight and snow load, and as mentioned before all loads are assumed to be evenly distributed along the whole span.

6.2.2.1 Self-weight

The characteristic self-weight of the ribbon is calculated from the material density and the cross-section area. In addition to the ribbon self-weight, extra dead load is applied, corresponding to the self-weight of tertiary load-carrying members, insulation, roof cover, air ducts etc. The additional self-weight is roughly assumed to be 1 kN/m^2.

By assuming that the self-weight is applied as a uniformly distributed load along the span length rather than along the actual ribbon length an underestimation of the load is introduced. This is however assumed to be compensated by overestimating the magnitude of the additional self-weight.

6.2.2.2 Snow load

The building is assumed to be placed in Stockholm, Sweden. According to Figure C-2 in Boverket (2015, p. 39) the characteristic snow load is given as

$$s_{\mathrm{k}} = 2.0 \text{ kN/m}^2$$

The characteristic snow load should according to Section 5.3 in Eurocode SS-EN 1991-1-3 (CEN, 2005, p. 16) be multiplied by a shape factor considering the roof design and possible snow drift. The shape factor is here assumed to be

$$\mu_1 = 1.0$$

For the load combination a combination factor ψ_0 is required. According to Table B-1 in Boverket (2015, p. 21) this combination factor for snow with $s_{\mathrm{k}} = 2.0$ kN/m^2 is

$$\psi_{0.\mathrm{s}} = 0.7$$

6.2.2.3 Load combination

As mentioned before, the preliminary design only considers the load combination in ULS. As stated by Equations 6.10a and 6.10b in Boverket (2015, p. 22) the load combination, assuming non-favourable loads, should be performed using the less favourable of the following two expressions:

$$\gamma_{\mathrm{d}} \left(1.35 G_{\mathrm{kj,sup}} + 1.5 \sum \psi_{0,\mathrm{i}} Q_{\mathrm{k,i}} \right) \tag{6.5}$$

$$\gamma_{\mathrm{d}} \left(0.89 \cdot 1.35 G_{\mathrm{kj,sup}} + 1.5 Q_{\mathrm{k,1}} + 1.5 \sum \psi_{0,\mathrm{i}} Q_{\mathrm{k,i}} \right) \tag{6.6}$$

The factor $G_{\mathrm{kj,sup}}$ represents the permanent load on the structure and $Q_{\mathrm{k,i}}$ the i:th variable load with its corresponding combination factor $\psi_{0,\mathrm{i}}$. In Equation (6.6) the most unfavourable variable load is assigned main variable load, $Q_{\mathrm{k,1}}$. As seen in the equation this load should not be multiplied with a combination factor $\psi_{0,1}$. In this case the snow load is the only variable load considered, and is therefore the obvious main variable load.

The factor γ_{d} is a safety factor dependent on the Reliability Class of the member considered. According to Section A, 13§ in Boverket (2015, p. 6) the load-carrying construction of the building in question should be assigned Reliability Class 3. Section A, 14§ in Boverket (2015, p. 7) then states that

$$\gamma_{\mathrm{d}} = 1.0$$

6.2.3 Design procedure

The design is performed on the basis of the equations derived in Section 4.2 in the following order:

1. The horizontal force due to self-weight H is calculated according to Equation (4.12)
2. The cable shape z and its first derivative z' are determined by Equations (4.13) and (4.14)
3. The horizontal force due to variable load ΔH is calculated according to Equation (4.29)
4. The deflection w is given by Equation (4.25)
5. The normal force N_{Ed} is expressed according to Equation (4.30)
6. The bending moment M_{Ed} is calculated according to Equation (4.28)

When forces and moments acting on the system are known, the corresponding stresses are calculated and the cross-section capacity controlled.

The design tensile stress is obtained from the expression

$$\sigma_{\mathrm{t,0,d}} = \frac{N_{\mathrm{Ed}}}{A} \tag{6.7}$$

N_{Ed} Design normal force [N]

A Cross-section area [m^2]

The design bending stress is calculated according to Navier's formula, i.e.

$$\sigma_{\mathrm{m,y,d}} = \frac{M_{\mathrm{Ed}}}{I}\frac{h}{2} \tag{6.8}$$

M_{Ed} Design bending moment [Nm]

h Cross-section height [m]

I Moment of inertia [m^4]

The capacity with regard to combined axial tension and bending is, according to Equation 6.17 in Eurocode SS-EN 1995-1-1 (CEN, 2009, p. 43), sufficient if the following relation is true:

$$\frac{\sigma_{\mathrm{t,0,d}}}{f_{\mathrm{t,0,d}}} + \frac{\sigma_{\mathrm{m,y,d}}}{f_{\mathrm{m,y,d}}} \leq 1 \tag{6.9}$$

6.2.3.1 Iterations

The relation between tensile and bending behaviour in the ribbon is dependent on the cross-section shape; with increasing bending stiffness EI, the ribbon will tend to adopt more beam behaviour and less cable-like behaviour. A consequence of a change of cross-section shape is thus redistribution between normal force and bending moment.

The cross-section dimensions must therefore be provided for the analysis. However, the dimensions are also the result of the design, and there is thus a problem with the dimensions being both input and output.

To handle this, the analysis is performed iteratively. The iterations are performed manually in the calculation procedure presented in Appendices B1 and B2, adopting the simple scheme shown in Figure 6.2.

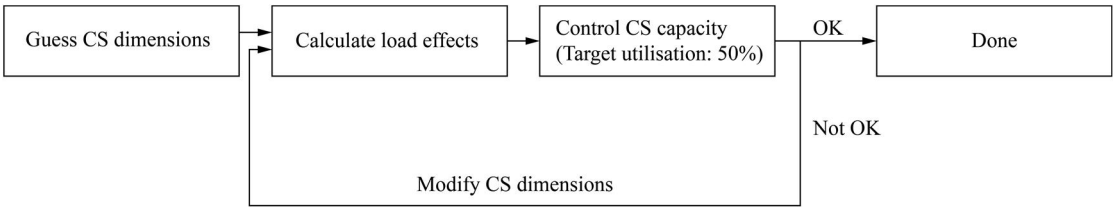

Figure 6.2 Iteration scheme.

6.2.4 Results

The results of the preliminary design are presented in Table 6.3, Table 6.4 and Table 6.5.

The main result of the ULS design is the required cross-section dimensions. The member dimensions have, when possible, been chosen from standard cross-section data given by Carling (2001) and VTT (2009), see Appendix A. However, in the result tables some proposals are included, where standard cross-section dimensions are not used (Proposals 1b and 3b in Table 6.3, Proposal 1b in Table 6.4, and Proposal 1 in Table 6.5). The reason for this is discussed later in this section.

Deflection is a problem related to design in SLS rather than ULS. The maximum deflection $w_{\max}$ is though included in the results, mainly to prove that unreasonably large deformations are not present; apart from that the deflection is not further considered.

As seen in Table 6.3, Table 6.4 and Table 6.5, the relation between bending and tensile stresses is included in the results. This data is of particular interest, as the point of the SR concept is to stress the ribbons primarily in tension and thereby utilise the material better; a lower value is thus preferable. The relation between bending and tensile stresses is further discussed later in this section.

The characteristic self-weight of the ribbons g_{k} is used to compare the material efficiency of the different proposals. However, it should be noticed that the values presented in the result tables consider the self-weight of ribbons only. Other structural members required in the different systems, e.g. tertiary system, are not included, and the results can therefore only be considered as an indication of the material usage. A more complete comparison of the material efficiency of the systems, considering all the structural elements, is performed in Section 6.6.

Table 6.3 Design results – 24 m span.

Proposal No.		1a	1b	2	3a	3b
h	[mm]	675	315	180	27	15[1)]
b	[mm]	215	430[1)]	78	∞[3)]	∞[3)]
c	[m]	8.0[2)]	8.0[2)]	0.8[2)]	n/a	n/a
w_{max}	[mm]	19	21	20	16	28
H	[kN]	977	981	98	125[4)]	122[4)]
H_{col}	[kN]	977	981	983	1000	987
N_{Ed}	[kN]	1060	1064	107	136[4)]	133[4)]
M_{Ed}	[kNm]	18.78	3.86	0.12	0.003	0.001
$\sigma_{m,y,d}/\sigma_{t,0,d}$	[-]	0.16	0.07	0.04	0.005	0.003
Util. tension	[%]	43	50	45	29	51
Util. bending	[%]	6	3	1	0	0
Util. total	[%]	49	52	46	29	51
g_k	[kg/m^2]	8.7	8.1	8.4	13.8	7.7

Table 6.4 Design results – 36 m span.

Proposal No.		1a	1b	2	3
h	[mm]	1620	765	315	33
b	[mm]	215	430[1)]	90	∞[3)]
c	[m]	8.0[2)]	8.0[2)]	0.8[2)]	n/a
w_{max}	[mm]	38	42	48	63
H	[kN]	2182	2242	224	278[4)]
H_{col}	[kN]	2182	2242	2237	2227
N_{Ed}	[kN]	2267	2329	233	289[4)]
M_{Ed}	[kNm]	232.12	52.50	0.81	0.01
$\sigma_{m,y,d}/\sigma_{t,0,d}$	[-]	0.38	0.18	0.07	0.006
Util. tension	[%]	39	45	49	51
Util. bending	[%]	13	7	3	0
Util. total	[%]	51	51	51	51
g_k	[kg/m^2]	20.9	19.7	17.0	16.8

Table 6.5 Design results – 48 m span.

Proposal No.		1	2	3
h	[mm]	1575	315	63
b	[mm]	430[1)]	165	∞[3)]
c	[m]	8.0[2)]	0.8[2)]	n/a
w_{max}	[mm]	61	81	102
H	[kN]	4069	408	208[4)]
H_{col}	[kN]	4069	4079	4062
N_{Ed}	[kN]	4160	417	520[4)]
M_{Ed}	[kNm]	383.85	1.37	0.06
$\sigma_{m,y,d}/\sigma_{t,0,d}$	[-]	0.35	0.06	0.01
Util. tension	[%]	39	48	48
Util. bending	[%]	11	3	0
Util. total	[%]	50	50	48
g_k	[kg/m^2]	40.6	31.2	32.1

[1)] Non-standard dimension
[2)] Predetermined value according to Section 5.2/5.3
[3)] Equal to building width
[4)] Force per unit width (1 m)

h, b	Cross-section dimensions
c	Ribbon spacing
$w_{\max}$	Maximum deflection
H	Horizontal force in ribbon
H_{col}	Total horizontal force at column
N_{Ed}	Design normal force in ribbon
M_{Ed}	Design bending moment in ribbon
$\frac{\sigma_{\text{m,y,d}}}{\sigma_{\text{t,0,d}}}$	Ratio bending stress/normal stress
g_{k}	Characteristic self-weight of ribbons per m^2 roof (sheeting not included)

Regarding Proposal 3, Kerto-Q is limited to a minimum standard thickness of 27 mm. However, in the case of 24 m span length a thickness of 27 mm results in a utilisation ratio of only 29 %, c.f. Proposal 3a in Table 6.3. The overcapacity provided influences the self-weight of the system, and the self-weight of Proposal 3a is therefore significantly larger than for the other proposals. In order to see the actual material required for the LVL system Proposal 3b is included, where the minimum standard thickness is disregarded. As seen in the results a thickness of only 15 mm is sufficient to reach the target utilisation of 50 %.

Regarding glulam, the maximum standard cross-section width is rather small, as explained in Section 2.2.1; the largest standard width according to Carling (2001) is 215 mm. For the first proposal, with sparse ribbons, this restriction is a problem as a large cross-section size is required in order to resist the large forces the ribbons are subjected to. With a restricted width, the height must be increased in order to reach sufficient cross-section area, but this leads to an undesirable increase of bending stiffness. In an effort to decrease the bending behaviour, Proposal 1b in the 24 and 32 m span cases (see Table 6.3 and Table 6.4) includes a cross-section wider than available standard widths. In the case of 48 m span length, there is no standard dimension with sufficient capacity, and a cross-section wider than standard is therefore a necessity. According to Carling (2001) and Crocetti et al. (2011) wider beams can be produced by gluing multiple beams side by side, and this is thus assumed in the concerned proposals. The chosen width of 430 mm corresponds to two beams of 215 mm width.

The reason for bending stress being undesirable is that it affects the material efficiency. As explained in Section 3.1, tension is a more efficient way of carrying loads than bending. In the result tables it can be observed that the increase of self-weight follows the increase of the ratio between bending and tensile stress. In turn, the ratio between bending and tensile stress is dependent on the stiffness of the cross-section, and larger cross-section height implies stiffer cross-section. Thus, higher cross-section means higher ratio between bending and tensile stress, which ultimately leads to less material efficiency.

To illustrate how the distribution between bending and tensile stresses vary with changed cross-section dimensions, a graph showing the ratio $\sigma_{\text{m}}/\sigma_{\text{t}}$ as a function of the ratio of cross-section h/b is plotted, see Figure 6.3. The ratio $\sigma_{\text{m}}/\sigma_{\text{t}}$ is though not

only dependent on the ratio h/b, but is also affected by the span length L and sag f. The results are therefore shown for a number of different cases.

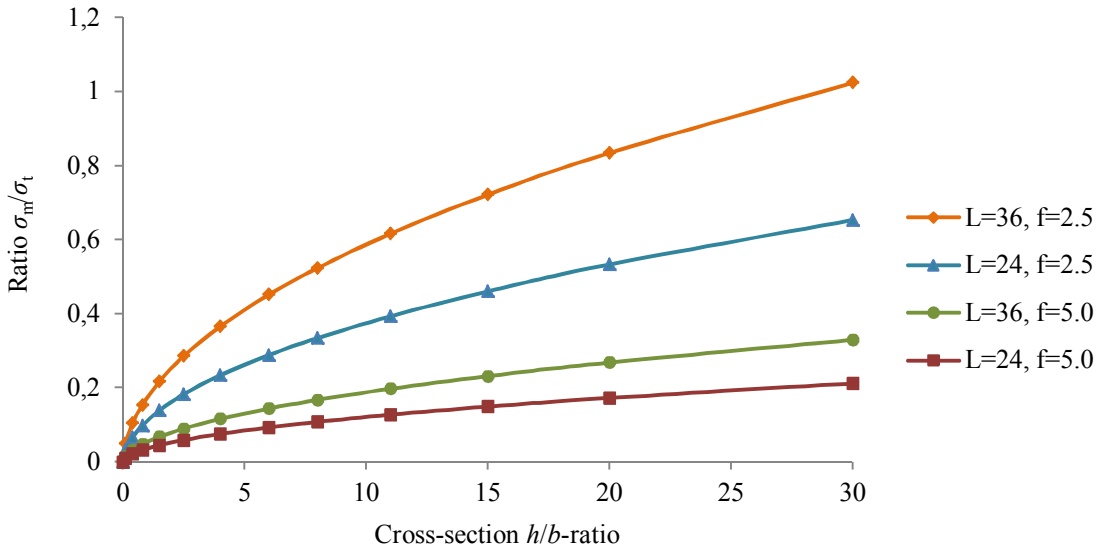

Figure 6.3 Graph showing the ratio σ_m/σ_t as a function of the ratio h/b.

Notice that in the graph unreasonably high h/b-ratios are provided, only to illustrate the continuously increasing bending behaviour. With regard to manageability, reasonable cross-section shapes are within $h/b \leq 10$ (Carling, 2001).

As explained in Section 6.2.1.3, creep is not considered in the preliminary ULS design. However, in order to get an indication of how much the influence of creep affects the results, an example where it is considered is here provided. Table 6.6 shows the deflection and member forces of Proposal 2, 24 m span length, with and without consideration to creep.

Table 6.6 Design results with consideration to creep – Proposal 2, 24 m span.

Proposal No.	w_{max} [mm]	H [kN]	H_{col} [kN]	N_{Ed} [kN]	M_{Ed} [kNm]	$\frac{\sigma_{m,y,d}}{\sigma_{t,0,d}}$
2	20	98	983	107	0.12	0.04
2_{creep}	22	98	982	106	0.11	0.04
Deviation	10.0 %	-0.1 %	-0.1 %	-0.1 %	-0.7 %	0.0 %

As seen, the change in member forces is very small, and the effect of creep does thus not affect the ULS design significantly.

6.3 Ribbon design – Fire

As mentioned in the introduction of this thesis a beneficial property of timber is its behaviour during fire; the uncharred core of a timber member exposed to fire maintains its load-carrying capacity, and thus no additional fire proofing is required, provided that the member cross-section is sufficiently large. In order to see if and how the three proposals designed in the previous section are affected by fire requirements

a preliminary design with regard to fire is performed. Of particular interest is the third proposal consisting of LVL panels, since the thin cross-section of the panels is assumed to be more vulnerable than the other proposals.

The fire exposure time t considered here is 60 minutes, which is the requirement for the reference building presented in Section 5.1.1. No measures to protect the members from fire are assumed.

The calculations are based on cross-section dimensions from the ULS design, as presented in Section 6.2.4. The cross-section design is altered only if proven necessary.

6.3.1 Geometry

The procedure for design with regard to fire considered here is a simplified method adopting a reduced cross-section. The method is presented in Section 4.2.2 in Eurocode SS-EN 1995-1-2 (CEN, 2010, p. 31).

An effective cross-section is calculated by reducing the original cross-section dimensions by d_{ef}, i.e.

$$b_{\mathrm{ef}} = b - d_{\mathrm{ef}} \tag{6.10}$$

$$h_{\mathrm{ef}} = h - d_{\mathrm{ef}} \tag{6.11}$$

The term d_{ef} is, according to Equation (4.1) in Eurocode SS-EN 1995-1-2 (CEN, 2010, p. 31) defined as

$$d_{\mathrm{ef}} = d_{\mathrm{char,n}} + k_0 d_0 \tag{6.12}$$

$d_{\mathrm{char,n}}$ Equivalent design charring depth [m]

$k_0 d_0$ Thickness of non-charred material layer without strength and stiffness [m]

The value of d_0 is 7 mm and the factor k_0 is determined from Table 4.1 in Eurocode SS-EN 1995-1-2 (CEN, 2010, p. 32). For a fire exposure time $t \geq 20$ min, the value of k_0 is 1.0.

$d_{\mathrm{char,n}}$ is, according to Equation (3.2) in Eurocode SS-EN 1995-1-2 (CEN, 2010, p. 22), defined as

$$d_{\mathrm{char,n}} = \beta_{\mathrm{n}} t \tag{6.13}$$

β_{n} Equivalent design charring speed [mm/min]

The value of β_{n} is obtained from Table 3.1 in Eurocode SS-EN 1995-1-2 (CEN, 2010, p. 24). Both for glulam and LVL $\beta_{\mathrm{n}} = 0.7$, giving $d_{\mathrm{char,n}} = 42$ mm and $d_{\mathrm{ef}} = 49$ mm.

6.3.2 Material properties

6.3.2.1 Design strength

The design strength during fire is according to Equation (2.1) in Eurocode SS-EN 1995-1-2 (CEN, 2010, p. 31) calculated as

$$f_{\mathrm{d,fi}} = k_{\mathrm{mod,fi}} \frac{f_{20}}{\gamma_{\mathrm{M,fi}}} \tag{6.14}$$

$f_{\mathrm{d,fi}}$ Design strength during fire

f_{20} 20 %-fractile of strength at normal temperature

$k_{\mathrm{mod,fi}}$ Modification factor for duration of load and moisture content during fire

$\gamma_{\mathrm{M,fi}}$ Partial factor for material property during fire

The recommended value for $\gamma_{\mathrm{M,fi}}$ is 1.0. The factor $k_{\mathrm{mod,fi}}$ takes the reduction of strength at high temperatures into consideration. As explained in Section 6.3.1 this is here handled by reducing the cross-section area rather than the material strength, and the value of $k_{\mathrm{mod,fi}}$ is therefore set to 1.0.

The 20 %-fractile of the strength is, according to Equation (2.4) in Eurocode SS-EN 1995-1-2 (CEN, 2010, p. 17), calculated as

$$f_{20} = k_{\mathrm{fi}} f_{\mathrm{k}} \tag{6.15}$$

f_{k} Characteristic strength

k_{fi} Factor for calculation of 20 %-fractile

The value of k_{fi} is determined from Table 2.1 in Eurocode SS-EN 1995-1-2 (CEN, 2010, p. 18). For glulam $k_{\mathrm{fi}} = 1.15$ and for LVL $k_{\mathrm{fi}} = 1.1$.

6.3.2.2 Design modulus of elasticity

The design modulus of elasticity during fire is calculated in the same way as the design strength, i.e.

$$E_{\mathrm{d,fi}} = k_{\mathrm{mod,fi}} \frac{E_{20}}{\gamma_{\mathrm{M,fi}}} \tag{6.16}$$

The values of $k_{\mathrm{mod,fi}}$ and $\gamma_{\mathrm{M,fi}}$ are both 1.0, as explained above. E_{20} is, according to Equation (2.5) in Eurocode SS-EN 1995-1-2 (CEN, 2010, p. 17), calculated as

$$E_{20} = k_{\mathrm{fi}} E_{05} \tag{6.17}$$

E_{05} 5 %-fractile of modulus of elasticity at normal temperature

6.3.3 Loads

The design load effect can, according to Equation (2.8) in Eurocode SS-EN 1995-1-2 (CEN, 2010, p. 19), be calculated in a simplified way as

$$E_{\mathrm{d,fi}} = \eta_{\mathrm{fi}} E_{\mathrm{d}} \tag{6.18}$$

E_{d} Design load effect in ULS design

η_{fi} Reduction factor

The reduction factor η_{fi} is calculated from the less favourable of the two equations

$$\eta_{\text{fi}} = \frac{G_{\text{k}} + \psi_{\text{fi}} Q_{\text{k},1}}{\gamma_{\text{G}} G_{\text{k}} + \gamma_{\text{Q},1} Q_{\text{k},1}} \tag{6.19}$$

$$\eta_{\text{fi}} = \frac{G_{\text{k}} + \psi_{\text{fi}} Q_{\text{k},1}}{\xi \gamma_{\text{G}} G_{\text{k}} + \gamma_{\text{Q},1} Q_{\text{k},1}} \tag{6.20}$$

G_{k} Characteristic value of permanent load

$Q_{\text{k},1}$ Characteristic value of main variable load

γ_{G} Partial coefficient for permanent load

$\gamma_{\text{Q},1}$ Partial coefficient for main variable load

ψ_{fi} Combination factor for frequent variable load during fire

ξ Reduction factor for unfavourable permanent load

The values of γ_{G}, $\gamma_{\text{Q},1}$ and ξ are 1.35, 1.5 and 0.89 respectively, as seen in Equations (6.5) and (6.6). According to Eurocode SS-EN 1995-1-2 (CEN, 2010) the value of ψ_{fi} is either ψ_1 or ψ_2, and in Section A, 10§ in Boverket (2015, p. 5) it is stated that the frequent value, i.e. ψ_1, should be used in accidental design situations. The value of ψ_1 is obtained from Table B-1 in Boverket (2015, p. 21) as $\psi_1 = 0.4$.

6.3.4 Design procedure

The design procedure is similar to the ULS design, see Section 6.2.3. However, as seen in the ULS design results in Section 6.2.4, the influence of the bending strength is very small for cross-sections of small height. For this reason the bending strength is here neglected for the LVL alternative, i.e. pure cable-like behaviour is assumed.

The explicit calculations for the glulam and LVL proposals are presented in Appendices C1 and C2 respectively.

6.3.5 Results

The results are presented in Table 6.7, Table 6.8 and Table 6.9.

Table 6.7 Fire design results – 24 m span.

Proposal No.	h [mm]	b [mm]	h_{ef} [mm]	b_{ef} [mm]	$\frac{A_{ef}}{A}$	Utilisation [%]	g_k [kg/m^2]
1a	675	215	626	166	0.72	18	8.7
1b	315	430	226	381	0.75	17	8.1
2	180	78	131	29	0.27	0.44	8.4
3	57[1)]	∞[2)]	8	∞[2)]	0.14	29	29.1

Table 6.8 Fire design results – 36 m span.

Proposal No.	h [mm]	b [mm]	h_{ef} [mm]	b_{ef} [mm]	$\frac{A_{ef}}{A}$	Utilisation [%]	g_k [kg/m^2]
1a	1620	215	1526	166	0.75	18	20.9
1b	765	430	716	381	0.83	15	19.7
2	315	90	266	41	0.38	0.35	17.0
3	57[1)]	∞[2)]	8	∞[2)]	0.13	62	29.1

Table 6.9 Fire design results – 48 m span.

Proposal No.	h [mm]	b [mm]	h_{ef} [mm]	b_{ef} [mm]	$\frac{A_{ef}}{A}$	Utilisation [%]	g_k [kg/m^2]
1	1575	430	1526	381	0.86	15	40.6
2	315	165	266	116	0.59	23	31.2
3	63	∞[2)]	14	∞[2)]	0.21	63	32.1

[1)] Design value from ULS design altered to fulfil fire requirements
[2)] Equal to building width

As seen in the result tables, the cross-sections obtained in the ULS design are sufficient in most cases, also with regard to fire; the utilisation ratio is even lower than in the ULS design, despite the reduction of cross-section size. This can be explained by the large reduction of load in the fire design case; the reduction factor η_{fi} is in the interval $0.42 \leq \eta_{fi} \leq 0.45$ for all of the analysed cases, and the design load in case of fire is thus less than half of the ULS design load.

However, for span lengths of 24 and 36 m, the cross-sections of the third proposal obtained in the ULS design lacks sufficient capacity with consideration to fire. Given the reduction value $d_{ef} = 49$ mm, this is an obvious result; the cross-sections obtained for these cases in the ULS design are thinner than the layer of material charred, and the panel would thereby be entirely consumed. The required increase of cross-section height results in a significant increase in material usage, as seen in Table 6.10.

Table 6.10 – Material usage of Proposal 3, ULS/fire.

Span length [m]	$g_{k,ULS}$ [kg/m^2]	$g_{k,fire}$ [kg/m^2]	Increase [%]
24	13.8	29.1	111
36	16.8	29.1	73

6.4 Truss design

As illustrated in Figure 5.2, Figure 5.4 and Figure 5.6 the different proposals include primary trusses transferring forces from the ribbons to the columns. The first proposal includes only intermediate trusses inside the building, whereas the second and third proposals also require trusses along the building boundary. To get an estimation of required dimensions of these trusses a simplified design is here performed. Only load combination in ULS is considered. The material assumed is glulam of the same quality as in the ribbons, i.e. GL30h.

6.4.1 Intermediate truss

Due to the different layout of ribbons in the different proposals, three different load cases for the intermediate truss can be identified; Proposal 1 results in one centric point load, Proposal 2 in several point loads, and Proposal 3 in a uniformly distributed load. For simplicity, the design is here only performed for the case of uniformly distributed load. In accordance with Section 5.1.2 the length of the intermediate truss is assumed to be 16 m long. The considered truss design and load configuration is illustrated in Figure 6.4.

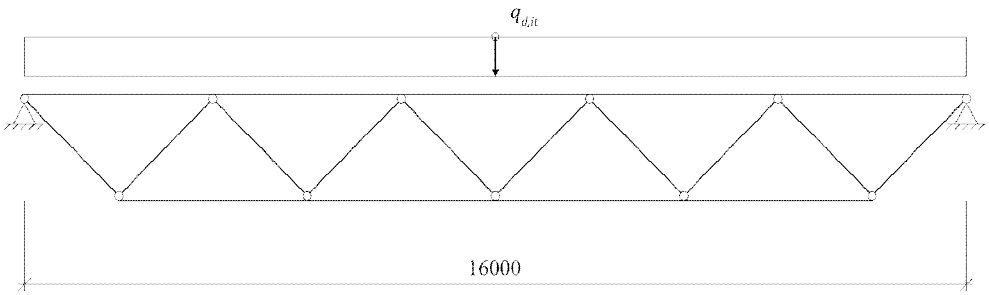

Figure 6.4 Intermediate truss model.

The maximum design load obtained in the ULS design of the ribbons is approximately $q_{\mathrm{d,max}} = 4.6$ kN/m^2. With influence from two adjacent spans the distributed load on the intermediate truss $q_{\mathrm{d,it}}$ is

$$q_{\mathrm{d,it}} = 2\, q_{\mathrm{d,max}} \frac{L}{2} = \begin{cases} 110 \text{ kN/m } (L = 24 \text{ m}) \\ 166 \text{ kN/m } (L = 36 \text{ m}) \\ 220 \text{ kN/m } (L = 48 \text{ m}) \end{cases}$$

The design is performed according to Eurocode SS-EN 1995-1-1 (CEN, 2009), using the software Strusoft WIN-Statik 6.4 Frame Analysis. An extract of the design procedure in the case of 24 m span length is presented in Appendix D.

The maximum sectional forces obtained in the analysis are presented in Table 6.11, and the resulting truss designs are presented in Figure 6.5, Figure 6.6 and Figure 6.7.

Table 6.11 Maximum sectional forces in intermediate truss. Note that the values represent the overall maximum, and do thus not coincide with each other.

Span length [m]	$N_{\mathrm{Ed,it}}$ [kN]	$V_{\mathrm{Ed,it}}$ [kN]	$M_{\mathrm{Ed,it}}$ [kNm]
24	-2143	198	111
36	-2340	285	219
48	-3434	394	225

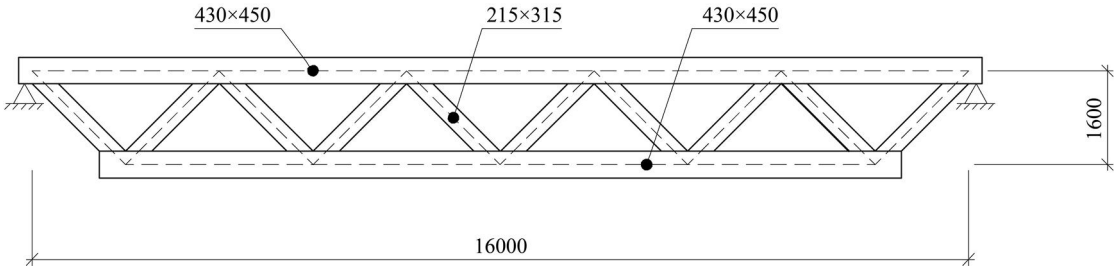

Figure 6.5 Design results – 24 m span. Total self-weight: 3055 kg.

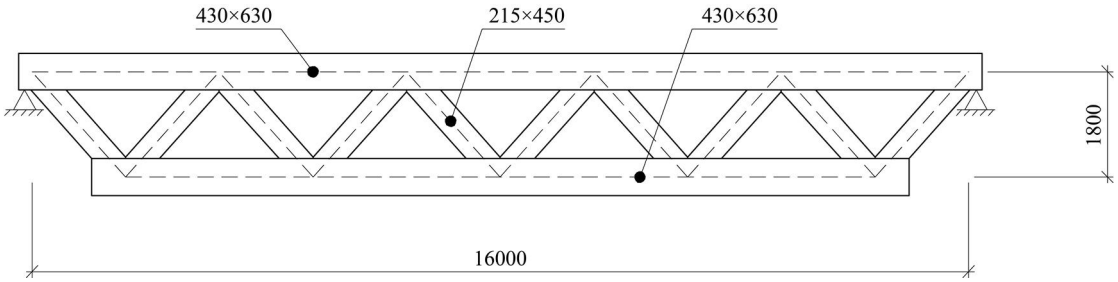

Figure 6.6 Design results – 36 m span. Total self-weight: 4357 kg.

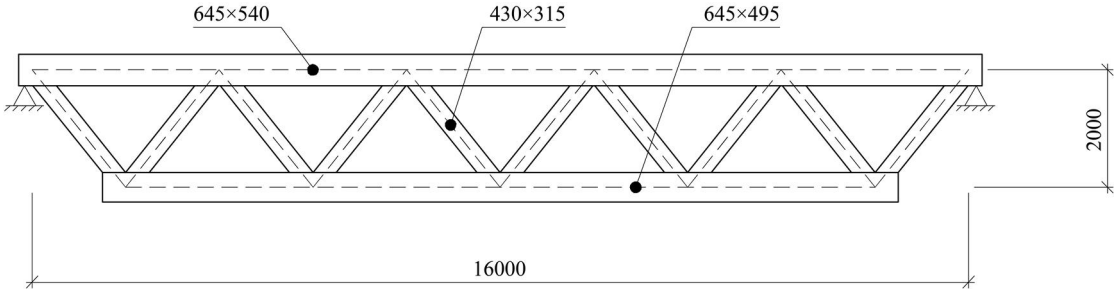

Figure 6.7 Design results – 48 m span. Total self-weight: 5645 kg.

6.4.2 Boundary truss

The boundary truss is only required in Proposals 2 and 3. As implied in Figure 5.4 and Figure 5.6 the truss is assumed to be inclined so that it is aligned with the tangent of the ribbon edge. In this way, the normal force in the ribbons can be directly transferred into the truss, which works only in its own plane (self-weight of the truss disregarded). It can be noticed that the concept is similar to the one adopted in the Stuttgart Trade Fair Exhibition Halls, as presented in Section 3.5.3. An alternative to

the inclined truss is to introduce two separate trusses; one vertical and one horizontal. The ribbon normal force would then be divided into its vertical and horizontal components, and handled separately. Another possible solution is to use a space truss, with load-bearing capacity in both directions. The two latter alternatives are however not considered in this thesis.

The boundary truss spans between the façade columns, which have a spacing of 8 m, according to Section 5.1.2. The truss design considered is illustrated in Figure 6.8. The load configuration is based on Proposal 2, i.e. point loads corresponding to the ribbon normal force, with a spacing of 0.8 m. With the chosen ribbon spacing and truss design, every other point load coincides with a truss node, as seen in Figure 6.8. This is beneficial as minimum local bending moment and shear is introduced in the lower chord of the truss. In the points where the ribbon connection does not coincide with a truss node a steel rod is introduced to transfer the force into a truss node. The same load configuration can be used for Proposal 3, assuming that the panel connections are arranged with a spacing of 0.8 m. Notice that the point loads at the two ends of the truss can be assumed to be directly transferred into the support, and do thus not affect the truss design.

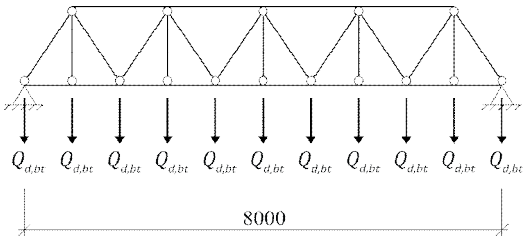

Figure 6.8 Boundary truss model.

As mentioned before, the point load magnitude corresponds to the ribbon normal force. For Proposal 2 these are (c.f. Table 6.3, Table 6.4 and Table 6.5):

$$Q_{\mathrm{d,bt}} = \begin{cases} 107\ \mathrm{kN}\ (L = 24\ \mathrm{m}) \\ 233\ \mathrm{kN}\ (L = 36\ \mathrm{m}) \\ 417\ \mathrm{kN}\ (L = 48\ \mathrm{m}) \end{cases}$$

For Proposal 3 the ribbon normal force is given as a distributed load in Table 6.3, Table 6.4 and Table 6.5. Converting these into corresponding point loads gives:

$$Q_{\mathrm{d,bt}} = \begin{cases} \dfrac{136\ \mathrm{kN/m} \cdot 8\ \mathrm{m}}{11} = 99\ \mathrm{kN} & (L = 24\ \mathrm{m}) \\ \dfrac{289\ \mathrm{kN/m} \cdot 8\ \mathrm{m}}{11} = 210\ \mathrm{kN} & (L = 36\ \mathrm{m}) \\ \dfrac{520\ \mathrm{kN/m} \cdot 8\ \mathrm{m}}{11} = 378\ \mathrm{kN} & (L = 48\ \mathrm{m}) \end{cases}$$

The design is here only performed for the proposal with the highest loads, i.e. Proposal 2.

For simplicity, the self-weight of the truss is assumed to act in the same direction as the ribbon forces. The design is performed according to Eurocode SS-EN 1995-1-1 (CEN, 2009), using the software Strusoft WIN-Statik 6.4 Frame Analysis. An extract of the design procedure in the case of 24 m span length is presented in Appendix E.

The maximum sectional forces obtained in the analysis are presented in Table 6.12, and the resulting truss designs are presented in Figure 6.9, Figure 6.10 and Figure 6.11.

Table 6.12 Maximum sectional forces in boundary truss. Note that the values represent the overall maximum, and do thus not coincide with each other.

Span length [m]	$N_{\mathrm{Ed,bt}}$ [kN]	$V_{\mathrm{Ed,bt}}$ [kN]	$M_{\mathrm{Ed,bt}}$ [kNm]
24	1243	52	54
36	1780	128	129
48	2542	311	358

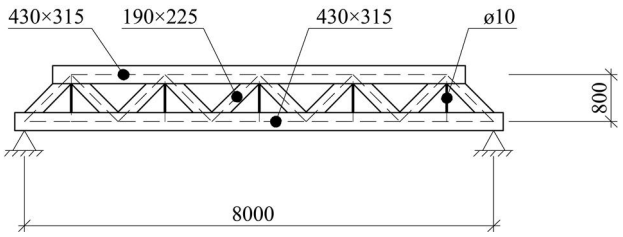

Figure 6.9 Design results – 24 m span. Total self-weight: 1049 kg.

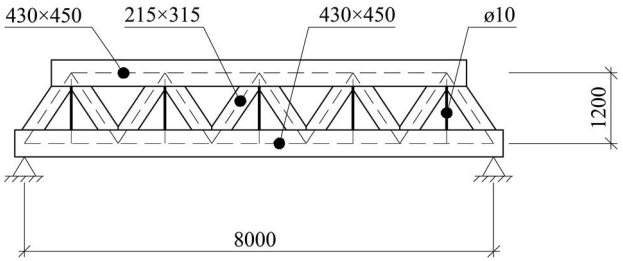

Figure 6.10 Design results – 36 m span. Total self-weight: 1609 kg.

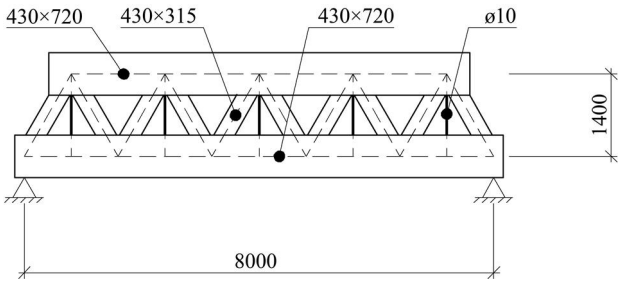

Figure 6.11 Design results – 48 m span. Total self-weight: 2861 kg.

The results of the truss design shows reasonable cross-section dimensions for all of the considered span lengths, and even the longest span length can therefore be considered possible with regard to truss design.

However, for longer spans the boundary truss is rather bulky, and other possible solutions could be investigated, if longer spans are desirable. One possible solution could be to simply decrease the column spacing, another to substitute the timber for another material, e.g. steel. For Proposal 3 also the possibility to transfer the loads to

the supports by shear in the continuous LVL sheet, and thus completely remove the boundary truss, could be investigated.

6.5 Boundary supports

As mentioned before, the three design proposals are compatible with different methods for resisting the horizontal forces and consequently, these are studied separately. Three different methods for resisting the horizontal forces of the ribbons are considered; compression strut from column to ground, tie from column to ground and bending stiff column (c.f. Figure 3.7b, c and d). Columns inside the building are assumed to be without significant horizontal forces, as horizontal forces from two adjacent spans are assumed to be in equilibrium. Thus, only columns at the building boundary are considered here.

In accordance with the constraints presented in Section 5.1.2, the columns are assumed to be 12 m high and have a spacing $c_{\mathrm{col,b}}$ of 8 m.

The design is only performed in ULS. The horizontal force is assumed to act at the top of the column, with a magnitude corresponding to the maximum value of H_{col} in Table 6.3, Table 6.4 and Table 6.5 respectively, i.e.

$$H_{\mathrm{col}} = \begin{cases} 1000 \text{ kN } (L = 24 \text{ m}) \\ 2245 \text{ kN } (L = 36 \text{ m}) \\ 4100 \text{ kN } (L = 48 \text{ m}) \end{cases}$$

The vertical load acting on the column is determined by the maximum vertical design load obtained from the design of the ribbons. With $q_{\mathrm{d,max}} = 4.6$ kN/m^2 the vertical load in the column is

$$V_{\mathrm{col}} = \frac{q_{\mathrm{d,max}} c_{\mathrm{col,b}} L}{2} = \begin{cases} 442 \text{ kN } (L = 24 \text{ m}) \\ 662 \text{ kN } (L = 36 \text{ m}) \\ 883 \text{ kN } (L = 48 \text{ m}) \end{cases}$$

6.5.1 Back-stay bar

In the alternative with a back-stay bar the vertical loads are assumed to be resisted by concrete columns and the horizontal forces by inclined steel bars. The geometrical constraints of the system are illustrated in Figure 6.12.

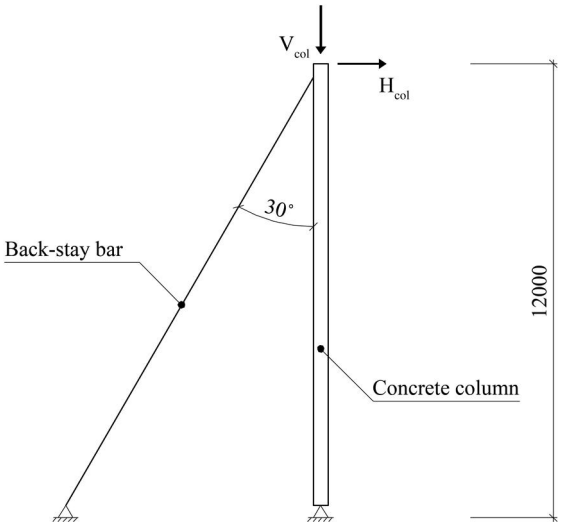

Figure 6.12 Geometrical constraints of back-stay bar system.

The reason for choosing steel rather than timber is that the member size can be kept down, minimising the possible conflict with surrounding activity. Furthermore, the choice of material enables introduction of prestressing, which is harder to perform with timber. No prestressing is though considered in these calculations.

The back-stay bar is designed by hand calculations according to Eurocode SS-EN 1993-1-1 (CEN, 2008b), by verifying that the following relation is satisfied:

$$\frac{N_{\mathrm{Ed}}}{N_{\mathrm{t,Rd}}} \leq 1 \tag{6.21}$$

N_{Ed} Design normal force [N]

$N_{\mathrm{t,Rd}}$ Design tensile capacity [N]

The design capacity is calculated according to Equation 2.1 in Eurocode SS-EN 1993-1-1 (CEN, 2008b, p. 23), i.e.

$$R_{\mathrm{d}} = \frac{R_{\mathrm{k}}}{\gamma_{\mathrm{M}}} \tag{6.22}$$

According to Section 6.1 in Eurocode SS-EN 1993-1-1 (CEN, 2008b, p. 45) the partial factor γ_{M} should be taken as γ_{M2} when considering tensile failure. According to Section E, 11§ in Boverket (2015, p. 86) the value of γ_{M2} is obtained from

$$\gamma_{\mathrm{M2}} = \min \begin{cases} 0.9\, f_{\mathrm{u}} / f_{\mathrm{y}} \\ 1.1 \end{cases} \tag{6.23}$$

f_{u} Ultimate steel strength [Pa]

f_{y} Steel yield strength [Pa]

Here the characteristic yield strength $f_{\mathrm{yk}} = 460$ MPa and ultimate strength $f_{\mathrm{uk}} = 610$ MPa is assumed.

The full back-stay bar design is presented in Appendix F.

The column design is performed according to Eurocode SS-EN 1992-1-1 (CEN, 2008a), with the software StruSoft WIN-Statik 6.4 Concrete Column. Concrete

with strength class C40/50 and reinforcement with a characteristic yield limit $f_{yk} =$ 500 MPa is assumed. An extract of the design in the case of 24 m span length is presented in Appendix G.

The result of the design is presented in Table 6.13, which includes required member dimensions, as well as the total mass of the different members. The latter property is used for comparison of the material efficiency of the different support proposals.

Table 6.13 Design results – Back-stay cable.

L [m]	h_{col} [mm]	b_{col} [mm]	m_{col} [m^3]	n_{rb} [-]	ϕ_{rb} [mm]	n_{bs} [-]	ϕ_{bs} [mm]	m_{bs} [kg]
24	350	350	3750	2+2	16	2	40	273
36	350	350	3750	2+2	20	2	60	615
48	400	400	4750	2+2	20	2	80	1094

h_{col} Concrete column cross-section height

b_{col} Concrete column cross-section width

m_{col} Column concrete mass

n_{rb} Number of reinforcement bars (top + bottom)

ϕ_{rb} Reinforcement bar diameter

n_{bs} Number of back-stay bars

ϕ_{bs} Back-stay steel bar diameter

m_{bs} Total back-stay steel mass

As seen in Table 6.13, the choice is made to use two back-stay bars per column. The two bars could be arranged with an angle between each other as seen in Figure 6.13. The bars could then also work as stabilisers for the column during construction and contribute to the horizontal stability of the building in the transverse direction.

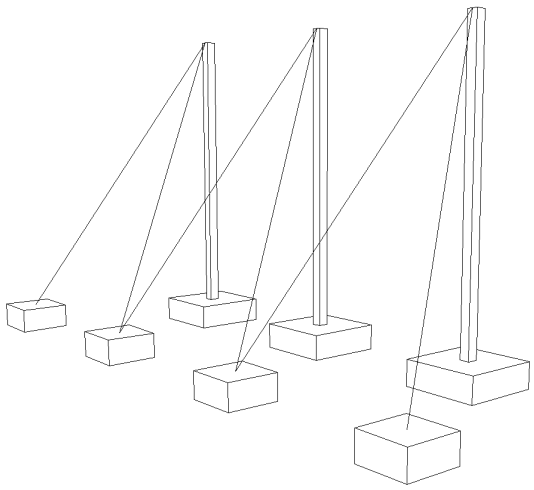

Figure 6.13 Possible arrangement of back-stay bars.

6.5.2 Inclined compression strut

The alternative with an inclined compression strut is similar to the back-stay alternative, with the only difference that the cable is exchanged for a steel compression member. The geometrical constrains of the system are illustrated in Figure 6.14.

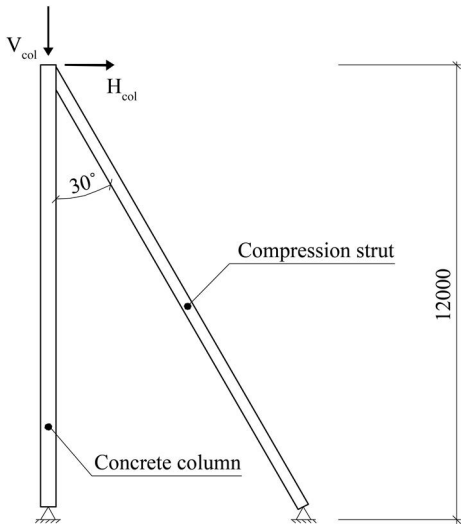

Figure 6.14 Geometrical constraints of compression strut system.

The member is assumed to have a rectangular hollow section made of steel with a characteristic yield limit $f_{\mathrm{yk}} = 355$ MPa.

The design of the compression strut is performed according to Eurocode SS-EN 1993-1-1 (CEN, 2008b), with the software StruSoft WIN-Statik 6.4 Frame Analysis. An extract of the design in the case of 24 m span length is presented in Appendix H.

The results are presented in Table 6.14. Similar to the back-stay bar results, required member dimensions, and the total mass of the different members are provided. For concrete column design, see Table 6.13 and Appendix G.

Table 6.14 Design results – Compression strut.

L [m]	h_{strut} [mm]	b_{strut} [mm]	t [mm]	m_{cs} [kg]
24	350	350	10.0	1473
36	400	400	16.0	2669
48	609.6[1)]		17.5	3545

[1)] Rectangular standard section of sufficient size is not available, and circular cross-section is therefore assumed. The number indicates cross-section diameter.

h_{strut} Strut cross-section height

b_{strut} Strut cross-section width

t Steel thickness

m_{cs} Compression strut steel mass

6.5.3 Bending stiff column

The alternative with a bending stiff column considers a reinforced concrete column, as illustrated in Figure 6.15.

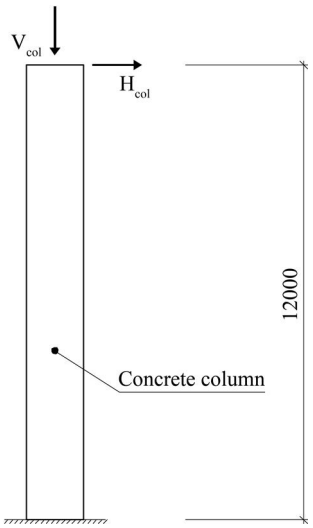

Figure 6.15 Geometrical constraints of bending stiff column system.

Concrete with strength class C40/50 and reinforcement with a characteristic yield limit $f_{\mathrm{yk}} = 500$ MPa is assumed. The design is performed according to Eurocode SS-EN 1992-1-1 (CEN, 2008a), with the software StruSoft WIN-Statik 6.4 Concrete Column. An extract of the design in the case of 24 m span length is presented in Appendix I.

The results are presented in Table 6.15.

Table 6.15 Design results – Bending stiff column.

L [m]	h_{col} [mm]	b_{col} [mm]	m_{col} [kg]	n_{rb} [-]	ϕ_{rb} [mm]	m_{rb} [kg]
24	1500	600	27000	28+28	32	4243
36	2000	800	36000	45+45	32	6818
48	2500	1000	75000	64+64	32	9697

m_{rb} Total mass of reinforcement bars

6.6 Summary of preliminary design

The primary purpose of the preliminary design is to perform a feasibility study of the different systems, and the general conclusion is that all the considered alternatives are possible, with regard to design of main members.

However, the preliminary design further aims at comparing the different proposals to each other, and evaluating their different properties. As one of the principal issues is the structural efficiency, a summary of the material usage for the different proposals is necessary for comparison of the three proposals. To achieve this, a case study is here performed, where the total material usage of the different systems is estimated for a building of given size.

The building considered for the comparison is assumed to be 144 m long and 128 m wide. These dimensions are chosen as they are divisible by the different span lengths and column spacing, and fairly similar to the reference building presented in Section 5.1.1.

The comparison includes the Stress Ribbons, primary and boundary trusses, and tertiary system. Additional members for horizontal support, columns and foundations are not included, as these members are assumed equal for the different proposals.

The total number of members for the different proposals and span lengths is calculated according to the equations below.

The number of SR spans is given by

$$n_{\text{span}} = \frac{144\ \text{m}}{L} \tag{6.24}$$

The total number of intermediate trusses is

$$n_{\text{it}} = n_{\text{span}} - 1 \tag{6.25}$$

The total number of Stress Ribbons is calculated from

$$n_{\text{SR}} = n_{\text{span}} \frac{128\ \text{m}}{c} \tag{6.26}$$

and the total number of boundary trusses is

$$n_{\text{bt}} = 2\frac{128\ \text{m}}{c_{\text{col,b}}} \tag{6.27}$$

The column spacing along the building boundary $c_{\text{col,b}}$ is, according to Section 5.1.2, 8 m.

The total ribbon length L_0 is calculated according to Equation (4.16), derived and presented in Section 4.1.1. The deviation from the span length L is though rather small;

$$L_0 = \begin{cases} 24.7\ \text{m} \\ 36.5\ \text{m} \\ 48.3\ \text{m} \end{cases}$$

6.6.1 Total material usage – Proposal 1

As seen in Section 6.2.4, alternative designs of Proposal 1 are generated for the 24 and 36 m span lengths. The systems considered here are the most structurally efficient, i.e. alternatives b. For Proposal 1 the ribbon spacing c is 8 m.

Regarding tertiary system, corrugated steel sheeting is assumed, and the self-weight of the sheeting is approximated to be 18 kg/m^2.

With the self-weight of the different structural members obtained in the preliminary design and Equations (6.24)-(6.27), the total material usage is calculated and presented in Table 6.16. Note that Proposal 1 requires no boundary trusses.

Table 6.16 Summary of material usage – Proposal 1.

L	[m]	24	36	48
n_{it}	[-]	40	24	16
m_{it}	[kg]	3055	4357	5645
$m_{\text{it,tot}}$	[10^3 kg]	122.2	104.6	90.3
n_{SR}	[-]	102	68	51
m_{SR}	[kg]	1719	5758	15716
$m_{\text{SR,tot}}$	[10^3 kg]	175.3	391.4	801.5
$g_{\text{k,sheet}}$	[kg/m^2]	18.0	18.0	18.0
$m_{\text{sheet,tot}}$	[10^3 kg]	331.8	331.8	331.8

n_{it} Number of primary trusses

m_{it} Self-weight of one primary truss

$m_{\text{it,tot}}$ Total primary truss mass

n_{SR} Number of Stress Ribbons

m_{SR} Self-weight of one Stress Ribbon

$m_{\text{SR,tot}}$ Total Stress Ribbon mass

$g_{\text{k,sheet}}$ Characteristic self-weight of steel sheeting

$m_{\text{sheet,tot}}$ Total steel sheeting mass

6.6.2 Total material usage – Proposal 2

Similar to Proposal 1 the total material usage is calculated from the self-weight of the different members obtained in the preliminary design, and Equations (6.24)-(6.27). Also here steel sheeting is assumed as tertiary system, but since the ribbon spacing is significantly smaller than for Proposal 1, a smaller sheet profile is sufficient. The self-weight of the sheeting is assumed to be 5 kg/m^2.

The results are presented in Table 6.17.

Table 6.17 Summary of material usage – Proposal 2.

L	[m]	24	36	48
n_{it}	[-]	40	24	16
m_{it}	[kg]	3055	4357	5645
$m_{\mathrm{it,tot}}$	[10^3 kg]	122.2	104.6	90.3
n_{bt}	[-]	32	32	32
m_{bt}	[kg]	1049	1609	2861
$m_{\mathrm{bt,tot}}$	[10^3 kg]	33.6	51.5	91.6
n_{SR}	[-]	618	932	1281
m_{SR}	[kg]	240	240	240
$m_{\mathrm{SR,tot}}$	[10^3 kg]	148.2	330.3	602.0
$g_{\mathrm{k,sheet}}$	[kg/m^2]	5.0	5.0	5.0
$m_{\mathrm{sheet,tot}}$	[10^3 kg]	92.2	92.2	92.2

n_{bt} Number of boundary trusses

m_{bt} Self-weight of one boundary truss

$m_{\mathrm{bt,tot}}$ Total boundary truss mass

6.6.3 Total material usage – Proposal 3

For the third proposal the revised design with regard to fire, see Section 6.3.5, is considered. Since the system consists of a continuous sheet, no tertiary system is required. The total material usage is presented in Table 6.18.

Table 6.18 Summary of material usage – Proposal 3.

L	[m]	24	36	48
n_{it}	[-]	40	24	16
m_{it}	[kg]	3055	4357	5645
$m_{\mathrm{it,tot}}$	[10^3 kg]	122.2	104.6	90.3
n_{bt}	[-]	32	32	32
m_{bt}	[kg]	1049	1609	2861
$m_{\mathrm{bt,tot}}$	[10^3 kg]	33.6	51.5	91.6
n_{SR}	[-]	n/a	n/a	n/a
m_{SR}	[kg/m]	717	1060	1553
$m_{\mathrm{SR,tot}}$	[10^3 kg]	550.9	542.6	596.5

6.6.4 Comparison

The results from the estimation of material usage for the various systems are compiled and presented in Figure 6.16. Furthermore, trend lines of how the material consumption of the different proposals varies with the span length are presented in Figure 6.17.

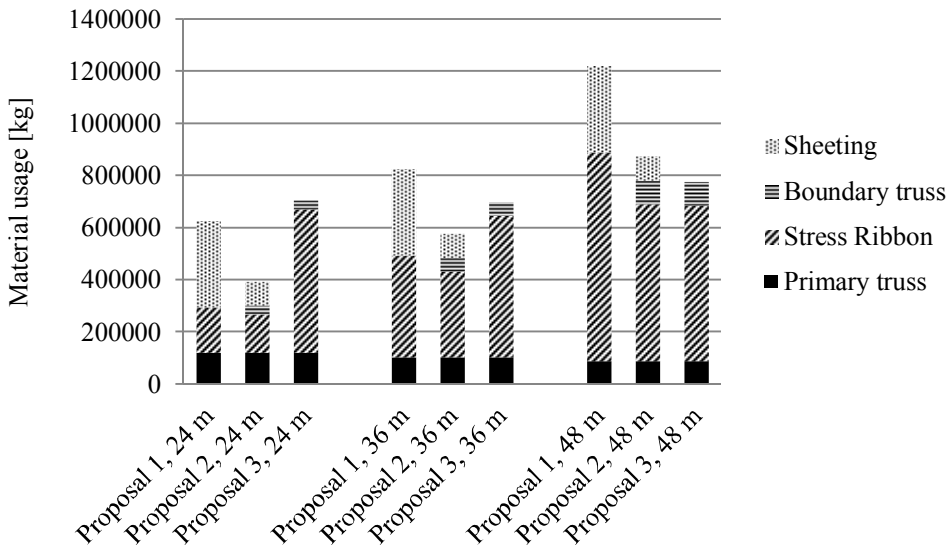

Figure 6.16 Total material usage.

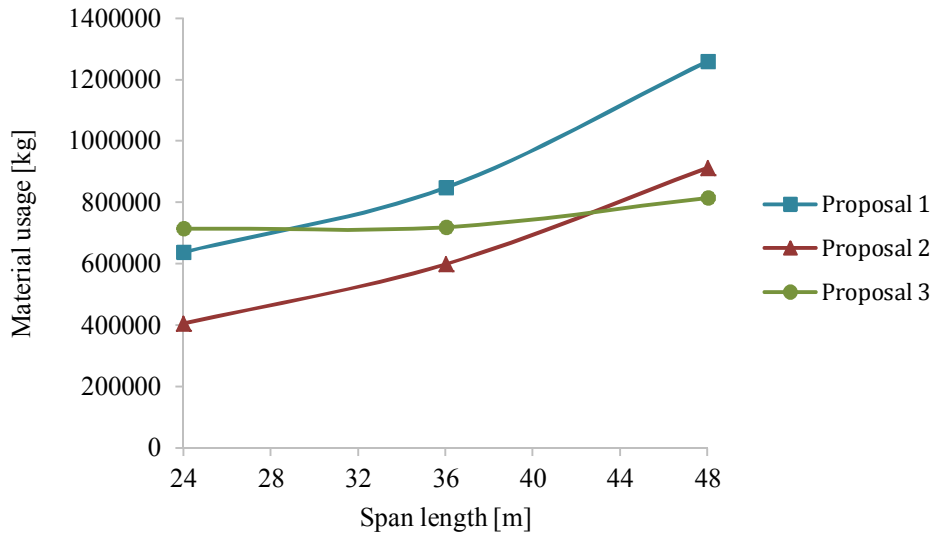

Figure 6.17 Total material usage – trend.

It should be noticed that the comparison includes numerous assumptions and unsolved issues. The results can thereby not be considered precise, but should rather be interpreted as mere indications of the total material consumption. Furthermore, the trend lines in Figure 6.17 are based only on three different span lengths. As shown in Section 6.3.5, Proposal 3 is affected by the fire requirements for the two shorter span lengths, but not for the longest one. To draw conclusions on the extension of this trend line is therefore difficult, but it can be assumed to adopt a shape similar to the trend lines of Proposal 1 and 2. The inclination of the trend line of Proposal 2 can be observed to be less steep than for Proposal 1, and thus an even less steep curve can be expected for Proposal 3. The results of the comparison are further discussed in Section 9.2.

7 Comparison to Conventional Systems

In order to assess the potential benefits of the SR concept the three proposals designed in Chapter 6, are in this chapter compared to more conventional systems with regard to material efficiency.

7.1 Steel truss system

As explained in Section 1.1, the main goal with introducing timber as construction material is to decrease the amount of steel, for environmental reasons. In order to quantify the reduction of steel in the three proposals, they are here compared to the steel truss system of IKEA in Umeå, presented in Section 5.1.1.

As in Section 6.6, the comparison is performed through a case study of a building of dimensions 144 m × 128 m. The comparison includes the primary, secondary and tertiary systems, as well as additional members for horizontal support of the ribbons. Columns and foundations are not included.

7.1.1 Material usage – IKEA Umeå

With the building layout presented in 5.1.1, and self-weight of the different members obtained from construction drawings, the total material usage is estimated. The results are presented in Table 7.1.

Table 7.1 Summary of material usage – IKEA Umeå.

System	L [m]	n_{pri} [-]	m_{pri} [kg]	$m_{\text{pri,tot}}$ [10^3 kg]	n_{sec} [-]	m_{sec} [kg]	$m_{\text{sec,tot}}$ [10^3 kg]	$g_{\text{k,sheet}}$ [kg/m^2]	m_{sheet} [10^3 kg]
Steel truss	24	49	4130	202.4	126	2124	267.6	13.31	214.7

n_{pri} Number of primary beams

m_{pri} Mass of one primary beam

$m_{\text{pri,tot}}$ Total mass of primary beams

n_{sec} Number of secondary beams

m_{sec} Mass of one secondary beam

$m_{\text{sec,tot}}$ Total mass of secondary beams

It should be noticed that the reference building is designed for a snow load which is 50 % higher than the one assumed for the SR proposals. This slightly affects the results as the dimensions, and thus the total mass, would be somewhat smaller for the steel system, if designed for a lower snow load.

7.1.2 Material usage – SR systems

Since the building studied here is the same as in Section 6.6, the material consumption of the different proposals is also the same. However, in addition to what is presented

there, the members for resisting horizontal forces are included here. The method for resisting horizontal forces considered is the one with back-stay bars.

The number of back-stay units is

$$n_{\mathrm{bs}} = 2\left(\frac{128\ \mathrm{m}}{c_{\mathrm{col,b}}} + 1\right) = 34$$

and with the self-weight per back-stay unit according to Table 6.13, the total mass is 10.2 tonnes for the span length of 24 m. Since the span length of the reference building is 24 m, this is the only SR span length considered in the comparison.

7.1.3 Comparison

The total material consumption for the different proposals is compiled and illustrated in Figure 7.1.

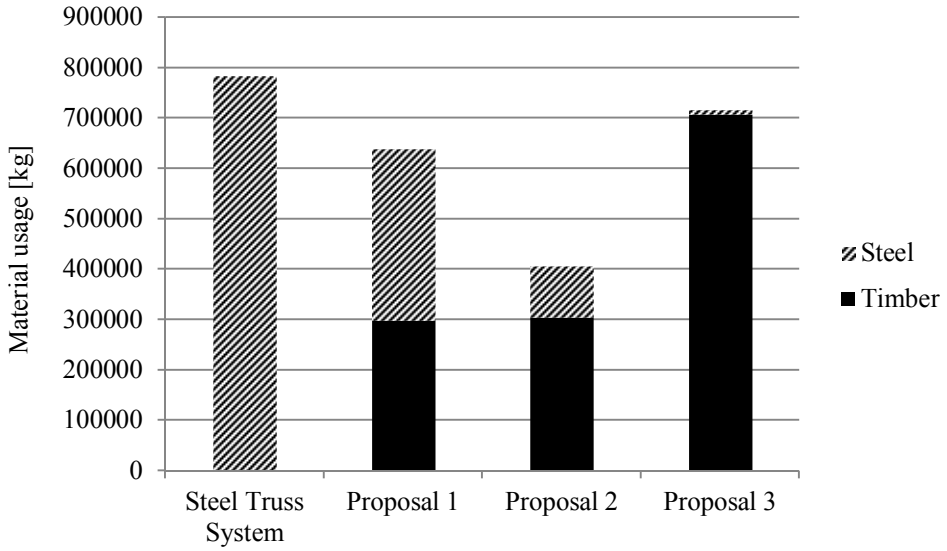

Figure 7.1 Comparison of material usage – Steel truss system and SR proposals, 24 m span length.

With the emission data presented in Section 2.3 the material consumption of the different systems can be translated into CO_2 equivalent, as seen in Table 7.2. As explained in Section 2.3, LCA is a science in itself and there are many factors to take into consideration when performing such an analysis. The aim of this thesis is not to make an accurate LCA, but to focus on development of possible design solutions and to perform a structural design. The data given in Table 7.2 should therefore not be used to draw definitive conclusions, but should rather be interpreted as preliminary indications of the environmental impact of the different systems. Examples of obvious error sources are that data for glulam is used also for LVL and that foundations are not incorporated in the comparison.

Table 7.2 Comparison of CO_2 eq.

System	CO_2 eq. [10^6 kg]			Comparison [%]		
	Generic	Martinsons	Moelven	Generic	Martinsons	Moelven
Steel truss	5.56	1.41	1.41	100	100	100
Proposal 1	2.57	0.95	1.00	46	17	18
Proposal 2	0.87	0.29	0.34	16	5	6
Proposal 3	0.40	0.07	0.18	7	1	3

A thorough discussion of the results is presented in Section 9.4. However, the general observation is that the material consumption is decreased for all of the proposals compared to the reference building. This, in combination with the substitution of steel for timber implies a significant reduction in CO_2 equivalent.

7.2 Timber system

The main benefit of the SR concept is material efficiency. However, as explained previously the system requires various additional components compared to a more conventional beam system in order to function properly. The overall material efficiency actually gained is therefore uncertain, and a comparison to a conventional system is required for assessment of the potential gain.

A comparison is here performed to a building consisting of solid glulam beams, located in Östersund, Sweden; the building is further presented in Section 7.2.1. Similar to the previous case study the comparison includes the primary, secondary and tertiary systems, as well as additional members for horizontal support of the ribbons. Columns and foundations are not included.

7.2.1 Overview – XXL Kv. Släpvagnen, Östersund

The reference building is a structure intended for a department store in Östersund, Sweden. Building data is collected from construction drawings of the structure.

The overall size of the building is approximately 96 m × 40 m. The structural system consists of primary and secondary solid glulam beams supported on glulam columns, arranged as presented in Figure 7.2. The cross-section dimensions of the primary beams are 215 mm × 1440 mm, and the secondary beams are of dimensions 190 mm × 1440 mm. Roof cover is provided by steel sheeting.

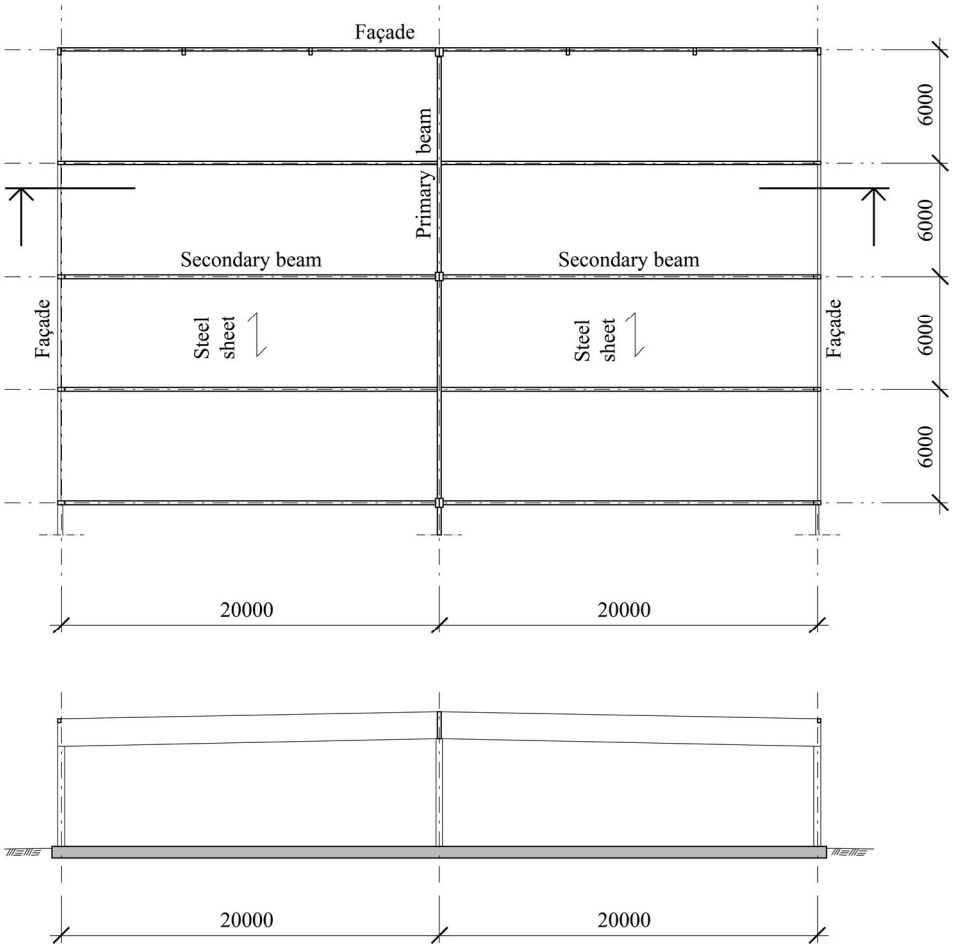

Figure 7.2 Principal roof plan and section of a part of the building.

7.2.2 Material usage – XXL Kv. Släpvagnen, Östersund

As seen in Section 7.2.1, the reference building is significantly smaller than the intended size of the buildings studied in this thesis, c.f. IKEA Umeå, Section 5.1.1. In order to get data comparable to the previous case studies the building dimensions must be extended. The choice is therefore made to assume a total reference building size of 140 m × 132 m. The chosen dimensions are divisible by the span length and column spacing of the reference building, and the total area covered is approximately the same as in the previous case studies.

Table 7.3 Summary of material usage – XXL Kv. Släpvagnen, Östersund.

System	L [m]	n_{pri} [-]	m_{pri} [kg]	$m_{\text{pri,tot}}$ [10^3 kg]	n_{sec} [-]	m_{sec} [kg]	$m_{\text{sec,tot}}$ [10^3 kg]	$g_{\text{k,sheet}}$ [kg/m^2]	m_{sheet} [10^3 kg]
Timber beam	24	66	1783	117.7	161	2627	422.9	15	277.2

Similar to the steel reference building, this building is designed for a snow load which is higher than the snow load assumed for the SR proposals, but here the difference is 25 %. This makes the comparison slightly unbalanced as the dimensions, and thus the total mass, would be somewhat smaller for the solid timber beam system, if designed for the lower snow load.

7.2.3 Comparison

The total material consumption for the different proposals is compiled and illustrated in Figure 7.3.

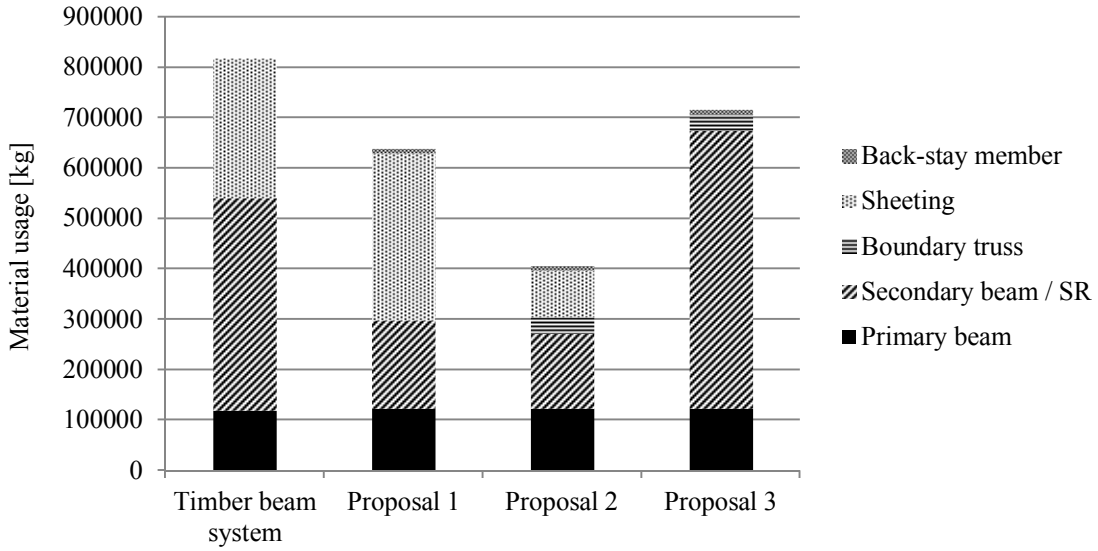

Figure 7.3 Comparison of material usage – Timber beam system and SR proposals.

Similar to the comparison to the steel truss system, the material consumption of the different systems is translated into CO_2 equivalent, as seen in Table 7.4. Also here the results should be considered preliminary indications rather than exact results.

Table 7.4 Comparison of CO_2 eq.

System	CO_2 eq. [10^6 kg]			Comparison [%]		
	Generic	Martinsons	Moelven	Generic	Martinsons	Moelven
Timber beam	2.23	0.81	0.90	100	100	100
Proposal 1	2.57	0.95	1.00	115	118	111
Proposal 2	0.87	0.29	0.34	39	36	38
Proposal 3	0.40	0.07	0.18	18	8	20

Also in this comparison it can be observed that the overall material usage is reduced for the SR proposals compared to the reference building. The results are further discussed in Section 9.4.

8 Details

This chapter treats details for the different proposals, mainly focusing on the connections between SRs and supporting trusses. The primary aim is to present possible principles, rather than final solutions. Thus, design calculations are not performed.

8.1 Ribbon-intermediate truss connection

There might be a variation in stiffness properties of different members, and tolerances for errors during manufacturing and assembly must also be accounted for. For this reason there might be a need for the possibility to adjust the ribbon sag, primarily during construction but also during the service life of the building. One way to achieve this is to provide a connection detail between the ribbon and the primary truss such that the span length, and thus the sag, is adjustable. Since the sag can be controlled by adjusting only one side of the ribbon span, every other connection can be non-adjustable as implied in Figure 8.1.

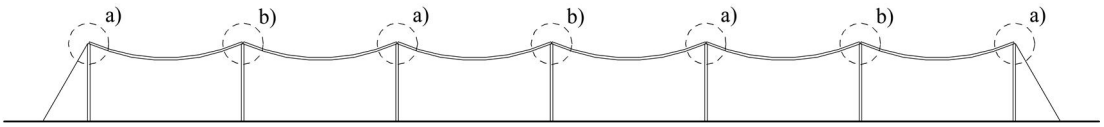

Figure 8.1 Possible arrangement of a) non-adjustable and b) adjustable connections.

With the expression for the ribbon length presented in Equation (4.16), it can be shown that a change of span length L of 0.1 m results in a change of sag f of 0.18 m, 0.26 m and 0.34 m for the span lengths of 24 m, 36 m and 48 m respectively. A considerable change in sag can thus be achieved by a rather small change in span length.

In Figure 8.2 and Figure 8.3 a proposal for how such a detail could be designed is provided. The proposal considered in the figures is Proposal 2, but since the only thing that separates the first and second proposal is the member size and spacing, a similar detail is assumed to be applicable also for Proposal 1. For Proposal 3, the LVL alternative, the detail would however look slightly different; instead of the slotted-in steel plates shown in Figure 8.3, the LVL sheet would be fastened by steel plates attached to the top and bottom of the sheet. Except for that the principle would be the same.

The adjustable connection is achieved by incorporating a turnbuckle at the end of the ribbon, as seen in Figure 8.3. The turnbuckle comprises two threaded rods, one with a left-hand thread and the other with a right-hand thread, connected to each other by a frame or bolt. The length can thus be adjusted by rotating the frame.

In order to only stress the turnbuckle with axial force, a compression strut from the ribbon to the lower chord of the truss is also incorporated. With this solution the connection between the slotted-in plates and the threaded rod is not required to transfer shear and bending moment, which is preferable. The drawback of the compression strut is that it constrains the ribbon end point to move along a circular arc with the radius equal to the strut length. Adjusting the ribbon length with the turnbuckle will thus not only imply an axial displacement of the ribbon end, but also a

vertical displacement. Assuming small adjustments this is however not considered a major problem.

As seen in the overview in Figure 8.2, the ribbon connections can be adapted to the truss so that three out of four connections fit in-between the truss diagonals, while every fourth connection is performed with a steel plate slotted-in in the meeting point of two diagonals. It should be noticed that in Figure 8.2 ribbons are only shown on one side of the truss, while there in fact would be ribbons on both sides, as implied in Figure 8.3.

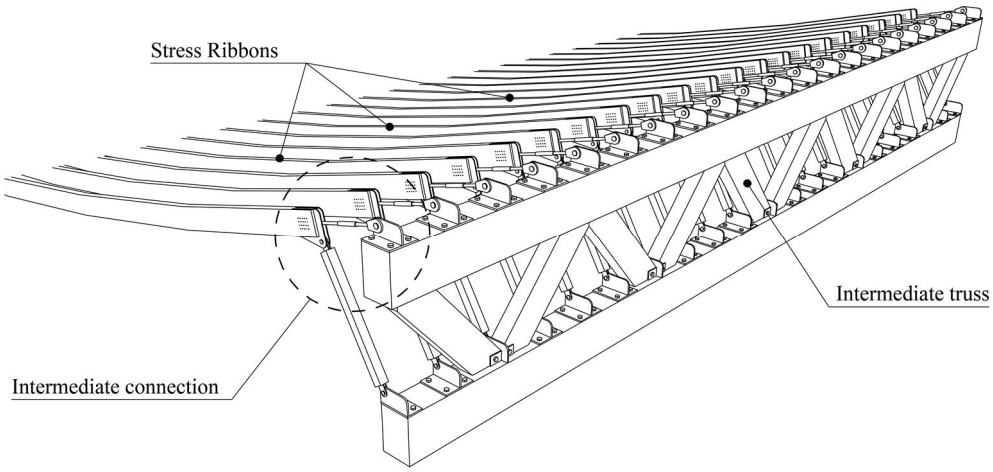

Figure 8.2 Overview of intermediate truss and ribbon connections. Note that the figure only illustrates the ribbon-truss connections. How the connection between truss and column is designed is not considered.

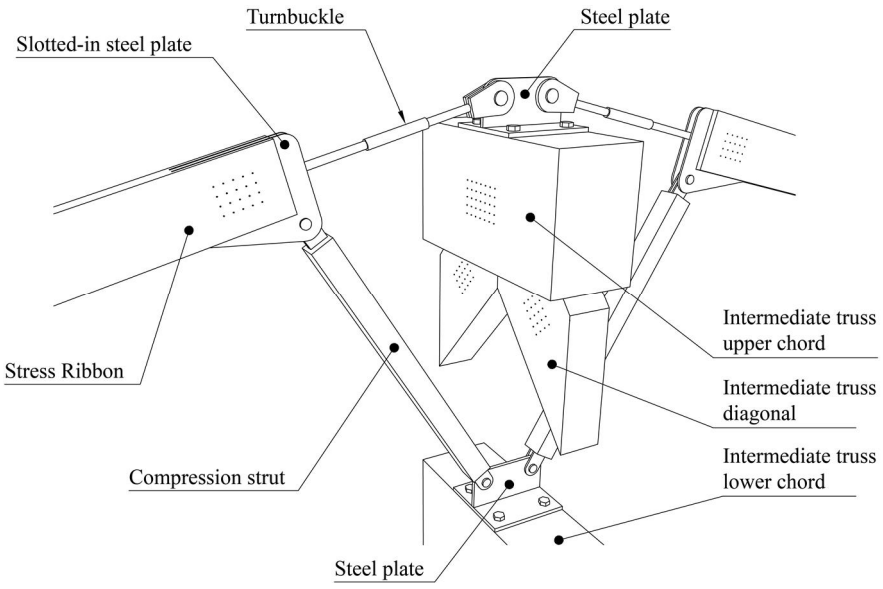

Figure 8.3 Adjustable intermediate connection.

In the connections where adjustability is not required, c.f. Figure 8.1, the ribbon can be directly connected to the top chord of the intermediate truss, as shown in Figure 8.4.

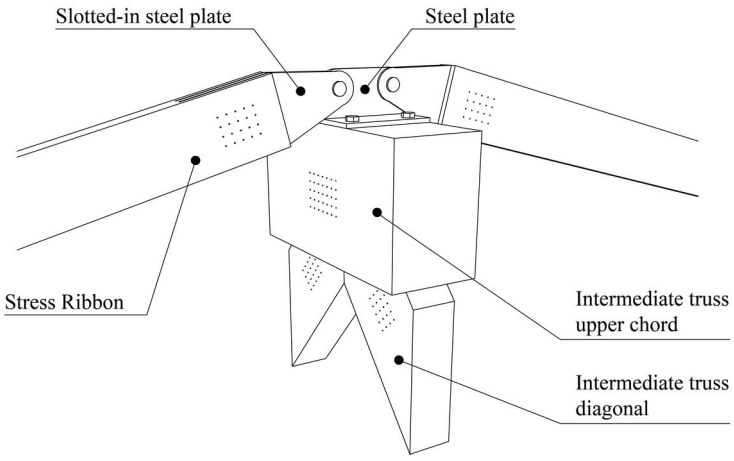

Figure 8.4 Non-adjustable intermediate connection.

8.2 Ribbon-boundary truss connection

As explained in the boundary truss design in Section 6.4.2, the ribbon spacing in Proposal 2 and the assumed connection spacing in Proposal 3, is chosen so that every other connection coincides with a truss node. Where they do not, a steel bar is added to transfer the ribbon force into a truss node. Examples of how such details could be designed are illustrated in Figure 8.5, Figure 8.6 and Figure 8.7. Also here the proposal considered in the figures is Proposal 2, but the principle can be adapted to apply also for Proposal 3.

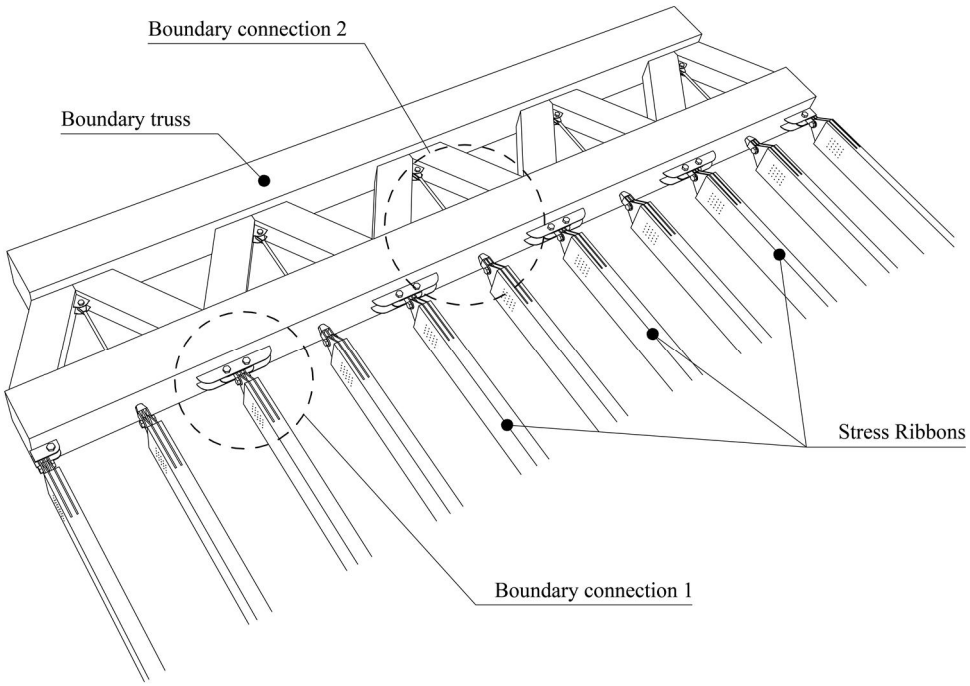

Figure 8.5 Overview of boundary truss and ribbon connections. Note that the figure only illustrates the ribbon-truss connections. How the connection between truss and column is designed is not considered.

In the connections where the ribbon coincides with a truss node, denoted Boundary connection 1, the detail could be designed as illustrated in Figure 8.6. The lower

chord and diagonals of the truss are assembled by slotted-in steel plates. Extruding these steel plates beyond the bottom of the lower chord allows for additional steel plates to be attached to the truss and the slotted-in steel plates of the ribbon to be pin connected with a single bolt.

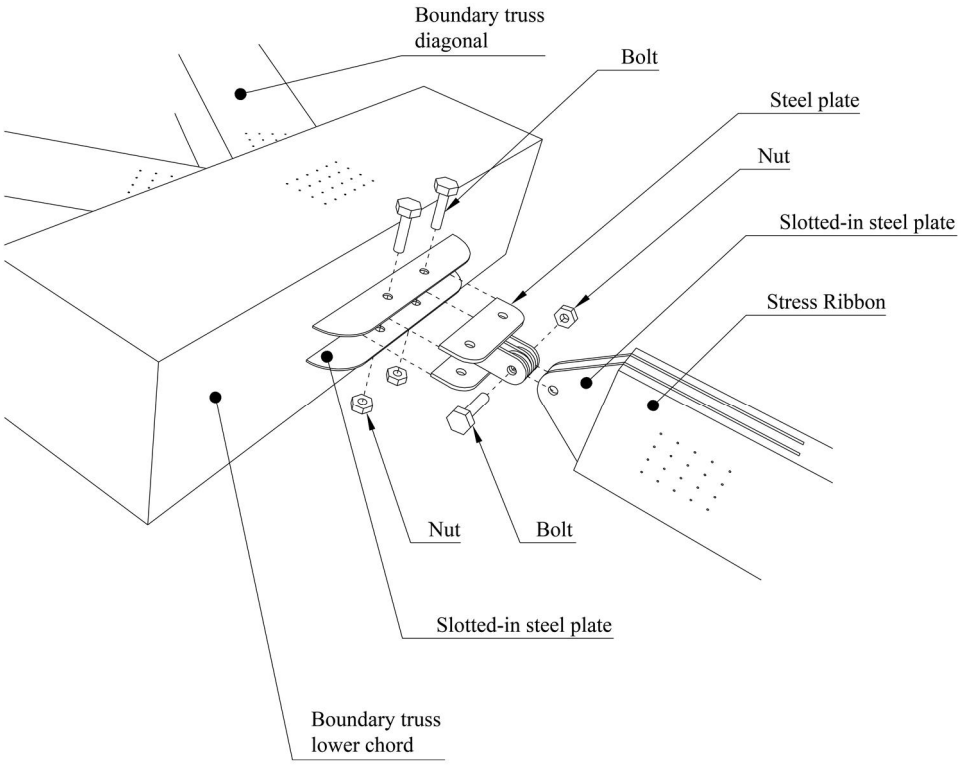

Figure 8.6 Boundary connection 1, exploded view.

In the connections where the ribbon does not coincide with a truss node, denoted Boundary connection 2, the detail could be designed as illustrated in Figure 8.7. A steel rod is attached to the slotted-in steel plates connecting the upper chord and the diagonals of the truss. The rod continues through a predrilled hole in the lower chord and a threaded rod end allows for a connection member to be screwed onto the rod. The slotted-in steel plates of the ribbon can then be pin connected to the truss by a single bolt.

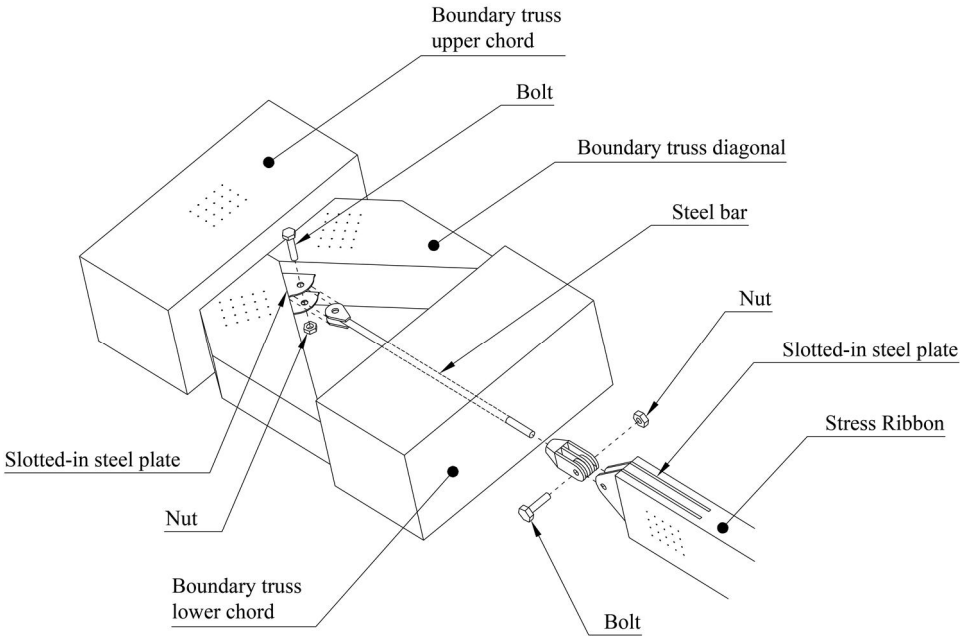

Figure 8.7 Boundary connection 2, exploded view.

8.3 Roof drainage

A function which has not yet been addressed, but is necessary for a roof structure, is the water runoff. Here no actual detail of the roof drainage is presented, but only ideas of how the overall structure can be adapted to introduce an inclination to allow for the water to drain off. Four possible solutions are illustrated in Figure 8.8.

The first alternative is to introduce a one-sided slope by changing the column height along the building. The water will then gather on one side of the building where rain gutters can be installed. For a building of large width also a large height of the apex is required in order to reach sufficient inclination with this alternative.

The second alternative is similar to the first, with the only difference that the roof instead has a two-sided inclination. The apex height can thus be somewhat reduced.

The third alternative has multiple slopes to allow for lower ridges and thus lower overall building height. In this alternative drainage must however be provided in the low point of the roof, i.e. inside the building. Furthermore, a blocked outlet would lead to very large amounts of water on the roof, with possibly devastating consequences. Also, this alternative implies a more complicated geometry of the trusses, as seen in Figure 8.8c.

In the fourth alternative the inclination is not created by an alternated column height, but instead by changing the sag of the SRs. With increasing sag towards the building edges the roof will adopt a double-curved shape with a saddle point in the middle. The complex geometry would lead to more difficult production and assembly, but the design can be considered both interesting and appealing.

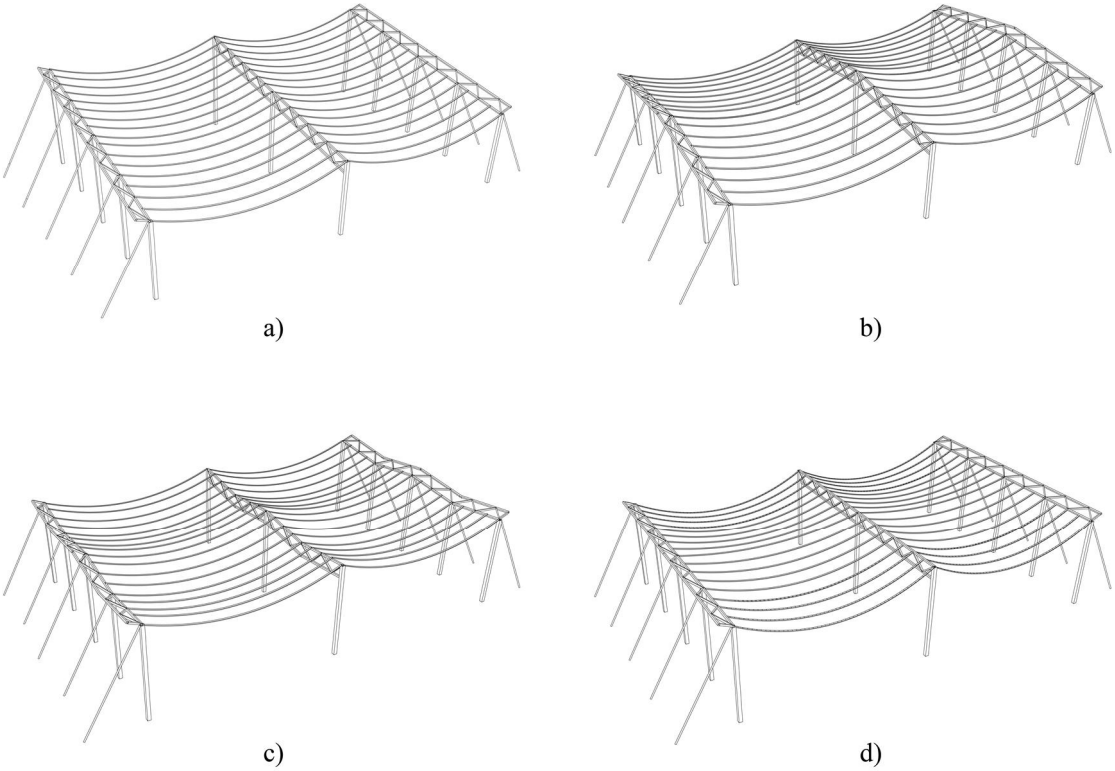

Figure 8.8 Possible method to achieve roof drainage, a) one-sided slope, b) two-sided slope, c) multiple slopes, d) double-curved surface .

In addition to the methods presented above, it should be mentioned that water runoff could also be achieved by alternating the material layers on top of the load-carrying structure rather than the alternating the load-carrying structure itself. For example, an inclination of the roof cladding can be achieved by alternating the thickness of the insulation along the roof.

9 Discussion

In this chapter the results of the preliminary design and the comparison of material efficiency are discussed and evaluated.

9.1 Span length

The preliminary design shows that sufficient capacity can be achieved with reasonable cross-section geometry for all the main members and all of the considered span lengths. A Stress Ribbon roof with a span length in the range of $24 \text{ m} \leq L \leq 48 \text{ m}$ can thereby be considered feasible. With regard to ribbon design even longer spans would be possible, at least for Proposal 2 and 3.

However, by looking at the comparison of material consumption for the different span lengths it can be observed that increased span length implies increased material usage. With increased material consumption less material efficiency is achieved for the superstructure, but also the foundation of the building is affected; naturally, longer span length means less foundations which implies less material consumption. It should though be noticed that an increased weight of the superstructure implies that the load on each foundation is increased. The accumulation of forces in the foundations are thus significantly higher for longer spans, which in fact might imply a net increase of material required for the foundations. The overall environmental gain is therefore uncertain for the longer and heavier alternatives.

Furthermore, with long span lengths the ribbons cannot be full length during transportation, but must be fabricated in smaller segments and joined together on site. This will add an element in the construction process, and will thus be time consuming and economically unfavourable.

The benefits of longer spans can thus be concluded not to be related to material efficiency nor production and assembly. If longer spans are desirable it must be motivated by other factors, such as the practical benefit in terms of flexibility for the end user or aesthetical aspects.

9.2 Proposal comparison

In the preliminary design and comparison of material consumption it can be observed that with regard to structural efficiency the different proposals are suitable in different situations.

Proposal 1 can be considered more suitable for short spans than for long spans. With an increased span length the cross-section size of the ribbons increases quite rapidly, thus reducing the material efficiency. As explained in Section 5.2, Proposal 1 does not require the boundary truss as the ribbons can be directly connected to the columns. This is beneficial since it can be assumed to simplify the assembly and decreases the material usage. However, as seen in the comparison in Figure 6.16 the contribution of the boundary truss to the overall material consumption is small, and the benefit of excluding the boundary truss in Proposal 1 is therefore negligible. On the other hand, the sheeting has a significant contribution to the total material consumption, especially for Proposal 1, which thus falls behind in the competition for material efficiency.

Proposal 2 is very material efficient, especially for short spans. This has much to do with the closer ribbon spacing than in Proposal 1, which implies less influence of the sheeting on the material efficiency. Apart from the contribution of the sheeting it can be observed that Proposals 1 and 2 are quite similar, at least for shorter span lengths.

Only considering ULS design, Proposal 3 is the alternative with the greatest potential with regard to material efficiency; as seen in the design results in Section 6.2.4, sufficient capacity in ULS is reached for a lower material self-weight for Proposal 3 than for the other two alternatives. In addition, the material self-weight presented there only includes the weight of the ribbons, while additional self-weight of the tertiary system required for Proposals 1 and 2 is left out.

However, in some sense the great potential of Proposal 3 is diminished as it suffers from being somewhat too material efficient. As seen in the fire design results in Section 6.3.5, the thin members of Proposal 3 are not sufficiently thick to fulfil the fire requirements, and the cross-section must therefore be increased. Furthermore, though not studied in this thesis, it should be remembered that the systems must also fulfil the SLS requirements; sufficient bending stiffness must be provided for the structure not to deform too much under non-uniform loading conditions, which might further increase the need for thicker members. Yet another thing that might affect the ribbon thickness, but is not studied in detail here, is the connection detail. With regard to the connection of the ribbons in Proposal 3, a sufficient ribbon thickness is required to allow for long enough dowels. As proposed in Section 8.1, the LVL sheets can be fastened by steel plates nailed to either side of the sheet. For practical reasons it would be favourable if the nails on the two sides of the member would not overlap, which then further restricts the minimum thickness of the LVL sheet. All of these factors lead to increased ribbon thickness and thus reduced material efficiency. These effects are though reduced with an increased span length; as seen in the comparison in Figure 6.16 the material consumption of Proposal 3 is higher than Proposals 1 and 2 for the two shorter span lengths considered, but for the longest span length Proposal 3 is the most material efficient solution. Furthermore, the trend lines in Figure 6.17 imply that for even longer span lengths than 48 m the superior structural efficiency of Proposal 3 would be yet more pronounced.

Apart from the material efficiency there are other aspects that separate the different proposals. One of these aspects is production and assembly. Proposal 1 has few members and no boundary truss, which implies a fast assembly. Proposal 3 has more members than Proposal 1, but on the other hand no tertiary system is required and thus one element in the assembly phase can be excluded. The assembly of Proposal 3 should therefore also be rather fast. With the large amount of members, Proposal 2 can be assumed to be the least efficient alternative with regard to assembly.

Regarding water runoff, the two glulam proposals can be considered more suitable than the LVL alternative with regard to the alternatives presented in Section 8.3; to install the glulam ribbons on different heights should not be too complicated, but to tilt the LVL sheets and get them in place to achieve the required inclination is assumed to be a difficult task. The drainage alternative with a double-curved surface can probably not at all be achieved with LVL sheets. For the LVL proposal other alternatives for achieving the required drainage should thus be considered, e.g. the alternative with varying insulation thickness, as previously discussed.

To summarise, the strengths and weaknesses of the different proposals are compiled in Table 9.1.

Table 9.1 Summary of strengths and weaknesses of the three design proposals.

Proposal	Strengths	Weaknesses
1	+ Few members, fast assembly + Requires no boundary beam	- Lacks material efficiency, especially for longer spans - Requires large tertiary span length
2	+ High material efficiency, regardless of span length + Small tertiary span length	- Many members, slow assembly
3	+ Straight-forward and appealing design + High material efficiency for long spans + Few members and no tertiary system, fast assembly	- Lacks material efficiency for short spans

9.3 Boundary supports

By comparing the results of the different support concepts it can be observed that the back-stay cable alternative is the most material efficient concept, and the bending stiff column alternative is the most material consuming concept. With the discussion about structural efficiency in Section 3.1 in mind, this result is hardly surprising. What is noticeable is the significant difference between the alternatives; the required amount of concrete is about 7-16 times larger for the bending stiff column than for the other two alternatives. Also the required amount of steel is substantially increased in the bending stiff column alternative; up to 16 times, dependent on span length and compared alternative. As the main purpose of adopting the SR concept is to achieve material efficiency, the alternative with bending stiff columns is thus considered unsuitable.

The difference in material efficiency between the two other concepts is smaller. In order to find the most suitable solution one would have to perform further studies on case specific circumstances, such as ground conditions, available space and user preferences. Moreover, other options could be investigated, e.g. by combining the strut, tie and bending stiff member in different ways.

9.4 Stress Ribbon structures versus conventional systems

As stated in the introduction of this thesis two of the main purposes of implementing timber Stress Ribbon systems in the context of this study are to decrease the amount of steel and to achieve structural efficiency.

With an IKEA store built-up by a system of steel trusses and steel sheeting as reference object, replacement of the main load-carrying members with timber members obviously results in a decrease of the amount of steel used. However, as seen in Figure 6.16 and stated in Section 9.2 the sheeting has a significant influence

on the overall material consumption. Because of this the amount of steel used is very different for the different proposals; as seen in Figure 7.1, the amount of steel used in Proposal 1 is almost half of the amount used in the steel truss system, whereas in Proposal 2 it is much less and in Proposal 3 almost none. It can be observed that this is also reflected in the estimation of CO_2 equivalent as Proposal 1 shows a lot higher values than Proposals 2 and 3. However, the most important point is that the comparison implies a significant decrease in both material usage and CO_2 equivalent for all of the proposals. To further decrease the amount of steel, other solutions for the tertiary system could be investigated, e.g. prefabricated timber panels.

The comparison with the timber beam system further emphasises the structural efficiency of the Stress Ribbon systems, and shows that structural and environmental benefits can be gained also in comparison to systems of the same material.

It should be remembered, as explained previously, that the reference buildings are both designed for a higher load than the SR proposals. If they were designed for the same load it is reasonable to assume that the difference in material consumption would be smaller. However, another thing that should not be forgotten when evaluating the results is that the SR proposals are designed to reach a utilization ratio of only 50%. Whether the weakening effect of the connections actually is as high as 50% is uncertain, and there might thus be additional capacity to gain there. Altogether, the generated results are considered a reasonable implication of the benefits of the SR systems, despite the various uncertainties.

10 Conclusions

The Stress Ribbon concept can be defined as a suspended structure with the shape of a hanging cable, provided with additional stiffness. Through the cable shape a Stress Ribbon structure transforms vertical load into axial tension, which improves the structural efficiency compared to ordinary beams acting in bending.

The three design proposals developed in this thesis can all be concluded to be feasible roof systems with regard to ULS design. Moreover, the systems are not only feasible, but it can also be concluded that the SR concepts studied are in general more material efficient than conventional systems. However, the study shows that the different proposals have different strengths and weaknesses, with regard to both material efficiency and other aspects. None of the considered proposals can therefore be ruled out or deemed more preferable, without consideration to case specific circumstances and desired properties.

A consequence of the adoption of cable action is large horizontal forces which must be resisted at the ribbon ends. Three methods for how to resist these forces were studied; the conclusions drawn are that a bending stiff column is not a suitable alternative, as it diminishes the material efficiency gained from the Stress Ribbon concept. The strut and the tie alternatives on the other hand, are far more material efficient and these alternatives are therefore the recommended solutions.

Altogether, it can be concluded that the Stress Ribbon concept is a very promising system for use in long-span roof structures, with structural efficiency as the main benefit.

11 Further studies

Since this thesis only covers preliminary design of the developed proposals there are a number of subjects to address in future research, in order to further develop the structural systems. Some recommendations for further studies are therefore listed below.

SLS analysis – The SR systems have relatively low bending stiffness, and might therefore be susceptible to deformations under non-uniform loads. Establishment of reasonable loading situations and studies on the deformations of the systems in SLS is therefore required. If the SLS analysis would show too large deformations additional measures to provide sufficient stiffness, c.f. Section 3.3, must be investigated.

Dynamic analysis – In order to further verify the structural rigidity of the systems, an analysis taking the dynamic behaviour into account is required. Here the most critical action is the wind load.

Connections – The connections presented in this thesis are just principles, and further development and design calculations have to be performed to verify the performance.

LVL behaviour – As explained in Section 5.4, the members of the LVL proposal are assumed to be produced without curvature. The behaviour of such a member has to be studied in order to assess whether additional loading is required during construction to achieve the desired shape, and to study if there is any risk of bending failure during construction. Furthermore, as mentioned in Section 6.4.2, the necessity of the boundary truss in the LVL alternative could be studied; the LVL sheet might have sufficient in-plane shear capacity to transfer the loads to the columns without the boundary truss.

Tertiary system – The tertiary system assumed in this thesis is corrugated steel sheeting. However, other possible solutions, such as prefabricated timber elements could be investigated in order to further reduce the steel consumption.

Construction method – An appropriate construction method has to be developed. One possible approach is the one adopted in the Nagano Olympic Memorial Arena, presented in Section 3.5.2, but also other methods could be investigated.

Environmental benefits – A more accurate study of the environmental benefits could be performed, with correct and verified data including the complete building.

12 References

12.1 Literature

Anisotropi (n.d). In Nationalencyklopedin. Retrieved 2016-02-17, from http://www.ne.se.proxy.lib.chalmers.se/uppslagsverk/encyklopedi/lång/anisotropi

Ban, S., Yoshida, A. & Motohashi, S. (1998) Nagano Olympic Memorial Arena: Design and Construction. *IABSE reports = Rapports AIPC = IVBH Berichte,* Volume 79, pp. 737-742. doi: 10.5169/seals-59969

Baus, U. & Schlaich, M. (2008). *Footbridges: Construction, Design, History.* Basel: Birkhäuser.

Bechthold, M. & Schodek, D. L. (2008). *Structures.* 6th ed. Upper Saddle River, New Jersey: Pearson Prentice Hall.

Brüninghoff, H. (1993). The Essing Timber Bridge, Germany. *Structural Engineering International,* 3(2), pp. 70-72.

Carling, O. (2001). *Limträhandbok.* Stockholm: Svenskt Limträ AB.

Crocetti R., Johansson M., Johnsson H., Kliger R., Mårtensson A., Norlin B., Pousette A., Thelandersson S. (2011). *Design of Timber Structures.* Stockholm: Swedish Forest Industries Federation.

Frühwald, A., Welling, J. & Scharai-Rad, M. (2003). *Comparison of Wood Products and Major Substitutes with Respect to Environmental and Energy Balances.* Retrieved from https://www.unece.org/fileadmin/DAM/timber/docs/sem-1/papers/r32Fruehwald.doc

Goldack, A., Schlaich, M. & Meiselbach, M. (2016). Stress Ribbon Bridges: Mechanics of the Stress Ribbon on the Saddle. *Journal of Bridge Engineering,* 21(5). doi: 10.1061/(ASCE)BE.1943-5592.0000869

Johansson, L., Samuelsson, S. & Engström, D. (2000). *Stora Träkonstruktioner* (Trita-ARK. Forskningspublikation, 2000:2). Stockholm: Trita-ARK.

Ludescher, G., Braun, F. & Bachmann, U. (2007). Stress-Ribbon Structures of the New Stuttgart Trade Fair Exhibition Halls. *Structural Engineering International,* 17(1), pp. 22-27. Retrieved from http://www.ingentaconnect.com.proxy.lib.chalmers.se/content/iabse/sei/2007/00000017/00000001/art00007

Marti, P. (2013). *Theory of Structures: Fundamentals, Framed Structures, Plates and Shells.* Berlin: Wilhelm Ernst & Sohn.

Peñaloza, D.(2015). *Exploring Climate Impacts of Timber Buildings - The Effects from Including Non-Traditional Aspects in Life Cycle Impact Assessment* (Licentiate Thesis, KTH Royal Institute of Technology, Department of Civil and Architectural Engineering). Retrieved from http://kth.diva-portal.org/smash/get/diva2:793941/FULLTEXT01.pdf

Samuelsson, A. & Wiberg, N.-E. (1980). *Byggnadsstatikens Bärverk.* Lund: Studentlitteratur.

Strasky, J. (2011). *Stress Ribbon and Cable-Supported Pedestrian Bridges,* London: ICE Publishing.

12.2 Regulations and codes

Boverket (2015) BFS 2015:6, EKS 10. Boverkets föreskrifter om ändring i verkets föreskrifter och allmänna råd (2011:10) om tillämpning av europeiska konstruktionsstandarder (eurokoder). Retrieved at http://www.boverket.se/

CEN (2005). SS-EN 1991-1-3. Eurocode 1 – Actions on structures – Part 1-3: General actions – Snow loads. Stockholm: SIS Förlag AB. Retrieved at https://enav.sis.se/

CEN (2008a). SS-EN 1992-1-1. Eurocode 2: Design of concrete structures – Part 1-1: General rules and rules for buildings. Stockholm: SIS Förlag AB. Retrieved at https://enav.sis.se/

CEN (2008b). SS-EN 1993-1-1. Eurocode 3: Design of steel structures – Part 1-1: General rules and rules for buildings. Stockholm: SIS Förlag AB. Retrieved at https://enav.sis.se/

CEN (2009). SS-EN 1995-1-1. Eurocode 5: Design of timber structures – Part 1-1: General – Common rules and rules for buildings. Stockholm: SIS Förlag AB. Retrieved at https://enav.sis.se/

CEN (2010). SS-EN 1995-1-2. Eurocode 5: Design of timber structures – Part 1-2: General – Structural fire design. Stockholm: SIS Förlag AB. Retrieved at https://enav.sis.se/

CEN (2013) SS-EN 14080:2013. Timber structures – Glued laminated timber and glued solid timber – Requirements. Stockholm: SIS Förlag AB. Retrieved at https://enav.sis.se/

VTT (2009) VTT Certificate No 184/03. Retrieved at https://www.moelven.com/Documents/Toreboda/Kerto/Kerto%20VTT%20Certificate%20No%20184-03%20Revision%2024%20March%202009,%20Gamla%20Kertohandboken%20Engelska.pdf

12.3 Images

Listed in order of appearance.

[1] Figure 3.8: *"Holzbrücke in Essing"* by Friedhelm Dröge – Licenced under the Creative Commons Attribution-Share Alike 4.0 International license. Retrieved at https://upload.wikimedia.org/wikipedia/commons/8/82/Essing_Holzbr%C3%BCcke_fd_%283%29.JPG

[2] Figure 3.10: *"Wooden bridge ober the Altmuehl/Main-Danube Canal at Essing"* by Brego – Licenced under GNU Free Documentation License, Version 1.2 or later version published by Free Software Foundation. Retrieved at https://upload.wikimedia.org/wikipedia/commons/7/7b/Holzbr%C3%BCcke_bei_Essing_1.jpg

[3] Figure 3.12: "日本語: エムウェーブの外観写真。デジカメで撮影" by Maclourin – Licensed under the Creative Commons Attribution-Share Alike 3.0 Unported license. Retrieved at https://commons.wikimedia.org/wiki/File:M-wave.JPG

[4] Figure 3.14: *"Hall 4 of the fairgrounds Stuttgart, Germany"* by JuergenG – Licenced under GNU Free Documentation License, Version 1.2 or later version published by Free Software Foundation. Retrieved at

https://upload.wikimedia.org/wikipedia/commons/8/87/Stuttgart_Messe_Halle4_P1270692.JPG

[5] Figure 3.15: *"Standard Hall – cross sections"* – Photo from: Ludescher, G., Braun, F. & Bachmann, U. (2007). Stress-Ribbon Structures of the New Stuttgart Trade Fair Exhibition Halls. *Structural Engineering International,* 17(1), pp. 22-27. Retrieved from http://www.ingentaconnect.com.proxy.lib.chalmers.se/content/iabse/sei/2007/00000017/00000001/art00007

[6] Figure 3.16: *"Grand Hall – erection of roof shell"* – Photo from: Ludescher, G., Braun, F. & Bachmann, U. (2007). Stress-Ribbon Structures of the New Stuttgart Trade Fair Exhibition Halls. *Structural Engineering International,* 17(1), pp. 22-27. Retrieved from http://www.ingentaconnect.com.proxy.lib.chalmers.se/content/iabse/sei/2007/00000017/00000001/art00007

[7] Figure 3.17: *"Main terminal of Washington Dulles International Airport (IAD/KIAD), in Fairfax and Loudoun counties in Virginia, United States, designed by Finnish architect Eero Saarinen"* by JetBlastBWI – Released into the public domain by its author. Retrieved at https://upload.wikimedia.org/wikipedia/commons/a/a8/Dulles_Airport_Terminal.jpg

Appendix A – Standard Dimensions of Glulam And Kerto

In this Appendix the standard dimension of glulam and Kerto are presented.

A.1 Standard dimensions of glulam

Table A-1 Standard cross-section dimensions of glulam.

Height [mm]	Width [mm]									
	42	56	66	78	90	115	140	165	190	215
180	x	x	x	x	x	x	x	x	x	x
225	x	x	x	x	x	x	x	x	x	x
270	x	x	x	x	x	x	x	x	x	x
315	x	x	x	x	x	x	x	x	x	x
360	x	x	x	x	x	x	x	x	x	x
405	x	x	x	x	x	x	x	x	x	x
450	x	x	x	x	x	x	x	x	x	x
495	x	x	x	x	x	x	x	x	x	x
540	x	x	x	x	x	x	x	x	x	x
585	x	x	x	x	x	x	x	x	x	x
630	x	x	x	x	x	x	x	x	x	x
675	x	x	x	x	x	x	x	x	x	x
720		x	x	x	x	x	x	x	x	x
765		x	x	x	x	x	x	x	x	x
810		x	x	x	x	x	x	x	x	x
855			x	x	x	x	x	x	x	x
900			x	x	x	x	x	x	x	x
945			x	x	x	x	x	x	x	x
990				x	x	x	x	x	x	x
1035				x	x	x	x	x	x	x
1080				x	x	x	x	x	x	x
1125					x	x	x	x	x	x
1170					x	x	x	x	x	x
1225					x	x	x	x	x	x
1260						x	x	x	x	x
1305						x	x	x	x	x
1350						x	x	x	x	x
1395							x	x	x	x
1440							x	x	x	x
1485							x	x	x	x
1530							x	x	x	x
1575							x	x	x	x
1620							x	x	x	x

x = Available dimensions

A.2 Standard dimensions of Kerto

Table A-2 Standard dimensions of Kerto.

Product[1)]	Thickness [mm]	Width / height [mm]								
		200	225	260	300	360	400	450	500	600
S/Q	27	x	x							
S/Q	33	x	x	x						
S/Q	39	x	x	x	x					
S/Q	45	x	x	x	x	x				
S/Q	51	x	x	x	x	x	x			
S/Q	57	x	x	x	x	x	x	x		
S/Q	63	x	x	x	x	x	x	x	x	
S/Q	69	x	x	x	x	x	x	x	x	x
S	75	x	x	x	x	x	x	x	x	x
S	81	x	x	x	x	x	x	x	x	x
S	90	x	x	x	x	x	x	x	x	x

1) Kerto-Q is also available in widths of 1800/2500 mm or sawn into required width.

x = Available dimensions

Appendix B1 - Calculation Procedure ULS design - Glulam

In this Appendix the calculation procedure for the ULS design of glulam ribbons is presented. The considered proposal is Proposal 2 and the span length is 24 m. However, the procedure is the same for Proposal 1, and for other span lengths.

B1.1 Geometry

Span length $L := 24\ m$

Span width $B := 8\ m$

Ribbon spacing $c := 0.8\ m$

Initial sag $f := 2.5\ m$

Assumed SR cross-section $b := 78\ mm$ $h := 180\ mm$ $A_{cs} := b \cdot h = 0.014\ m^2$

Moment of inertia $I_y := \frac{b \cdot h^3}{12} = \left(3.791 \cdot 10^{-5}\right)\ m^4$

B1.2 Material Properties

SR material Glulam GL30h

Density $\rho_{g.mean} := 4.8\ \frac{kN}{m^3}$

Partial factor for glulam $\gamma_{M.g} := 1.25$

Service class 1

Load duration Medium term action

Modification factor for load duration and service class $k_{mod} := 0.8$

Creep factor $k_{def} := 0$ (Creep not considered)

Factor for quasi-permanent snow load $\psi_{2.s} := 0.2$

Characteristic mean modulus of elasticity parallel to fibre $E_{0.g.mean} := 13.6\ GPa$

Final char. mean modulus of elasticity parallel to fibre $E_{0.g.mean.fin} := \frac{E_{0.g.mean}}{1 + \psi_{2.s} \cdot k_{def}} = 13.6\ GPa$

Design mean modulus of elasticity parallel to fibre

$$E_{0.g.d} := \frac{E_{0.g.mean.fin}}{\gamma_{M.g}} = 10.88\ GPa$$

Size factor for tensile strength

$$k_{h.t} := \begin{cases} \min\left(\left(\frac{600\ mm}{b}\right)^{0.1}, 1.1\right) & \text{if } b < 600\ mm \\ 1 & \text{else} \end{cases} = 1.1$$

Characteristic tensile strength parallel to fibres

$$f_{t.0.g.k} := 24\ MPa$$

Design tensile strength parallel to fibres

$$f_{t.0.g.d} := k_{mod} \cdot k_{h.t} \frac{f_{t.0.g.k}}{\gamma_{M.g}} = 16.896\ MPa$$

Size factor for bending strength

$$k_{h.m} := \begin{cases} \min\left(\left(\frac{600\ mm}{h}\right)^{0.1}, 1.1\right) & \text{if } h < 600\ mm \\ 1 & \text{else} \end{cases} = 1.1$$

Characteristic bending strength

$$f_{m.g.k} := 30\ MPa$$

Design bending strength

$$f_{m.g.d} := k_{mod} \cdot k_{h.m} \frac{f_{m.g.k}}{\gamma_{M.g}} = 21.12\ MPa$$

B1.3 Loads

B1.3.1 Self-weight

SR self-weight

$$g_{k.SR} := \rho_{g.mean} \cdot A_{cs} = 0.067\ \frac{kN}{m}$$

Additional self-weight (sheeting etc.)

$$g_{k.add} := 1\ \frac{kN}{m^2} \cdot c = 0.8\ \frac{kN}{m}$$

Total characteristic self-weight

$$g_k := g_{k.SR} + g_{k.add} = 0.867\ \frac{kN}{m}$$

B1.3.2 Snow load

Characteristic snow load

$$s_k := 2.0\ \frac{kN}{m^2} \cdot c = 1.6\ \frac{kN}{m}$$

Snow shape factor

$$\mu_1 := 1.0$$

Factor for combination value of snow $\psi_{0.s} := 0.7$

B1.3.3 Load combination

Security factor $\gamma_d := 1.0$

Total design load (eq. 6.10a) $q_{d.6.10a} := \gamma_d \cdot \langle 1.35\ g_k + 1.5\ \psi_{0.s} \cdot \mu_1 \cdot s_k \rangle = 2.851\ \frac{kN}{m}$

Total design load (eq. 6.10b) $q_{d.6.10b} := \gamma_d \cdot \langle 0.89 \cdot 1.35\ g_k + 1.5\ \mu_1 \cdot s_k \rangle = 3.442\ \frac{kN}{m}$

Design self-weight

$$G_d := \begin{cases} \text{if } q_{d.6.10a} \geq q_{d.6.10b} \\ \quad \gamma_d \cdot 1.35\ g_k \\ \text{else} \\ \quad \gamma_d \cdot 0.89 \cdot 1.35\ g_k \end{cases} = 1.042\ \frac{kN}{m}$$

Design imposed load

$$Q_d := \begin{cases} \text{if } q_{d.6.10a} \geq q_{d.6.10b} \\ \quad \gamma_d \cdot 1.5\ \psi_{0.s} \cdot \mu_1 \cdot s_k \\ \text{else} \\ \quad \gamma_d \cdot 1.5\ \mu_1 \cdot s_k \end{cases} = 2.4\ \frac{kN}{m}$$

B1.4 Analysis

Horizontal reaction force from self-weight $H_g := \frac{G_d \cdot L^2}{8\ f} = 0.03\ MN$

Cable shape function $z(x) := -\frac{4\ f}{L^2}\ x^2 + \frac{4\ f}{L}\ x$

First derivative of cable shape function $z'(x) := -\frac{8\ f}{L^2}\ x + \frac{4\ f}{L}$

Factor λ $\lambda(\Delta H) := \sqrt{\frac{H_g + \Delta H}{E_{0.g.d} \cdot I_y}}$

Initial guess value for ΔH $\Delta H_{guess} := H_g$

Equation for calculation of horizontal force from variable load:

$$\Delta H_{guess} = \frac{Q_d - G_d \frac{\Delta H_{guess}}{H_g}}{2\ \langle H_g + \Delta H_{guess} \rangle}\ 16\ f \cdot E_{0.g.d} \cdot A_{cs} \cdot \left(\frac{1}{12} - \frac{1}{\langle \lambda \langle \Delta H_{guess} \rangle \cdot L \rangle^2} + \frac{2\ tanh\left(\frac{\lambda \langle \Delta H_{guess} \rangle \cdot L}{2} \right)}{\langle \lambda \langle \Delta H_{guess} \rangle \cdot L \rangle^3} \right)$$

orizontal force from variable oad — $\Delta H := \text{find}(\Delta H_{guess}) = 0.068\ MN$

Redefinition of factor λ — $\lambda := \lambda(\Delta H) = 0.488\ \frac{1}{m}$

Total horizontal load — $H := H_g + \Delta H = 0.098\ MN$

Deflection:

$$w(x) := \frac{Q_d - G_d \frac{\Delta H}{H_g}}{2\ H} \left(\frac{L^2}{4} - \frac{2}{\lambda^2} + \frac{2\ \cosh\left(\lambda \cdot \left(x - \frac{L}{2}\right)\right)}{\lambda^2\ \cosh\left(\frac{\lambda \cdot L}{2}\right)} - \left(x - \frac{L}{2}\right)^2 \right)$$

First two derivatives of the deflection:

$$w'(x) := \frac{Q_d - G_d \frac{\Delta H}{H_g}}{H} \left(\operatorname{sech}\left(\frac{\lambda \cdot L}{2}\right) \sinh\left(\lambda \cdot \left(x - \frac{L}{2}\right)\right) \frac{1}{\lambda} - \left(x - \frac{L}{2}\right) \right)$$

$$w''(x) := \frac{Q_d - G_d \frac{\Delta H}{H_g}}{H} \left(\operatorname{sech}\left(\frac{\lambda \cdot L}{2}\right) \cosh\left(\lambda \cdot \left(x - \frac{L}{2}\right)\right) - 1 \right)$$

Normal force in SR — $N(x) := H \sqrt{1 + (z'(x) + w'(x))^2}$

Bending moment in SR — $M(x) := -E_{0.g.d} \cdot I_y\ w''(x)$

B1.5 Results

Maximum deflection — $w_{max} := w\left(\frac{L}{2}\right) = 0.02\ m$

Maximum total sag (incl. deflection) — $f_{max} := f + w_{max} = 2.52\ m$

Horizontal force due to self-weight — $H_g = 30.015\ kN$

Horizontal load due to variable load — $\Delta H = 68.301\ kN$

Total horizontal load in SR — $H = 98.316\ kN$

Total horizontal load at column — $H_{tot} := H \cdot \frac{B}{c} = 983.156\ kN$

Design normal force in SR $N_{Ed.SR} := N(0\ m) = 106.618\ kN$

Design tensile stress $\sigma_{t.0.d} := \frac{N_{Ed.SR}}{A_{cs}} = 7.594\ MPa$

Design bending moment in SR $M_{Ed.SR} := M\left(\frac{L}{2}\right) = 0.1186\ kN \cdot m$

Design bending stress $\sigma_{m.y.d} := \frac{M_{Ed.SR}}{I_y}\ \frac{h}{2} = 0.282\ MPa$

Ratio between bending and normal stress $ratio := \frac{\sigma_{m.y.d}}{\sigma_{t.0.d}} = 0.037$

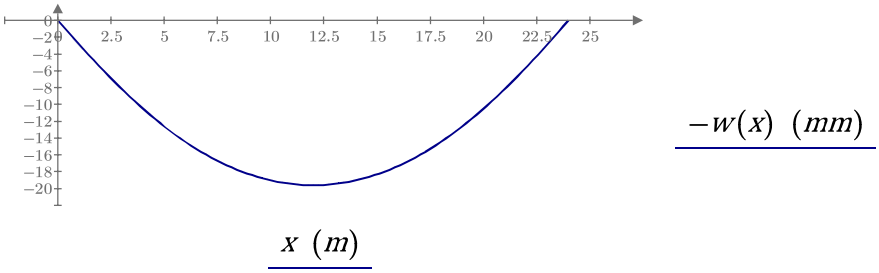

Figure B1.1 Deflection of SR.

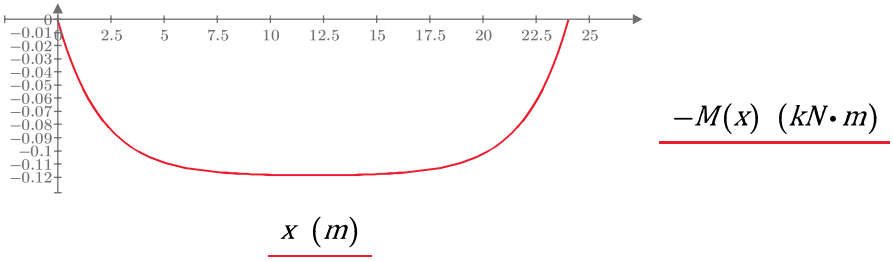

Figure B1.2 Bending moment distribution.

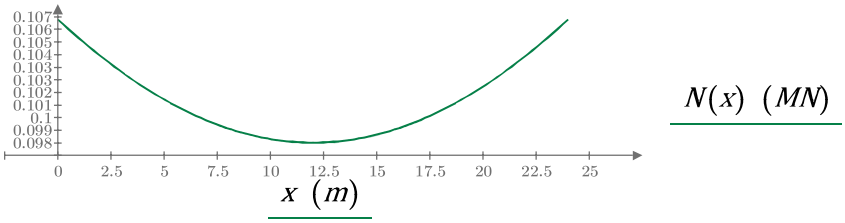

Figure B1.3 Normal force distribution.

B1.6 Utilisation check

Utilization in tension $util_t := \frac{\sigma_{t.0.d}}{f_{t.0.g.d}} = 0.449$

Utilization in bending $util_m := \frac{\sigma_{m.y.d}}{f_{m.g.d}} = 0.013$

Total utilization $util_{tot} := \frac{\sigma_{m.y.d}}{f_{m.g.d}} + \frac{\sigma_{t.0.d}}{f_{t.0.g.d}} = 0.463$

Appendix B2 - Calculation Procedure ULS design - LVL

In this Appendix the calculation procedure for the ULS design of LVL ribbons is presented. The considered proposal is Proposal 3 and the span length is 24 m. However, the procedure is the same for other span lengths.

B2.1 Geometry

Span length $L := 24\ m$

Span width $B := 8\ m$

Ribbon spacing $c := 1\ m$

Initial sag $f := 2.5\ m$

Assumed SR cross-section $b := 1000\ mm \qquad h := 27\ mm \qquad A_{cs} := b \cdot h = 0.027\ m^2$

Moment of inertia $I_y := \frac{b \cdot h^3}{12} = \left(1.640 \cdot 10^{-6}\right)\ m^4$

B2.2 Material Properties

Stress Ribbon material LVL (Kerto-Q)

Density $\rho_{Q.mean} := 5.1\ \frac{kN}{m^3}$

Partial factor for glulam $\gamma_{M.Q} := 1.2$

Service class 1

Load duration Medium term action

Modification factor for load duration and service class $k_{mod} := 0.8$

Creep factor $k_{def} := 0$ (Creep not considered)

Factor for quasi-permanent snow load $\psi_{2.s} := 0.2$

Characteristic mean modulus of elasticity parallel to fibre $E_{0.Q.mean} := 10.5\ GPa$

Final char. mean modulus of elasticity parallel to fibre $E_{0.Q.mean.fin} := \frac{E_{0.Q.mean}}{1 + \psi_{2.s} \cdot k_{def}} = 10.5\ GPa$

Design mean modulus of elasticity parallel to fibre

$$E_{0.Q.d} := \frac{E_{0.Q.mean.fin}}{\gamma_{M.Q}} = 8.75\ GPa$$

Characteristic tensile strength parallel to fibres

$$f_{t.0.Q.k} := 26\ MPa$$

Design tensile strength parallel to fibres

$$f_{t.0.Q.d} := k_{mod}\ \frac{f_{t.0.Q.k}}{\gamma_{M.Q}} = 17.333\ MPa$$

Characteristic bending strength

$$f_{m.Q.k} := 36\ MPa$$

Design bending strength

$$f_{m.Q.d} := k_{mod}\ \frac{f_{m.Q.k}}{\gamma_{M.Q}} = 24\ MPa$$

B2.3 Loads

B2.3.1 Self-weight

SR self-weight

$$g_{k.SR} := \rho_{Q.mean} \cdot A_{cs} = 0.138\ \frac{kN}{m}$$

Additional self-weight (sheeting etc.)

$$g_{k.add} := 1\ \frac{kN}{m^2} \cdot c = 1\ \frac{kN}{m}$$

Total characteristic self-weight

$$g_k := g_{k.SR} + g_{k.add} = 1.138\ \frac{kN}{m}$$

B2.3.2 Snow load

Characteristic snow load

$$s_k := 2.0\ \frac{kN}{m^2} \cdot c = 2\ \frac{kN}{m}$$

General shape factor

$$\mu_1 := 1.0$$

Factor for combination value of snow

$$\psi_{0.s} := 0.7$$

B2.3.3 Load combination

Security factor

$$\gamma_d := 1.0$$

Total design load (eq. 6.10a)

$$q_{d.6.10a} := \gamma_d \cdot \langle 1.35\ g_k + 1.5\ \psi_{0.s} \cdot \mu_1 \cdot s_k \rangle = 3.636\ \frac{kN}{m}$$

Total design load (eq. 6.10b)

$$q_{d.6.10b} := \gamma_d \cdot \langle 0.89 \cdot 1.35\ g_k + 1.5\ \mu_1 \cdot s_k \rangle = 4.367\ \frac{kN}{m}$$

Design self-weight

$$G_d := \begin{cases} \gamma_d \cdot 1.35\ g_k & \text{if } q_{d.6.10a} \geq q_{d.6.10b} \\ \gamma_d \cdot 0.89 \cdot 1.35\ g_k & \text{else} \end{cases} = 1.367\ \frac{kN}{m}$$

Design imposed load

$$Q_d := \begin{cases} \gamma_d \cdot 1.5\ \psi_{0.s} \cdot \mu_1 \cdot s_k & \text{if } q_{d.6.10a} \geq q_{d.6.10b} \\ \gamma_d \cdot 1.5\ \mu_1 \cdot s_k & \text{else} \end{cases} = 3\ \frac{kN}{m}$$

B2.4 Analysis

Horizontal reaction force from self-weight

$$H_g := \frac{G_d \cdot L^2}{8\ f} = 0.039\ MN$$

Cable shape function

$$z(x) := -\frac{4\ f}{L^2}\ x^2 + \frac{4\ f}{L}\ x$$

First derivative of cable shape function

$$z'(x) := -\frac{8\ f}{L^2}\ x + \frac{4\ f}{L}$$

Factor λ

$$\lambda(\Delta H) := \sqrt{\frac{H_g + \Delta H}{E_{0.Q.d} \cdot I_y}}$$

Initial guess value for ΔH

$$\Delta H_{guess} := H_g$$

Equation for calculation of horizontal force from variable load:

$$\Delta H_{guess} = \frac{Q_d - G_d \frac{\Delta H_{guess}}{H_g}}{2\ \left(H_g + \Delta H_{guess}\right)}\ 16\ f \cdot E_{0.Q.d} \cdot A_{cs} \cdot \left(\frac{1}{12} - \frac{1}{\left(\lambda\left(\Delta H_{guess}\right) \cdot L\right)^2} + \frac{2\ tanh\left(\frac{\lambda\left(\Delta H_{guess}\right) \cdot L}{2}\right)}{\left(\lambda\left(\Delta H_{guess}\right) \cdot L\right)^3} \right)$$

Horizontal force from variable load

$$\Delta H := \mathbf{find}\left(\Delta \mathbf{H}_{\mathbf{guess}}\right) = 0.086\ MN$$

Redefinition of factor λ

$$\lambda := \lambda(\Delta H) = 2.951\ \frac{1}{m}$$

Total horizontal load

$$H := H_g + \Delta H = 0.125\ MN$$

Deflection:

$$w(x) := \frac{Q_d - G_d \frac{\Delta H}{H_g}}{2\ H} \left(\frac{L^2}{4} - \frac{2}{\lambda^2} + \frac{2\ \cosh\left(\lambda \cdot \left(x - \frac{L}{2}\right)\right)}{\lambda^2\ \cosh\left(\frac{\lambda \cdot L}{2}\right)} - \left(x - \frac{L}{2}\right)^2 \right)$$

First two derivatives of the deflection:

$$w'(x) := \frac{Q_d - G_d \frac{\Delta H}{H_g}}{H} \left(\operatorname{sech}\left(\frac{\lambda \cdot L}{2}\right) \sinh\left(\lambda \cdot \left(x - \frac{L}{2}\right)\right) \frac{1}{\lambda} - \left(x - \frac{L}{2}\right) \right)$$

$$w''(x) := \frac{Q_d - G_d \frac{\Delta H}{H_g}}{H} \left(\operatorname{sech}\left(\frac{\lambda \cdot L}{2}\right) \cosh\left(\lambda \cdot \left(x - \frac{L}{2}\right)\right) - 1 \right)$$

Normal force in SR $N(x) := H \sqrt{1 + (z'(x) + w'(x))^2}$

Bending moment in SR $M(x) := -E_{0.Q.d} \cdot I_y \, w''(x)$

B2.5 Results

Maximum deflection $w_{max} := w\left(\frac{L}{2}\right) = 0.016 \ m$

Maximum total sag (incl. deflection) $f_{max} := f + w_{max} = 2.516 \ m$

Horizontal force due to self-weight $H_g = 39.368 \ kN$

Horizontal load due to variable load $\Delta H = 85.616 \ kN$

Total horizontal load in SR $H = 124.984 \ kN$

Total horizontal load at column $H_{tot} := H \cdot \frac{B}{c} = 999.869 \ kN$

Design normal force in SR $N_{Ed.SR} := N(0 \ m) = 135.521 \ kN$

Design tensile stress $\sigma_{t.0.d} := \frac{N_{Ed.SR}}{A_{cs}} = 5.019 \ MPa$

Design bending moment in SR $M_{Ed.SR} := M\left(\frac{L}{2}\right) = 0.0031 \ kN \cdot m$

Design bending stress $\sigma_{m.y.d} := \frac{M_{Ed.SR}}{I_y} \frac{h}{2} = 0.026 \ MPa$

Ratio between bending and normal stress $ratio := \frac{\sigma_{m.y.d}}{\sigma_{t.0.d}} = 0.005$

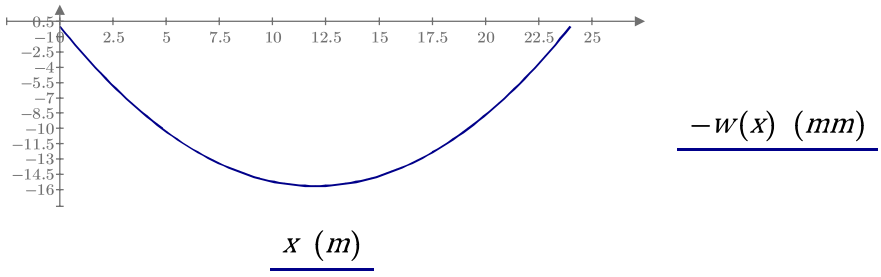

Figure B2.1 Deflection of SR.

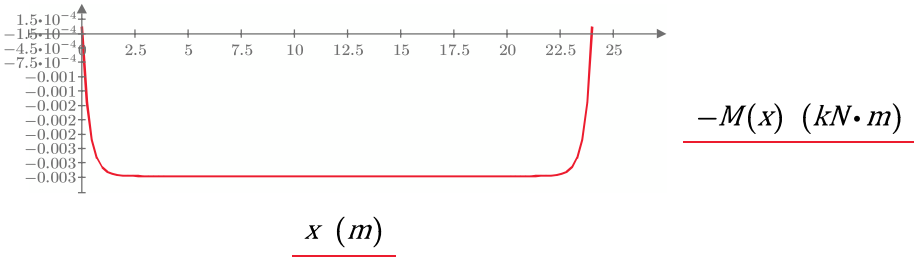

Figure B2.2 Bending moment distribution.

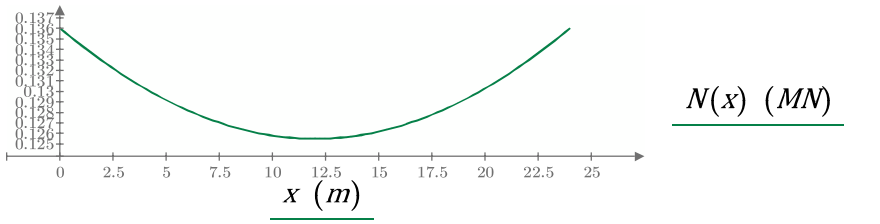

Figure B2.3 Normal force distribution.

B2.6 Utilisation check

Utilization in tension $util_t := \frac{\sigma_{t.0.d}}{f_{t.0.Q.d}} = 0.29$

Utilization in bending $util_m := \frac{\sigma_{m.y.d}}{f_{m.Q.d}} = 0.001$

Total utilization $util_{tot} := \frac{\sigma_{m.y.d}}{f_{m.Q.d}} + \frac{\sigma_{t.0.d}}{f_{t.0.Q.d}} = 0.291$

Appendix C1 - Calculation procedure fire design - Glulam

In this Appendix the calculation procedure for the fire design of glulam ribbons is presented. The considered proposal is Proposal 2 and the span length is 24 m. However, the procedure is the same for Proposal 1, and for other span lengths.

C1.1 Geometry

Span length $L := 24\ m$

Ribbon spacing $c := 0.8\ m$

Initial sag $f := 2.5\ m$

Assumed SR cross-section $b := 78\ mm$ $h := 180\ mm$ $A_{cs} := b \cdot h = 0.014\ m^2$

Fire exposure time $t_{fire} := 60\ min$

Equivalent design charring speed $\beta_n := 0.7\ \frac{mm}{min}$

Equivalent design charring depth $d_{char.n} := \beta_n \cdot t_{fire} = 42\ mm$

Distance d_0 $d_0 := 7\ mm$

Factor k_0

$$k_0 := \begin{cases} \frac{t_{fire}}{20\ min} & \text{if } t_{fire} < 20\ min \\ 1 & \text{else} \end{cases} = 1$$

Effective charring depth $d_{ef} := d_{char.n} + k_0 \cdot d_0 = 49\ mm$

Effective cross-section width $b_{ef} := b - d_{ef} = 29\ mm$

Effective cross-section height $h_{ef} := h - d_{ef} = 131\ mm$

Remaining cross-section area $A_r := b_{ef} \cdot h_{ef} = 0.004\ m^2$

Effective second moment of inertia $I_{y.fi} := \frac{b_{ef} \cdot h_{ef}^3}{12} = \left(5.433 \cdot 10^{-6}\right)\ m^4$

C1.2 Material Properties

SR material	Glulam GL30h
Density	$\rho_{g.mean} := 4.8 \ \frac{kN}{m^3}$
Partial factor for glulam	$\gamma_{M.g.fi} := 1.0$
Modification factor for tensile strength and E-modulus	$k_{mod.fi} := 1.0$
Characteristic modulus of elasticity	$E_{0.g.k} := 11.3 \ GPa$
Factor k_{fi}	$k_{fi} := 1.15$
Modulus of elasticity, 20 %-fractile	$E_{0.g.20} := k_{fi} \cdot E_{0.g.k} = 12.995 \ GPa$
Design mean modulus of elasticity parallel to fibre	$E_{0.g.d.fi} := k_{mod.fi} \ \frac{E_{0.g.20}}{\gamma_{M.g.fi}} = 12.995 \ GPa$
Characteristic tensile strength parallel to fibres	$f_{t.0.g.k} := 24 \ MPa$
Tensile strength parallel to fibres, 20 %-fractile	$f_{t.0.g.20} := k_{fi} \cdot f_{t.0.g.k} = 27.6 \ MPa$
Design tensile strength parallel to fibres	$f_{t.0.g.d.fi} := k_{mod.fi} \ \frac{f_{t.0.g.20}}{\gamma_{M.g.fi}} = 27.6 \ MPa$
Characteristic bending strength	$f_{m.g.k} := 30 \ MPa$
Bending strength, 20 %-fractile	$f_{m.g.20} := k_{fi} \cdot f_{m.g.k}$
Design bending strength	$f_{m.g.d.fi} := k_{mod.fi} \ \frac{f_{m.g.20}}{\gamma_{M.g.fi}}$

C1.3 Loads

C1.3.1 Self-weight

Self-weight of Stress Ribbons	$g_{k.SR} := \rho_{g.mean} \cdot A_{cs} = 0.067 \ \frac{kN}{m}$

Additional self-weight (sheeting etc.)

$$g_{k.add} := 1\ \frac{kN}{m^2} \cdot c = 0.8\ \frac{kN}{m}$$

Total characteristic self-weight

$$g_k := g_{k.SR} + g_{k.add} = 0.867\ \frac{kN}{m}$$

C1.3.2 Snow load

Characteristic snow load

$$s_k := 2.0\ \frac{kN}{m^2} \cdot c = 1.6\ \frac{kN}{m}$$

Snow shape factor

$$\mu_1 := 1.0$$

Factor for combination value of snow

$$\psi_{0.s} := 0.7$$

Factor for frequent value of snow

$$\psi_{1.s} := 0.4$$

C1.3.3 Load combination

Security factor

$$\gamma_d := 1.0$$

Total design load (eq. 6.10a)

$$q_{d.6.10a} := \gamma_d \cdot \left\langle 1.35\ g_k + 1.5\ \psi_{0.s} \cdot \mu_1 \cdot s_k \right\rangle = 2.851\ \frac{kN}{m}$$

Total design load (eq. 6.10b)

$$q_{d.6.10b} := \gamma_d \cdot \left\langle 0.89 \cdot 1.35\ g_k + 1.5\ \mu_1 \cdot s_k \right\rangle = 3.442\ \frac{kN}{m}$$

Design self-weight - ULS

$$G_d := \begin{cases} \gamma_d \cdot 1.35\ g_k & \text{if } q_{d.6.10a} \geq q_{d.6.10b} \\ \gamma_d \cdot 0.89 \cdot 1.35\ g_k & \text{else} \end{cases} = 1.042\ \frac{kN}{m}$$

Design variable load - ULS

$$Q_d := \begin{cases} \gamma_d \cdot 1.5\ \psi_{0.s} \cdot \mu_1 \cdot s_k & \text{if } q_{d.6.10a} \geq q_{d.6.10b} \\ \gamma_d \cdot 1.5\ \mu_1 \cdot s_k & \text{else} \end{cases} = 2.4\ \frac{kN}{m}$$

Load reduction factor

$$\eta_{fi} := \frac{g_k + \psi_{1.s} \cdot s_k \cdot \mu_1}{1.35\ g_k + 1.5\ \mu_1 \cdot s_k} = 0.422$$

Design self-weight - fire

$$G_{d.fi} := \eta_{fi} \cdot G_d = 0.44\ \frac{kN}{m}$$

Design variable load - fire

$$Q_{d.fi} := \eta_{fi} \cdot Q_d = 1.013\ \frac{kN}{m}$$

C1.4 Analysis

Horizontal reaction force from self-weight

$$H_g := \frac{G_{d.fi} \cdot L^2}{8\ f} = 0.013\ \ MN$$

Cable shape function

$$z(x) := -\frac{4\ f}{L^2}\ x^2 + \frac{4\ f}{L}\ x$$

First derivative of cable shape function

$$z'(x) := -\frac{8\ f}{L^2}\ x + \frac{4\ f}{L}$$

Factor λ

$$\lambda(\Delta H) := \sqrt{\frac{H_g + \Delta H}{E_{0.g.d.fi} \cdot I_{y.fi}}}$$

Initial guess value for ΔH

$$\Delta H_{guess} := H_g$$

Equation for calculation of horizontal force from variable load:

$$\Delta H_{guess} = \frac{Q_{d.fi} - G_{d.fi}\ \frac{\Delta H_{guess}}{H_g}}{2\ \left(H_g + \Delta H_{guess}\right)}\ 16\ f \cdot E_{0.g.d.fi} \cdot A_r \cdot \left(\frac{1}{12} - \frac{1}{\left(\lambda\left(\Delta H_{guess}\right) \cdot L\right)^2} + \frac{2\ tanh\left(\frac{\lambda\left(\Delta H_{guess}\right) \cdot L}{2}\right)}{\left(\lambda\left(\Delta H_{guess}\right) \cdot L\right)^3} \right)$$

Horizontal force from variable load

$$\Delta H := \mathbf{find}\left(\Delta \mathbf{H}_{\mathbf{guess}}\right) = 0.029\ \ MN$$

Redefinition of factor λ

$$\lambda := \lambda(\Delta H) = 0.766\ \frac{1}{m}$$

Total horizontal load

$$H := H_g + \Delta H = 0.041\ \ MN$$

Deflection:

$$w(x) := \frac{Q_{d.fi} - G_{d.fi}\ \frac{\Delta H}{H_g}}{2\ H} \left(\frac{L^2}{4} - \frac{2}{\lambda^2} + \frac{2\ \cosh\left(\lambda \cdot \left(x - \frac{L}{2}\right)\right)}{\lambda^2\ \cosh\left(\frac{\lambda \cdot L}{2}\right)} - \left(x - \frac{L}{2}\right)^2 \right)$$

First two derivatives of the deflection:

$$w'(x) := \frac{Q_{d.fi} - G_{d.fi}\ \frac{\Delta H}{H_g}}{H} \left(\operatorname{sech}\left(\frac{\lambda \cdot L}{2}\right) \sinh\left(\lambda \cdot \left(x - \frac{L}{2}\right)\right) \frac{1}{\lambda} - \left(x - \frac{L}{2}\right) \right)$$

$$w''(x) := \frac{Q_{d.fi} - G_{d.fi}\ \frac{\Delta H}{H_g}}{H} \left(\operatorname{sech}\left(\frac{\lambda \cdot L}{2}\right) \cosh\left(\lambda \cdot \left(x - \frac{L}{2}\right)\right) - 1 \right)$$

Normal force in SR

$$N(x) := H \sqrt{1 + \left(z'(x) + w'(x)\right)^2}$$

Bending moment in SR

$$M(x) := -E_{0.g.d.fi} \cdot I_{y.fi}\ w''(x)$$

C1.5 Results

Total horizontal load $H_{tot} := H + \Delta H = 70.163\ kN$

Design normal force in SR $N_{Ed.SR.fi} := N(0\ m) = 44.93\ kN$

Design tensile stress $\sigma_{t.0.d.fi} := \frac{N_{Ed.SR.fi}}{A_r} = 11.827\ MPa$

Design bending moment in SR $M_{Ed.SR.fi} := M\left(\frac{L}{2}\right) = 0.0255\ kN \cdot m$

Design bending stress $\sigma_{m.y.d.fi} := \frac{M_{Ed.SR.fi}}{I_{y.fi}} \frac{h_{ef}}{2} = 0.307\ MPa$

Ratio between bending and normal stress $ratio := \frac{\sigma_{m.y.d.fi}}{\sigma_{t.0.d.fi}} = 0.026$

C1.6 Utilisation check

Utilization in tension $util_t := \frac{\sigma_{t.0.d.fi}}{f_{t.0.g.d.fi}} = 0.429$

Utilization in bending $util_m := \frac{\sigma_{m.y.d.fi}}{f_{m.g.d.fi}} = 0.009$

Total utilization $util_{tot} := \frac{\sigma_{m.y.d.fi}}{f_{m.g.d.fi}} + \frac{\sigma_{t.0.d.fi}}{f_{t.0.g.d.fi}} = 0.437$

Appendix C2 - Calculation procedure fire design - LVL

In this Appendix the calculation procedure for the fire design of LVL ribbons is presented. The considered proposal is Proposal 3 and the span length is 24 m. However, the procedure is the same for other span lengths.

C2.1 Geometry

Span length $L := 24\ m$

Ribbon spacing $c := 1\ m$

Initial sag $f := 2.5\ m$

Assumed SR cross-section $b := 1000\ mm$ $h := 57\ mm$ $A_{cs} := b \cdot h = 0.057\ m^2$

Fire exposure time $t_{fire} := 60\ min$

Equivalent design charring speed $\beta_n := 0.7\ \frac{mm}{min}$

Equivalent design charring depth $d_{char.n} := \beta_n \cdot t_{fire} = 42\ mm$

Distance d_0 $d_0 := 7\ mm$

Factor k_0

$$k_0 := \begin{cases} \frac{t_{fire}}{20\ min} & \text{if } t_{fire} < 20\ min \\ 1 & \text{else} \end{cases} = 1$$

Effective charring depth $d_{ef} := d_{char.n} + k_0 \cdot d_0 = 49\ mm$

Effective cross-section width $b_{ef} := b - d_{ef} = 951\ mm$

Effective cross-section height $h_{ef} := h - d_{ef} = 8\ mm$

Remaining cross-section area $A_r := b_{ef} \cdot h_{ef} = 0.008\ m^2$

C2.2 Material Properties

SR material LVL (Kerto-Q)

Density $\rho_{Q.mean} := 5.1\ \frac{kN}{m^3}$

Partial factor for LVL $\gamma_{M.Q.fi} := 1.0$

Modification factor for tensile strength and E-modulus $k_{mod.fi} := 1.0$

Characteristic modulus of elasticity $E_{0.Q.k} := 8.8\ GPa$

Factor k_{fi} $k_{fi} := 1.1$

Modulus of elasticity, 20 %-fractile $E_{0.Q.20} := k_{fi} \cdot E_{0.Q.k} = 9.68\ GPa$

Design mean modulus of elasticity parallel to fibre $E_{0.Q.d.fi} := k_{mod.fi} \frac{E_{0.Q.20}}{\gamma_{M.Q.fi}} = 9.68\ GPa$

Characteristic tensile strength parallel to fibres $f_{t.0.Q.k} := 26\ MPa$

Tensile strength parallel to fibres, 20 %-fractile $f_{t.0.Q.20} := k_{fi} \cdot f_{t.0.Q.k} = 28.6\ MPa$

Design tensile strength parallel to fibres $f_{t.0.Q.d.fi} := k_{mod.fi} \frac{f_{t.0.Q.20}}{\gamma_{M.Q.fi}} = 28.6\ MPa$

C2.3 Loads

C2.3.1 Self-weight

Self-weight of Stress Ribbons $g_{k.SR} := \rho_{Q.mean} \cdot A_{cs} = 0.291\ \frac{kN}{m}$

Additional self-weight (sheeting etc.) $g_{k.add} := 1\ \frac{kN}{m^2} \cdot c = 1\ \frac{kN}{m}$

Total characteristic self-weight $g_k := g_{k.SR} + g_{k.add} = 1.291\ \frac{kN}{m}$

C2.3.2 Snow load

Characteristic snow load $s_k := 2.0\ \frac{kN}{m^2} \cdot c = 2\ \frac{kN}{m}$

Snow shape factor $\mu_1 := 1.0$

Factor for combination value of snow $\psi_{0.s} := 0.7$

Factor for frequent value of snow $\psi_{1.s} := 0.4$

C2.3.3 Load combination

Security factor $\gamma_d := 1.0$

Total design load (eq. 6.10a) $q_{d.6.10a} := \gamma_d \cdot \langle 1.35\ g_k + 1.5\ \psi_{0.s} \cdot \mu_1 \cdot s_k \rangle = 3.842\ \frac{kN}{m}$

Total design load (eq. 6.10b) $q_{d.6.10b} := \gamma_d \cdot \langle 0.89 \cdot 1.35\ g_k + 1.5\ \mu_1 \cdot s_k \rangle = 4.551\ \frac{kN}{m}$

Design self-weight - ULS

$$G_d := \begin{cases} \text{if } q_{d.6.10a} \geq q_{d.6.10b} \\ \quad \gamma_d \cdot 1.35\ g_k \\ \text{else} \\ \quad \gamma_d \cdot 0.89 \cdot 1.35\ g_k \end{cases} = 1.551\ \frac{kN}{m}$$

Design variable load - ULS

$$Q_d := \begin{cases} \text{if } q_{d.6.10a} \geq q_{d.6.10b} \\ \quad \gamma_d \cdot 1.5\ \psi_{0.s} \cdot \mu_1 \cdot s_k \\ \text{else} \\ \quad \gamma_d \cdot 1.5\ \mu_1 \cdot s_k \end{cases} = 3\ \frac{kN}{m}$$

Load reduction factor $\eta_{fi} := \frac{g_k + \psi_{1.s} \cdot s_k \cdot \mu_1}{1.35\ g_k + 1.5\ \mu_1 \cdot s_k} = 0.441$

Design self-weight - fire $G_{d.fi} := \eta_{fi} \cdot G_d = 0.684\ \frac{kN}{m}$

Design variable load - fire $Q_{d.fi} := \eta_{fi} \cdot Q_d = 1.323\ \frac{kN}{m}$

C2.4 Analysis

Horizontal reaction force $H := \frac{\langle G_{d.fi} + Q_{d.fi} \rangle \cdot L^2}{8\ f} = 0.058\ MN$

Cable shape function $z(x) := -\frac{4\ f}{L^2}\ x^2 + \frac{4\ f}{L}\ x$

First derivative of cable shape function $z'(x) := -\frac{8\ f}{L^2}\ x + \frac{4\ f}{L}$

Normal force in SR $N(x) := H \sqrt{1 + (z'(x))^2}$

C2.5 Results

Horizontal force $H = 57.779\ kN$

Design normal force in SR $N_{Ed.SR} := N(0\ m) = 62.594\ kN$

Design tensile stress $\sigma_{t.0.d.fi} := \frac{N_{Ed.SR}}{A_r} = 8.227\ MPa$

C2.6 Utilisation check

Utilization in tension $util_t := \frac{\sigma_{t.0.d.fi}}{f_{t.0.Q.d.fi}} = 0.288$

Appendix D – Intermediate Truss Design

In this Appendix an extract of the intermediate truss design is presented. The design is performed with the software Strusoft WIN-Statik 6.4 Frame Analysis, and all the data and figures presented are extracted from the software. The ribbon span length considered in the example is 24 m.

Joints

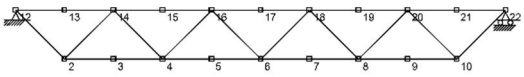

Member

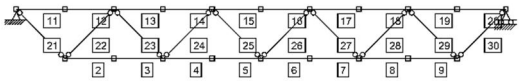

Section data

Name	Dir.	Area (m^2)	I (m^4)	h (m)	z (m)	E-modulus (kN/m^2)
430x450 / GL 30h	y-y	1.935e-1	3.27e-3	0.450	0.225	9.40e6
215×315 / GL 30h	y-y	6.772c-2	5.60c-4	0.315	0.158	9.40c6

Section/Member

Member	Section	Dir.	Length (m)	Weight (kg)	Member	Section	Dir.	Length (m)	Weight (kg)
2	430x450 / GL 30h	y-y	1.600	133.128	18	430x450 / GL 30h	y-y	1.600	133.128
3	430x450 / GL 30h	y-y	1.600	133.128	19	430x450 / GL 30h	y-y	1.600	133.128
4	430x450 / GL 30h	y-y	1.600	133.128	20	430x450 / GL 30h	y-y	1.600	133.128
5	430x450 / GL 30h	y-y	1.600	133.128	21	215×315 / GL 30h	y-y	2.263	65.895
6	430x450 / GL 30h	y-y	1.600	133.128	22	215×315 / GL 30h	y-y	2.263	65.895
7	430x450 / GL 30h	y-y	1.600	133.128	23	215×315 / GL 30h	y-y	2.263	65.895
8	430x450 / GL 30h	y-y	1.600	133.128	24	215×315 / GL 30h	y-y	2.263	65.895
9	430x450 / GL 30h	y-y	1.600	133.128	25	215×315 / GL 30h	y-y	2.263	65.895
11	430x450 / GL 30h	y-y	1.600	133.128	26	215×315 / GL 30h	y-y	2.263	65.895
12	430x450 / GL 30h	y-y	1.600	133.128	27	215×315 / GL 30h	y-y	2.263	65.895
13	430x450 / GL 30h	y-y	1.600	133.128	28	215×315 / GL 30h	y-y	2.263	65.895
14	430x450 / GL 30h	y-y	1.600	133.128	29	215×315 / GL 30h	y-y	2.263	65.895
15	430x450 / GL 30h	y-y	1.600	133.128	30	215×315 / GL 30h	y-y	2.263	65.895
16	430x450 / GL 30h	y-y	1.600	133.128					
17	430x450 / GL 30h	y-y	1.600	133.128	Sum			51.427	3055.254

Basic loadcase: G

Basic loadcase - G

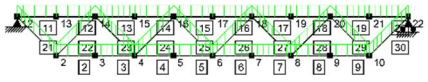

Self weight

Member	q(kN/m)	Member	q(kN/m)	Member	q(kN/m)	Member	q(kN/m)	Member	q(kN/m)
2	0.816	8	0.816	15	0.816	21	0.286	27	0.286
3	0.816	9	0.816	16	0.816	22	0.286	28	0.286
4	0.816	11	0.816	17	0.816	23	0.286	29	0.286
5	0.816	12	0.816	18	0.816	24	0.286	30	0.286
6	0.816	13	0.816	19	0.816	25	0.286		
7	0.816	14	0.816	20	0.816	26	0.286		

Basic loadcase: Q

Basic loadcase - Q

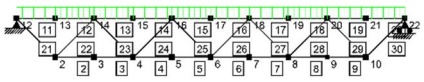

Uniform load

Member	Dir.	Load intensity	L1(m)	L2(m)	Member	Dir.	Load intensity	L1(m)	L2(m)
11	Y / q(kN/m)	110.000	0	0	13	Y / q(kN/m)	110.000	0	0
12	Y / q(kN/m)	110.000	0	0	14	Y / q(kN/m)	110.000	0	0

Basic loadcase

Name	Des.	Name	Des.
G	B1	Q	B2

Loadcase

	Name	Combination	Limit	Type	Dependency
1	1	1,2*B1+B2	ULS		

Results

Loadcase: 1

Member	Ratio of utilization	Member	Ratio of utilization	Member	Ratio of utilization	Member	Ratio of utilization
16	0.966	13	0.909	17	0.832	2	0.560
15	0.966	7	0.891	14	0.832	27	0.433
30	0.921	4	0.891	20	0.718	24	0.433
21	0.921	29	0.879	11	0.718	28	0.405
19	0.910	22	0.879	8	0.682	23	0.405
12	0.910	6	0.875	3	0.682	26	0.008
18	0.909	5	0.875	9	0.560	25	0.008

Appendix E – Boundary Truss Design

In this Appendix an extract of the boundary truss design is presented. The design is performed with the software Strusoft WIN-Statik 6.4 Frame Analysis, and all the data and figures presented are extracted from the software. The ribbon span length considered in the example is 24 m.

Joints

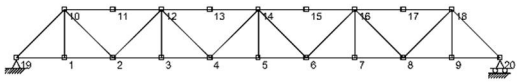

Member

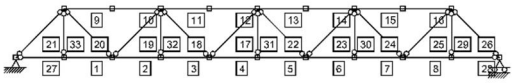

Section data

Name	Dir.	Area (m²)	I (m^4)	h (m)	z (m)	E-modulus (kN/m²)
315x430 / GL 30h	y-y	1.354e-1	1.12e-3	0.315	0.158	9.40e6
190×225 / GL 30h	y-y	4.275e-2	1.80e-4	0.225	0.113	9.40e6
Rund 10 / S355	y-y	7.854e-5	4.91e-10	0.010	0.005	2.10e8

Section/Member

Member	Section	Dir.	Length (m)	Weight (kg)	Member	Section	Dir.	Length (m)	Weight (kg)
1	315x430 / GL 30h	y-y	0.800	46.595	19	190×225 / GL 30h	y-y	1.131	20.797
2	315x430 / GL 30h	y-y	0.800	46.595	20	190×225 / GL 30h	y-y	1.131	20.797
3	315x430 / GL 30h	y-y	0.800	46.595	21	190×225 / GL 30h	y-y	1.131	20.797
4	315x430 / GL 30h	y-y	0.800	46.595	22	190×225 / GL 30h	y-y	1.131	20.797
5	315x430 / GL 30h	y-y	0.800	46.595	23	190×225 / GL 30h	y-y	1.131	20.797
6	315x430 / GL 30h	y-y	0.800	46.595	24	190×225 / GL 30h	y-y	1.131	20.797
7	315x430 / GL 30h	y-y	0.800	46.595	25	190×225 / GL 30h	y-y	1.131	20.797
8	315x430 / GL 30h	y-y	0.800	46.595	26	190×225 / GL 30h	y-y	1.131	20.797
9	315x430 / GL 30h	y-y	0.800	46.595	27	315x430 / GL 30h	y-y	0.800	46.595
10	315x430 / GL 30h	y-y	0.800	46.595	28	315x430 / GL 30h	y-y	0.800	46.595
11	315x430 / GL 30h	y-y	0.800	46.595	29	Rund 10 / S355	y-y	0.800	0.493
12	315x430 / GL 30h	y-y	0.800	46.595	30	Rund 10 / S355	y-y	0.800	0.493
13	315x430 / GL 30h	y-y	0.800	46.595	31	Rund 10 / S355	y-y	0.800	0.493
14	315x430 / GL 30h	y-y	0.800	46.595	32	Rund 10 / S355	y-y	0.800	0.493
15	315x430 / GL 30h	y-y	0.800	46.595	33	Rund 10 / S355	y-y	0.800	0.493
16	315x430 / GL 30h	y-y	0.800	46.595					
17	190×225 / GL 30h	y-y	1.131	20.797		Sum		29.714	1049.147
18	190×225 / GL 30h	y-y	1.131	20.797					

Basic loadcase: G

Basic loadcase - G

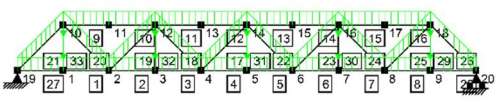

Self weight

Member	q(kN/m)	Member	q(kN/m)	Member	q(kN/m)	Member	q(kN/m)	Member	q(kN/m)
1	0.571	8	0.571	15	0.571	22	0.180	29	-0.006
2	0.571	9	0.571	16	0.571	23	0.180	30	-0.006
3	0.571	10	0.571	17	0.180	24	0.180	31	-0.006
4	0.571	11	0.571	18	0.180	25	0.180	32	-0.006
5	0.571	12	0.571	19	0.180	26	0.180	33	-0.006
6	0.571	13	0.571	20	0.180	27	0.571		
7	0.571	14	0.571	21	0.180	28	0.571		

Basic loadcase: Q

Basic loadcase - Q

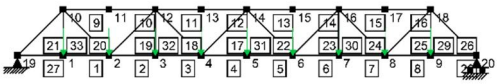

Joint load

Joint	Dir.	Load intensity	Joint	Dir.	Load intensity	Joint	Dir.	Load intensity
1	Y / P(kN)	107.000	4	Y / P(kN)	107.000	7	Y / P(kN)	107.000
2	Y / P(kN)	107.000	5	Y / P(kN)	107.000	8	Y / P(kN)	107.000
3	Y / P(kN)	107.000	6	Y / P(kN)	107.000	9	Y / P(kN)	107.000

Basic loadcase

Name	Des.	Name	Des.
G	B1	Q	B2

Loadcase

	Name	Combination	Limit	Type	Dependency
1	1	1,2*B1+B2	ULS		

Results

Loadcase: 1

Member	Ratio of utilization	Member	Ratio of utilization	Member	Ratio of utilization	Member	Ratio of utilization
5	0.915	20	0.781	28	0.473	23	0.394
4	0.915	14	0.732	27	0.473	18	0.394
26	0.805	11	0.732	8	0.473	24	0.368
21	0.805	13	0.726	1	0.473	19	0.368
7	0.788	12	0.726	32	0.467	22	0.023
2	0.788	15	0.571	30	0.467	17	0.023
6	0.788	10	0.571	9	0.447		
3	0.788	33	0.488	16	0.447		
25	0.781	29	0.488	31	0.408		

Appendix F - Back-stay bar design

In this Appendix the design of the back-stay member is presented. The design is performed for the three span lengths 24, 36 and 48 m simultaneously. Individual data is given in vector form, where the first position corresponds to 24 m span, second position to 36 m span and third position to 48 m span.

F.1 Geometry

Back-stay bar angle $\alpha := 30\ °$

Column height $H_{col} := 12\ m$

Back-stay cable length $l_{bs} := \frac{H_{col}}{\cos(\alpha)} = 13.856\ m$

Assumed number of back-stay bars $n_{bs} := [2\ \ 2\ \ 2]^{T}$

F.2 Material Properties

Steel quality S460

Characteristic yield strength $f_{yk} := 460\ MPa$

Characteristic ultimate strength $f_{uk} := 610\ MPa$

Partial factor for steel with regard to tensile failure $\gamma_{M2} := min\left(0.9\ \frac{f_{uk}}{f_{yk}}, 1.1\right) = 1.1$

Design yield strength $f_{yd} := \frac{f_{yk}}{\gamma_{M2}} = 418.182\ MPa$

Steel density $\rho_s := 7850\ \frac{kg}{m^3}$

F.3 Loads

Horizontal force at column $H_{col} := \begin{bmatrix} 1000 \\ 2245 \\ 4100 \end{bmatrix} kN$

Normal force in back-stay $N_{bs} := \frac{H_{col}}{\sin(\alpha)} = \begin{bmatrix} 2 \cdot 10^3 \\ 4.49 \cdot 10^3 \\ 8.2 \cdot 10^3 \end{bmatrix} kN$

F.4 Design

Required cross-section area

$$A_{req} := \frac{N_{bs}}{f_{yd}} = \begin{bmatrix} 0.005 \\ 0.011 \\ 0.02 \end{bmatrix} \ m^2$$

Required cross-section diameter

$$\phi_{req} := 2 \overrightarrow{\sqrt{\frac{A_{req}}{\pi}} \cdot \frac{1}{n_{bs}}} = \begin{bmatrix} 39.017 \\ 58.461 \\ 79.004 \end{bmatrix} \ mm$$

F.5 Results

Chosen cross-section dimension

$$\phi_{bs} := \begin{bmatrix} 40 & 60 & 80 \end{bmatrix}^T \ mm$$

Back-stay cross-section area

$$A_{bs} := \frac{\pi \cdot \phi_{bs}^{\ 2}}{4} = \begin{bmatrix} 0.001 \\ 0.003 \\ 0.005 \end{bmatrix} \ m^2$$

Back-stay steel volume

$$V_{bs} := \overrightarrow{n_{bs} \cdot A_{bs} \cdot l_{bs}} = \begin{bmatrix} 0.035 \\ 0.078 \\ 0.139 \end{bmatrix} \ m^3$$

Backstay steel mass

$$m_{bs} := V_{bs} \cdot \rho_s = \begin{bmatrix} 0.273 \\ 0.615 \\ 1.094 \end{bmatrix} \ tonne$$

Appendix G – Non-bending stiff column design

In this Appendix an extract of the design of the concrete column used in the back-stay and the compression strut alternatives is presented. The design is performed with the software Strusoft WIN-Statik 6.4 Concrete Column, and all the data and figures presented are extracted from the software. The ribbon span length considered in the example is 24 m.

Input - Eurocode concrete / EN 1992-1-1 (Swedish annex)

Column: 24 m - Ultimate limit state

General

Designation	Value	Designation	Value
Exposure class:	X0 Very dry	Quality control and reduced deviations:	No
Life class:	L50	Reduced or measured geometrical data:	No

Column geometry

Designation	Value	Designation	Value	Designation	Value
Column length (m):	12.0	Buckling length, L_{cz} (m):	12.0	Stabilized L_{cy}/i:	No
Buckling length, L_{cy} (m):	12.0	Column type:	Slender	Stabilized L_{cz}/i:	No

Concrete Material C40/50

Design values for Ultimate Limit State (MPa)	Value [MPa]	Design values for Ultimate Limit State (MPa)	Value [MPa]	Design values for Ultimate Limit State (MPa)	Value [MPa]
f_{cd}	26.67	ε_{c1}	0.0020	Low strength variation:	No
f_{ctd}	1.64	ε_{cu}	0.0035		
E_{cd}	29350	γ_c	1.50		

Design values for Ultimate Limit State (MPa)

Designation	Bottom Designation B500B Diameter, mm 16	Top Designation B500B Diameter, mm 16	Stirrup Designation B500B Diameter, mm 8
f_{yd}	435	435	435
f_{ycd}	435	435	435
E_{sd}	200000	200000	200000

Reinforcement details

	Bottom	Code	Top	Code
Cover	26	26	26	26
Cover (side)	26	26		
Distance between bars				
In same layer	20	20	20	20
In different layers	20	20	20	20
Vibration space 0 (mm)				
Largest aggregate size 10 (mm)				
Cover tolerance 10 (mm)				
Stirrup details				
Angle (deg) 90.0				

Section Loadcase: 24 m
Section: 350x350

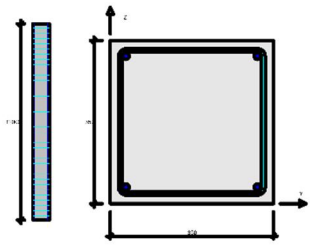

Loadcase dependent parameters

Loadcase	Creep coefficient
24 m (Effective creep)	0

Loadcase

Designation	Mz [kNm]	My [kNm]	N [kN]	Limit state	Type
24 m	0	0	-442.0	ULS	

Column: 24 m - Calculation settings

Design settings	
Use compression reinforcement	Yes
Use minimum bend reinforcement	Yes
Use sudden release (EN 8.10.2.2)	No
Monolithic construction (EN 9.2.1.2)	No
2nd order moment calculation	Stiffness method (EN 5.8.7)

Design results

Column: 24 m - Ultimate limit state

Slender bending capacity

Buckling data	Calculated WITH 2nd order moment according to the Stiffness method (EN 5.8.7)
Required reinforcement	2 ø 16 + 2 ø 16
Moment from load	M_y = 0 kNm
Moment from initial bow imperfection	M_{eiy} = 13.3 kNm
Addition from 2nd order effects	M_{y2} = 63.6 kNm
Total design moment	M_{yd2} = 0 + 13.3 + 63.6 = 76.9 kNm
Minumum moment with respect to unintentional load eccentricity according to EN 6.1.	M_y = 8.8 kNm
Moment capacity	M_{Rdy} = 115.0 kNm
Utilization ratio	M_{yd2}/M_{Ryd} = 76.9/115.0 = 0.67
Moment from load	M_z = 0 kNm
Moment from initial bow imperfection	M_{eiz} = 13.3 kNm
Addition from 2nd order effects	M_{z2} = 63.6 kNm
Total design moment	M_{zd2} = 0 + 13.3 + 63.6 = 76.9 kNm
Minumum moment with respect to unintentional load eccentricity according to EN 6.1.	M_z = 8.8 kNm
Moment capacity	M_{Rdz} = 115.0 kNm
Utilization ratio	M_{zd2}/M_{Rzd} = 76.9/115.0 = 0.67

Slender compression capacity

Slender capacity	N_{xyu} = -555.7 kN
Utilization ratio	N/N_{xyu} = -442.0/-555.7 = 0.80
Slenderness factor	$\lambda_y = l_{cy}/i_y$ = 12.00/0.101 = 118.77< 133.17
Slender capacity	N_{xzu} = -555.7 kN
Utilization ratio	N/N_{xzu} = -442.0/-555.7 = 0.80
Slenderness factor	$\lambda_z = l_{cz}/i_z$ = 12.00/0.101 = 118.77< 133.17

Minimum stirrups

Minimum transverse reinforcement according to EN 1992-1-1 9.5.3	Stirrups ø 8 s 320

Appendix H – Compression strut design

In this Appendix an extract of the design of the compression strut is presented. The design is performed with the software Strusoft WIN-Statik 6.4 Frame Analysis, and all the data and figures presented are extracted from the software. The ribbon span length considered in the example is 24 m.

Joints

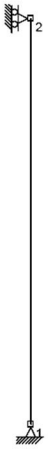

Member

Section data

Name	Dir.	Area (m^2)	I (m^4)	h (m)	z (m)	E-modulus (kN/m^2)
VKR 350x350-10 / S355	y-y	1.360e-2	2.60e-4	0.350	0.175	2.10e8

Section/Member

Member	Section	Dir.	Length (m)	Weight (kg)
1	VKR 350x350-10 / S355	y-y	13.900	1473.400
Sum			13.900	1473.400

Basic loadcase: 24 m

Basic loadcase - 24 m

Basic loadcase

Name	Des.
24 m	B1

Loadcase

	Name	Combination	Limit	Type	Dependency
1	24 m	B1	ULS		

Results

Loadcase: 24 m

Member	Ratio of utilization
1	0.896

Appendix I – Bending Stiff Column Design

In this Appendix an extract of the design of the bending stiff column is presented. The design is performed with the software Strusoft WIN-Statik 6.4 Concrete column, and all the data and figures presented are extracted from the software.. The ribbon span length considered in the example is 24 m.

Input - Eurocode concrete / EN 1992-1-1 (Swedish annex)

Column: 24 m - Ultimate limit state

General

Designation	Value	Designation	Value
Exposure class:	X0 Very dry	Quality control and reduced deviations:	No
Life class:	L50	Reduced or measured geometrical data:	No

Column geometry

Designation	Value	Designation	Value	Designation	Value
Column length (m):	12.0	Buckling length, L_{cz} (m):	24.0	Stabilized L_{cy}/i:	No
Buckling length, L_{cy} (m):	24.0	Column type:	Slender	Stabilized L_{cz}/i:	No

Concrete Material C40/50

Design values for Ultimate Limit State (MPa)	Value [MPa]	Design values for Ultimate Limit State (MPa)	Value [MPa]	Design values for Ultimate Limit State (MPa)	Value [MPa]
f_{cd}	26.67	ε_{c1}	0.0020	Low strength variation:	No
f_{ctd}	1.64	ε_{cu}	0.0035		
E_{cd}	29350	γ_c	1.50		

Design values for Ultimate Limit State (MPa)

Designation	Bottom Designation B500B Diameter, mm 32	Top Designation B500B Diameter, mm 32	Stirrup Designation B500B Diameter, mm 8
f_{yd}	435	435	435
f_{ycd}	435	435	435
E_{sd}	200000	200000	200000

Reinforcement details

	Bottom	Code	Top	Code
Cover	42	42	42	42
Cover (side)	42	42		
Distance between bars				
In same layer	32	32	32	32
In different layers	32	32	32	32
Vibration space 0 (mm)				
Largest aggregate size 10 (mm)				
Cover tolerance 10 (mm)				
Stirrup details				
Angle (deg) 90.0				

Section Loadcase: 24 m
Section: 1500x600

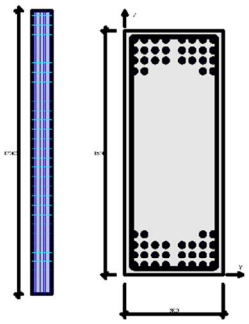

Loadcase dependent parameters

Loadcase	Creep coefficient
24 m (Effective creep)	0

Loadcase

Designation	Mz [kNm]	My [kNm]	N [kN]	Limit state	Type
24 m	0	12000.0	-442.0	ULS	

Column: 24 m - Calculation settings

Design settings	
Use compression reinforcement	Yes
Use minimum bend reinforcement	Yes
Use sudden release (EN 8.10.2.2)	No
Monolithic construction (EN 9.2.1.2)	No
2nd order moment calculation	Stiffness method (EN 5.8.7)

Design results

Column: 24 m - Ultimate limit state

Slender bending capacity

Buckling data	Calculated WITH 2nd order moment according to the Stiffness method (EN 5.8.7)
Required reinforcement	28 ø 32 + 28 ø 32
Moment from load	M_y = 12000.0 kNm
Moment from initial bow imperfection	M_{ciy} = 26.5 kNm
Addition from 2nd order effects	M_{y2} = 112.4 kNm
Total design moment	M_{yd2} = 12000.0 + 26.5 + 112.4 = 12138.9 kNm

Slender bending capacity

Minumum moment with respect to unintentional load eccentricity according to EN 6.1.	M_y = 22.1 kNm
Moment capacity	M_{Rdy} = 12466.8 kNm
Utilization ratio	M_{yd2}/M_{Ryd} = 12138.9/12466.8 = 0.97

Moment from load	M_z = 0 kNm
Moment from initial bow imperfection	M_{ciz} = 26.5 kNm
Addition from 2nd order effects	M_{z2} = 3.3 kNm
Total design moment	M_{zd2} = 0 + 26.5 + 3.3 = 29.8 kNm
Minumum moment with respect to unintentional load eccentricity according to EN 6.1.	M_z = 8.8 kNm
Moment capacity	M_{Rdz} = 3844.2 kNm
Utilization ratio	M_{zd2}/M_{Rzd} = 29.8/3844.2 = 0.01

Utilization ratio, biaxially	$(M_{dy2}/M_{Rdy})^a + (M_{dz2}/M_{Rdz})^a =$ $= (12138.9/12466.8)^{1.0} + (29.8/3844.2)^{1.0} = 0.98$

Slender compression capacity

Slender capacity	N_{xyu} = -43581.7 kN
Utilization ratio	N/N_{xyu} = -442.0/-43581.7 = 0.01
Slenderness factor	$\lambda_y = l_{cy}/i_y$ = 24.00/0.433 = 55.43< 639.16
Slender capacity	N_{xzu} = -4790.4 kN
Utilization ratio	N/N_{xzu} = -442.0/-4790.4 = 0.09
Slenderness factor	$\lambda_z = l_{cz}/i_z$ = 24.00/0.173 = 138.56< 456.17

Minimum stirrups

Minimum transverse reinforcement according to EN 1992-1-1 9.5.3	Stirrups ø 8 s 400